SECOND GENERATION PHOTOACTIVATED INSULINS

A DISSERTATION IN

Pharmaceutical sciences
and
Chemistry

Presented to the Faculty of the University
of Missouri-Kansas City in partial fulfillment of
the requirements for the degree

DOCTOR OF PHILOSOPHY

by
VENKATA SRIKRISHNA KARTHIK NADENDLA

M.Pharm., Manipal University, 2012
B.Pharm., Manipal University, 2010

Kansas City, Missouri
2020

SECOND GENERATION PHOTOACTIVATED INSULINS

Venkata Srikrishna Karthik Nadendla, Doctor of Philosophy

University of Missouri-Kansas City, 2020

ABSTRACT

The photoactivated depot (PAD) is a minimally invasive approach developed for a continuously variable light stimulated release of insulin. In this approach, a protein depot that can last for days is injected under the skin. A light source placed on the skin above the site of injection can trigger protein release into the blood with a transcutaneous irradiation. Since the insulin photorelease is a photochemical reaction, the amount released can be tightly controlled by varying the duration of irradiation. PAD is beneficial for diabetics as it can deliver insulin in a continuously variable fashion and can be automated as an artificial pancreas to avoid dosing errors.

A first-generation material was constructed by covalently linking insulin to an insoluble polymer via a photocleavable group. Insolubility is a key requirement of the PAD material to allow retention at the site of injection, prior to irradiation. *In vitro* and *in vivo* experiments demonstrated its ability to deliver insulin on exposure to light. However, it needed further improvements due to the use of the polymer. Due to its large size, the material had low insulin density and was injected using a lower gauge needle. The polymer was not eliminated from the injection site after irradiation. Thus, alternative polymer-free approaches were explored to confer insolubility to insulin.

In this work, photocleavable small molecules (tags) were explored to lower protein solubility. Firstly, non-polar peptidic and unnatural photocleavable tags were designed that could render insulin less soluble in aqueous conditions. Protein solubility also depends on its net charge. As an alternative approach, insulin solubility was lowered by balancing its charges with tags to be zero at physiological pH. A series of positively charged photocleavable groups were designed to raise the pI of insulin from 5.4 to 7.2.

Two ideal materials, one chosen from each category of tags, were tested in diabetic rats. A PAD dose-response relationship was developed for the first time in living systems. These observations can assist in the development of an automated of the delivery system in response to blood glucose (with a continuous glucose monitor) for the diabetics.

APPROVAL PAGE

The faculty listed below, appointed by the Dean of the School of Graduate Studies, have examined the dissertation titled "Second Generation Photoactivated Insulins" presented by Venkata Srikrishna Karthik Nadendla, candidate for the Doctor of Philosophy degree, and certify that in their opinion it is worthy of acceptance.

Supervisory Committee

Simon H. Friedman, Ph.D., Committee Chair
Department of Pharmacology and Pharmaceutical Sciences

Samuel Bouyain, DPhil.
Department of Cell Biology and Biophysics

Keith R. Buszek, Ph.D.
Department of Chemistry

William G. Gutheil, Ph.D.
Department of Pharmacology and Pharmaceutical Sciences

Kathleen V. Kilway, Ph.D.
Department of Chemistry

CONTENTS

LIST OF ILLUSTRATIONS

LIST OF TABLES

ACKNOWLEDGEMENTS

I sincerely thank my advisor, Prof. Simon H. Friedman, for giving an opportunity and supporting me in his lab. He was personally unavailable during my first year due to his chemotherapy, but still made sure that I had an excellent training by constantly keeping in touch over emails and skype. I am very grateful for his patience as this was a tedious task after going through multiple exhausting chemotherapy sessions. Also, this work would not have progressed without his advice on all the topics discussed here, the most important of them being the azine issue and the analysis of isoelectric point shifts in Lantus.

I am very thankful to Dr. Karen Kover, who worked with us extensively on testing the PAD *in vivo*. Her inputs on insulin insensitivity in rats were crucial in the standardization of the rat model. She did not hesitate to work with me for over 8 months to ensure that our PAD results were reliable. I am also thankful for her very interesting discussions on pancreatic endocrinology while performing these experiments.

I also thank my committee members Dr. Samuel Bouyain, Dr. Keith Buszek, Dr. William Gutheil, and Dr. Kathleen Kilway for their time, interest and recommendations. They have not only taught me principles of chemistry and biology, but also taught how to apply them to explore science through their coursework. This work is based on, and discusses most of the principles discussed in the classrooms.

I acknowledge all my former and present colleagues in the lab, and the department who have laid the foundation for, helped, and supported my work here.

Dr. Cameron Lindsay kindly provided us with a sample of Lantus. Special thanks to Dr. Mridul Mukherji and Dr. Bi-Botti Youan for sharing their resources (multimode reader and zeta sizer). This work was supported by the University of Missouri Fast Track Award, UMKC-SOP Deans Bridge Fund, and NIH-1DP3DK106921-01.

Finally, I thank my family so much for their sacrifices to support my journey.

CHAPTER 1

INTRODUCTION

Insulin and diabetes

Insulin plays a critical role in the maintenance of glucose homeostasis. It is secreted by the β cells of pancreas during hyperglycemic conditions and functions by signaling other tissues in the body to absorb glucose from blood[1]. Hence, insulin dependent glucose absorption is a vital process that allows cells to store (glycogen) or produce energy (adenosine triphosphate). This process not only enables the tissues to carry out daily functions, but also protects biological molecules in the extracellular fluids from being exposed to a high concentration of sugar.

In type 1 diabetics, the β cells in pancreas are destroyed due to autoimmunity[2]. Thus, they can neither produce insulin nor utilize glucose from blood. Type 2 diabetics become insulin insensitive due to unknown reasons, though the β cells produce insulin in the initial stages. Since the blood glucose is not lowered, β cells will be under constant stress to produce more insulin. After a while, the β cells stress out and lose their ability to produce insulin[3]. The consequence of both types of conditions is persistent elevation of blood glucose.

Under normal conditions, kidney reabsorbs any glucose passing through the urinary fluids. Since glucose is present in large excess in diabetics, their kidneys cannot reabsorb all glucose. This results in retention of glucose in urine[4]. Moreover, excess glucose is accumulated in the extracellular body fluids, and this raises the osmotic pressure in blood. Due to this increase in osmotic pressure, more water is

retained in the renal system. Hence diabetics have a higher frequency of urination (polyuria). Patients also feel thirsty throughout the day (polydipsia) due to loss of fluids. Another common consequence of the increase of osmotic pressure is the swelling of the lenses in the eye. This disables the patients to have a focused sight (blurry vision) and will ultimately lead to blindness if the condition is untreated[1]. Nutrient rich body fluids with high amounts of glucose also provide microorganisms such as yeasts the ideal conditions to grow[5]. Therefore, diabetics are also prone to infections.

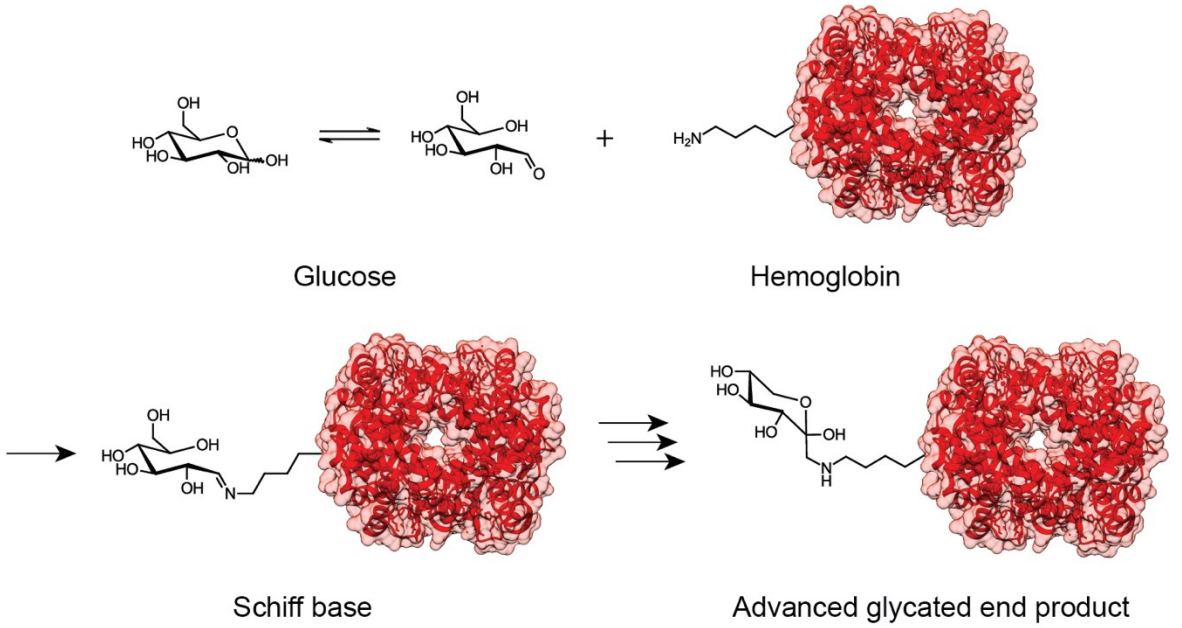

Figure 1 Formation of glycated proteins and AGEs

Many long-term complications of hyperglycemia, i.e. if the diabetic condition is not treated, are usually dangerous and lower the life span of patients. This is mainly due to the exposure of sugars to biological molecules. As shown in Figure 1, sugars react with nucleophilic groups on proteins and undergo further transformations to

form 'Advanced Glycation End products' or AGEs[6]. The rate of protein glycation is higher in diabetics in comparison to healthy individuals due to the higher concentration of glucose in blood. AGEs are either toxic or less active biologically and therefore modulate patient's physiology. Thus, diabetes begins as an imbalance in carbohydrate metabolism, which will eventually result in other physiological imbalances and the failure of the living being as a whole. The changes in blood flow and production of AGEs cause nerve damage making the patient less sensitive to pain. Patients are also observed to heal at a slower rate. Inability of the patient to feel the pain makes the injuries in regions in extremities less detectable. These injuries are ideal sites for infections in diabetics, which may spread to other tissues in later stages. In such cases, extremities are amputated to prevent the spread of infection[9]. Hyperglycemia over long periods may also result in strokes, heart attacks and kidney failures[10,11].

Glycated hemoglobin (HbA1c) is used as a marker to know the AGEs formation[7]. According to the American Diabetes Association, healthy individuals have <5.7% HbA1c in their blood. A percentage of >6.5% indicates that the patient is under constant hyperglycemia for a long duration and thus the diagnosis can be concluded as a diabetes[8]. Blood glucose levels at any instant can also be determined by the patients or at the clinics using point-of-care glucometers. The fasting glucose levels of a healthy person typically lies below 100 mg/dL (<5.6 mM). Mean fasting glucose levels of diabetics are observed to be above 125 mg/dL (>7 mM).

Therefore, insulin is exogenously administered to control the blood glucose concentration in diabetics[12]. The goal of this hormonal therapy is to assist the patient physiologically by reducing the blood glucose and prevent the formation of AGEs. However, patients must limit consumption of carbohydrate rich food and have a physically active lifestyle. Type 1 diabetics are dependent on insulin for their survival. Many type 2 diabetics also take insulin to treat the condition. About 422 million people suffer from diabetes around the world according to the World Health Organization. T1D can occur at a young age and constitute about 10% of the diabetic population. About 1.6 million deaths per year are caused due to diabetes.

Chemistry and types of insulin

Insulin is a protein consisting of two peptidic chains, A and B with a mass of 5808 Da. The two chains are connected with two disulfide linkages, and an additional intra-chain disulfide connectivity exists on the A chain. There are 21 and 30 amino acids in the A and B chains of human insulin respectively (Figure 2).

With the understanding of the chemical nature of insulin and advancements in the field of recombinant DNA technology, insulin can be readily manufactured on a large scale in *Escherichia coli*. Native human insulin has a characteristic pharmacokinetic profile depending on the dose administered – showing its onset of action at 30-60 minutes, peaking the concentration at 2-4 hours and showing its duration of action for 6-8 hours[13]. This profile may not always provide the best therapy and therefore, new insulin variants were designed to improve the treatment.

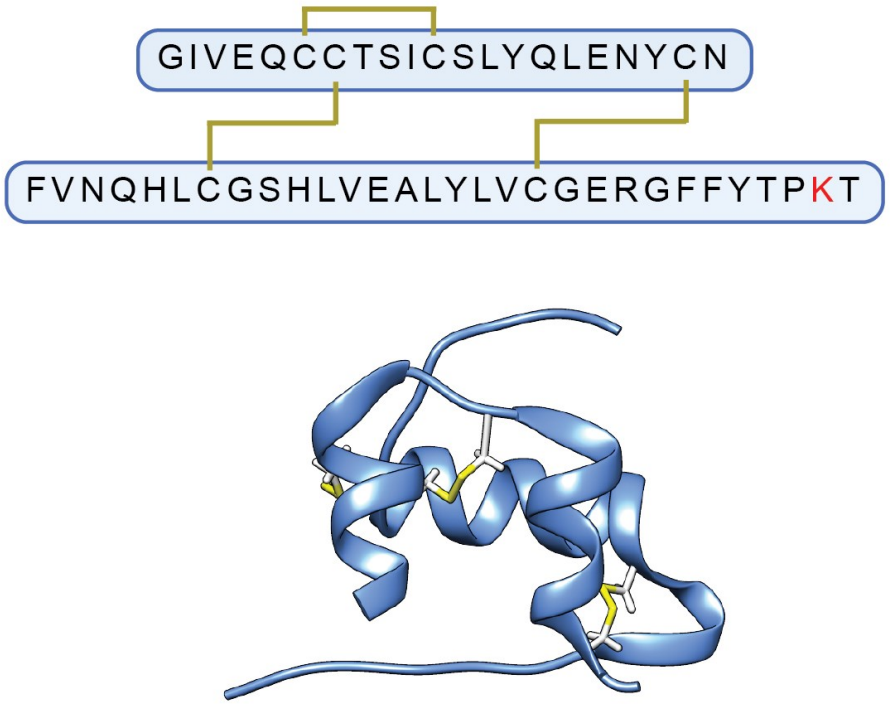

Figure 2 Primary and 3D structure of insulin. B29 lysine (red) shown in the sequence, is frequently modified to make designer insulins

Insulin was either chemically modified or genetically engineered to control its properties. These modifications altered insulin behavior including its rate of absorption and duration of action; this resulted in a variety of rapid/fast acting, intermediate acting and long acting insulins. The most common clinically available 'designer insulins' are discussed in Table 1.

Fast acting variants are engineered to modify their structure and prevent formation of hexamers/dimers[14]. Such associations between insulin molecules prevent rapid absorption into the blood. Neutral Protamine Hagedorn (NPH) insulin is neither chemically modified nor genetically engineered – but insulin is mixed with protamine to form insoluble complexes, thus lowering the rate at which the hormone

is absorbed into the blood[15]. Glargine is engineered to raise the isoelectric point close to the physiological pH, thus lowering its solubility and hence the rate of absorption from the site of injection[16]. Detemir is a fatty acid conjugate of insulin – this lowers the protein solubility and improves insulin binding to serum albumin and thus its half-life and duration of action[17]. Degludec consists of a hexadecanedioic acid conjugation which assists in the formation of insulin multi-hexamers at the site of injection[18]. These complexes slowly dissociate and have a long duration of action.

Table 1 Clinically available designer insulins

Type of insulin	Modification	Peak (hr)	Duration (hr)
Native		2 – 4	6 – 8
Fast-acting (modifications prevent hexamer/dimer formation)			
Lispro	B28P-29K reversed to B28K-29P	1 – 2	4 – 6
Aspart	B28P → B28D	1 – 2	4 – 6
Glulisine	B3N → B3K B29K → B29	1 – 2	4 – 6
Intermediate-acting			
NPH	Protamine complex	6 – 10	12+
Long acting			
Detemir	B29K – myristic acid conjugation	Flat, ~5	12 – 24
Glargine	A21N → A21G +B31R, +B32R	Flat, ~5	24
Degludec	B29K – hexadecanedioic acid conjugation	Flat	~42

Blood glucose dependent insulin delivery: importance

Human diet is not consistent. The amount of glucose varies from meal to meal. Moreover, the amount of food and the number of meals per day also depends on the habit of the individual. Thus, the increase in blood glucose due to consumption of each meal is non-uniform and unpredictable. This also means that the insulin should be delivered in the right amounts and time to bring blood glucose down to normal levels. In a healthy individual, this is achieved by the pancreas due to the inherent ability of β cells to sense glucose concentration – releasing insulin in a dose-dependent manner[19].

However, insulin administration to the diabetics is a challenge. Firstly, diabetics are required to monitor their blood glucose, and then deliver the right amount of insulin. Administration of excess insulin lowers the blood glucose below the optimum levels and will lead to hypoglycemia. Few cases of hypoglycemia and even deaths have been reported in diabetics due to errors in dosing. Such accidents may particularly occur during nights, while the patient is sleeping and not aware of the glucose levels. Therefore, it is extremely necessary to develop insulin delivery systems that can mimic the function of pancreas, i.e. deliver the right amount of insulin based on the patient's glucose levels, only at the right time.

Current (bolus) insulin delivery methods and challenges

Insulin is a protein hormone. So, its delivery is also associated with all the problems as with any other protein therapeutics. An oral insulin delivery is ideal and patient convenient. Many researchers failed in their attempts to develop an oral

insulin formulation as the protein will be digested by proteases in the gastrointestinal tract. Therefore, formulations such as injections and inhalations were developed and are now used to deliver a manually adjusted, single dose of insulin when required.

Subcutaneous injections

Subcutaneous insulin injection is the cheapest and the most popular method of administration in diabetics. Insulin solutions (regular and all fast/long acting insulin analogs) of known concentration are manufactured with additives and preservatives. These solutions are required to be stored at 2-8 C. After a meal, the patient is expected to measure the blood glucose with a glucometer. Depending on the blood sugar levels, right dose of insulin should be calculated and injected subcutaneously. Though this method of administration appears to be straight-forward, patients frequently face the following problems.

a. Manual calculation of dose and delivery of insulin with a syringe several times a day is a tedious process. Hypoglycemia can also be a problem if the dose is miscalculated by the patient. Insulin is not administered continuously throughout the day, and the dose is not varied automatically, i.e. this treatment does not mimic the action of pancreas. As a result, blood glucose is not maintained at optimum levels throughout the day. Long term complications (due to advanced glycation end products) of diabetes may still arise with this method of administration.
b. This process involves multiple pricks for glucose measurement and insulin delivery. The number of invasive steps varies from person to person. Based on an average diet of three meals a day, patients are required to prick six times a day

and thus, >2000 times a year. This is not a patient friendly approach since insulin should be administered for the rest of their lives.

c. Insulin structure and function is also dependent on temperature. Loss of activity is observed with the insulin solutions over time, especially in developing nations where refrigeration of the protein during transport and storage is not possible[20]. Insulin fibrillates at higher temperatures rendering the formulation inactive.

Inhalable insulin

Inhalable insulin is manufactured and supplied to the patients as dry powdered form and is required to be delivered via lungs with the help of an inhaler. It offers patients convenience with respect to delivery as it is a non-invasive approach. Additionally, it is observed that inhalable insulin is more rapid acting in comparison with a regular insulin delivered with a subcutaneous injection[21]. However, this formulation is not well accepted by the diabetics for several reasons[22].

a. Like injections inhalation cannot be automated, and thus the method does not mimic the action of pancreas. So, it is also difficult to maintain blood glucose at optimum levels with this method of administration. Therefore, long term complications of diabetes and the production of advanced glycation end products may be observed over time.

b. In order to make the protein inhalable, insulin is processed into a dry powder with very small particle size. Of the total amount of protein inhaled, only a fraction reaches the lower levels of lung's airways from where insulin is absorbed into the blood. Therefore, a large dose of insulin is required to be inhaled to achieve

therapeutic blood concentration. This also raises the costs of production and thus the price of insulin per dose.

c. Inhalation of dry powder causes irritation of the throat and ultimately results in cough. Furthermore, few patients using inhalable insulin contracted lung cancer. Though it was not concluded that cancer resulted from the inhalation of insulin, concerns were raised regarding this route of administration. Inhalable insulin should not be used if the patient is already suffering from pulmonary disorders such as COPD and asthma.
d. Unlike injections, the amount of insulin that can be inhaled is not easily adjustable. Therefore, unit doses of insulin (for instance 8 U, 10, U and 12 U) are supplied by the manufacturer – which should be consumed by the patient at once. This mode of delivery, in addition to the limited doses of inhalable insulin available does not give the patients flexibility to tightly control their blood glucose levels.
e. Finally, long acting inhalable insulins are not available and can be administered using injections only. Since some diabetics are treated with a combination of long and rapidly acting insulins, it is difficult to train the patients for both inhalation and injections.

Continuously variable insulin delivery – approaches and problems

As discussed earlier, pancreatic release of insulin is dependent on the concentration of glucose. This pattern of delivery, i.e. to monitor blood glucose and deliver insulin throughout the day in only the right amounts is called a continuously

variable delivery. This type of insulin delivery ensures that the blood glucose is maintained at optimum levels on every day of the year.

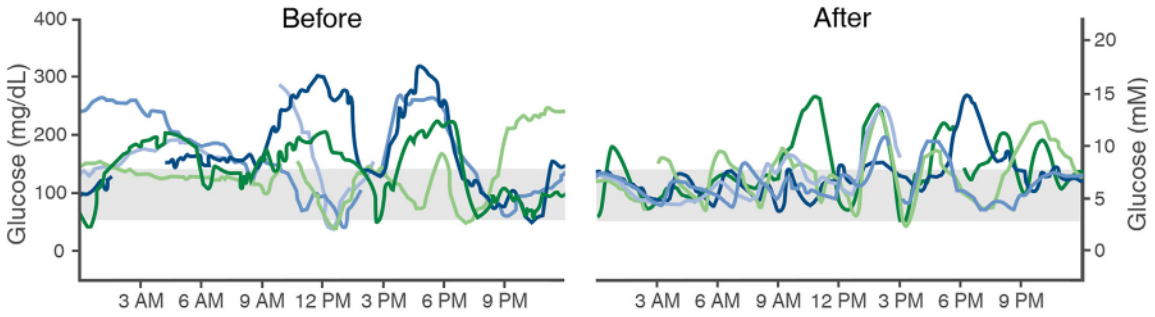

Figure 3 Comparison of 24-hour glucose profiles (left "Before" plot = bolus delivery, right "After" plot = continuously variable delivery). Image adapted[23]. Each line represents data from a single patient

Bolus insulin delivery lowers blood glucose in a predictable fashion. However, the glucose levels in blood varies drastically in these patients throughout the day, when observed using a continuous glucose monitor. But, a finer control of blood glucose was possible and thus maintained in optimum levels with a continuously variable insulin delivery as shown in Figure 3.

Such delivery was developed by automating the delivery device and integrating this system with a continuous glucose monitor (CGM). Therefore, the CGM measures blood glucose and digitally informs the delivery device to deliver the right amount of insulin. Such automated devices are also called artificial pancreas. Since blood glucose is maintained at normal levels efficiently, it is observed that the formation of AGEs (measured as HbA1c) is reduced when insulin is delivered in this fashion[24].

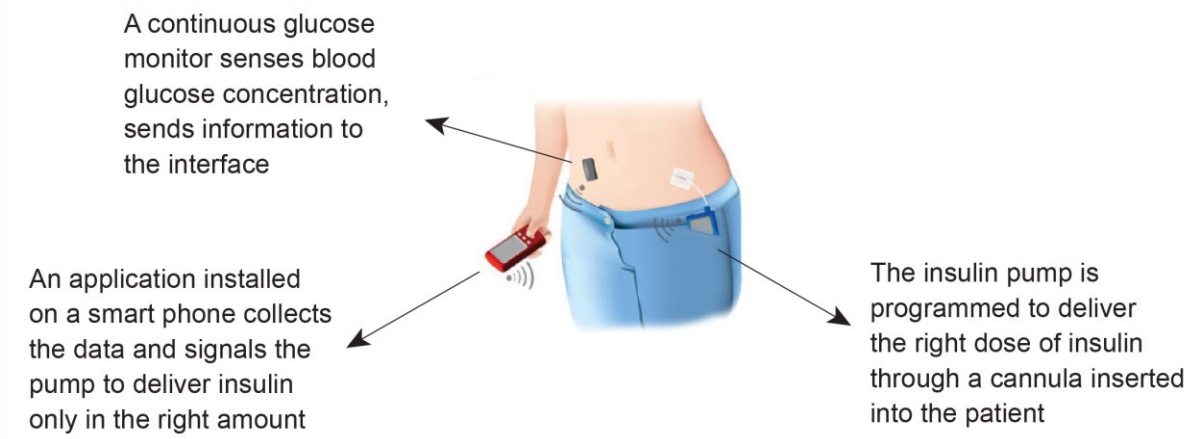

Figure 4 The artificial pancreas system consisting of insulin pump, an interface and a continuous glucose monitor.

The only device that can deliver insulin in a continuously variable fashion and can be automated is a pump. These are mechanical devices that contain a reservoir of insulin and pump the peptide solution into the patient through a constantly connected cannula (Figure 4). Insulin pumps and CGM usually communicate through an interface installed on the user's cell phone. The software also records data and efforts are being made to share this data directly with the patient's doctor to provide better health care.

Though pumps offer an almost ideal solution to the insulin delivery problem, it still is associated with issues. Most of these issues are associated with the design of the pumps; specifically, with the pumps requirement of a cannula to deliver the hormone[25–29]. This constant insertion of a needle-like cannula into the patient's skin results in biofouling. Biofouling is the deposition of biomolecules and microorganisms on the cannula. This leads to two issues – a) infections at the site of insertion, and b) clogging of the needle. Clogged cannulas do not deliver the protein

solution in a desirable fashion, resulting in variabilities in the amount of drug delivered. Many T1D patients are relatively young who have an active lifestyle with continuous physical movements. Therefore, it is possible that the delivery may be interrupted due to crimping or snagging of the cannula. Among the additional problems that have been frequently reported with the use of pumps is that the patients observe scarring of tissue around the site of insertion. Due to all the problems discussed above, site of insertion of cannula needs to be varied time to time. This again creates variation in the therapeutic response as insulin is absorbed at different rates from different regions of the body. Therefore, there is a need to develop better continuously variable delivery systems to provide a better health care to the diabetics.

The Photoactivated Insulin Depot

The idea

The Photo-Activated Depot (PAD) is developed as a new approach for a continuously variable insulin delivery. In this approach, insulin is injected under the skin as a depot that has a dose enough for days or weeks. Insulin release in therapeutic amounts from the depot into the blood can be controlled with the help of a light source of specific wavelength. The light source will be placed above the skin, over the site of injection as light easily penetrates through the upper layers of skin. This is beneficial and potentially makes the system superior to pumps because the insulin delivery is a non-invasive approach, i.e. does not require a physical connection (like cannula of pumps) to deliver insulin. But since a depot of insulin needs to be injected under the skin, the overall approach is therefore minimally invasive (Figure 5).

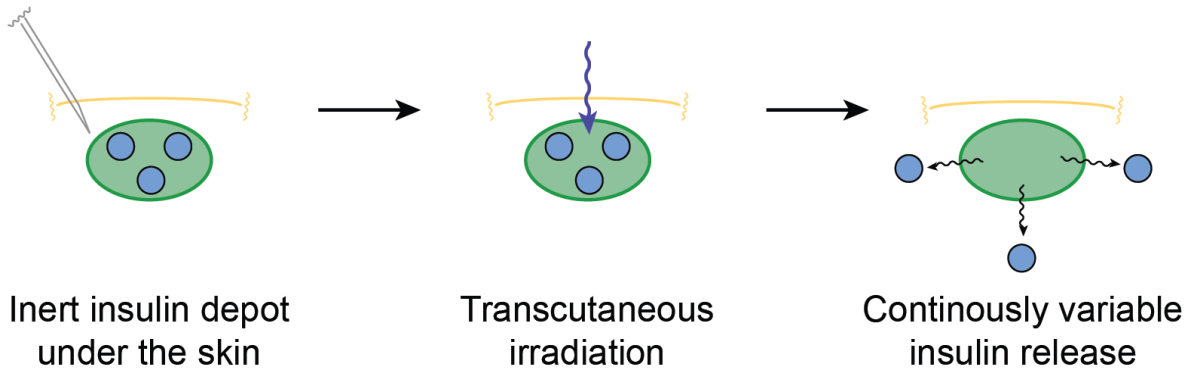

Figure 5 Photoactivated insulin depot - the idea

Advantages of PAD over pumps

Firstly, PAD is potentially superior to pumps as it will not have any issues associated with a physical connection. All the issues discussed earlier including biofouling, infections, crimping, snagging, etc., are eliminated with this design. Secondly, the release of insulin is finely controlled with light, i.e. releasing the right amount of insulin at right times. Insulin will be chemically engineered to react to light (photons); more light releases more insulin. This process can be easily controlled by manipulating the duration of irradiation. Thirdly, PAD can be easily automated; the light source can be easily turned on or off in response to a read out from a CGM. Therefore, the PAD captures the advantages of pumps by delivering insulin in a continuously variable fashion, while eliminating the problems associated with the physical connection of pumps.

First-generation PAD

A first-generation material was designed by chemically linking insulin to an insoluble polymer via a photocleavable group[30]. The polymer conferred insolubility

and allows creation of the depot when injected under the skin. Rink amide resin made of polyethylene glycol was used for this purpose. This polymer was used to carry out any tests in animal models too since polyethylene glycol is biocompatible. The DMNPE (dimethoxy nitro phenyl ethyl) was chosen as the photocleavable group in this material. A modified DMNPE was synthesized with an azido group and the insulin ester was made. This insulin-DMNPE-azide conjugate was then chemically linked on to the Rink amide resin using click chemistry. Chemical structure of the material is shown in the Figure 6. When this material was suspended in PBS and exposed to light of 365 nm wavelength, the DMNPE ester of insulin was photo-cleaved to release native insulin into the buffer. Rate of insulin release was determined, and the process was observed to occur in a predictable first order fashion.

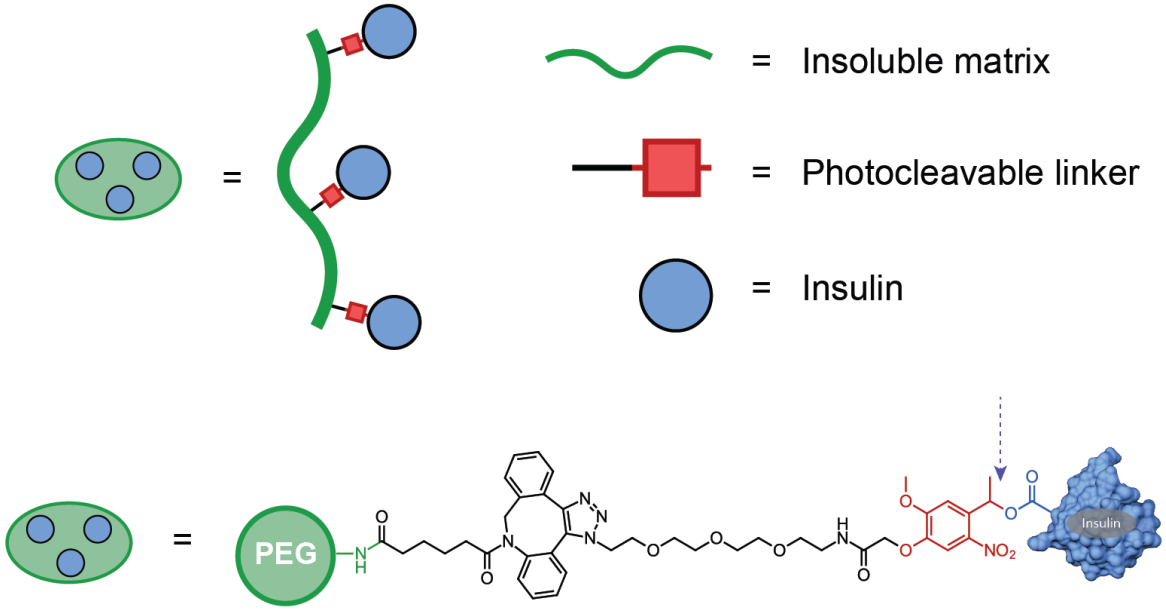

Figure 6 The first-generation PAD design and structure. The photolabile bond of the DMNPE photocleavable group is shown with an arrow

In addition to the *in vitro* experiments, the first-generation PAD was also tested in diabetic rats[31]. It was observed that therapeutic amounts of insulin were delivered into the rat's blood with a light stimulus, and a corresponding reduction in blood glucose levels was seen. These were the first experiments that indicated that the PAD can be potentially developed into an efficient continuously variable insulin delivery system.

Issues with the first-generation PAD

Though the PAD tests gave positive results in diabetic rats therapeutically, few issues were faced while pursuing these experiments. All these problems are due to the use of the insoluble polymer in the material. The PEG based Rink amide polymer is fairly bulky compared to the size/weight of the insulin protein itself. In the first-generation PAD, many insulin molecules were clicked on to the surface of the polymer. The overall insulin density was observed to be only 10% w/w of the material. This means that the polymer occupied 90% of the weight. Following issues were faced while pursuing animal experiments, majorly due to the size and density of the polymer:

1) A lower gauge, i.e. larger diameter needle had to be used to inject the material into the skin. This is because the polymer does not pass through a 31G needle, which is usually used to inject insulin subcutaneously by the patients.
2) As discussed above, the overall density of the therapeutic moiety is less. This also means that the density of photocleavable groups is lower. This problem actually discusses two issues, (a) that the depot will not last long and has to be

reloaded from time to time and (b) that it will be difficult for light to trigger insulin release as the overall photocleavable group density is lower – thus increasing the duration of irradiation.

3) After insulin photo-release, the polymer is not removed from the site of injection. Polyethylene glycol is not biodegradable and this retention of the polymer over a period may result in unforeseen reactions at the site of injection.

Preliminary studies on the first-generation PAD showed that insulin delivery from an intradermal depot can be controlled with the help of transcutaneous light. It also showed that the depot can release a second dose of insulin with a second irradiation. Photo-released insulin was observed to be functional and lowered the blood glucose to normal levels. While these studies demonstrated the therapeutic abilities of PAD, there is still a need for the design of new materials. Since all the issues arose due to the use of polymer, it will be ideal to design next generation PAD without the use of such polymeric materials.

CHAPTER 2

THE TAG APPROACH

Design of the new generation PAD

The polymer used for the construction of the first-generation PAD makes about 90% of the material by weight. In addition, the polymer does not have any role in the therapy and can't be eliminated from the site of injection by the animal. Furthermore, injecting bulky materials is not feasible as a larger diameter needle can't be used. Therefore, the new generation PAD materials are expected to have:

1) High insulin density: By lowering the amount of polymer (or support materials) used, the density of the therapeutic moiety can be increased. This also means that the same amount of material by weight can theoretically last for much longer time when injected as a depot. Lowering the weight percentage of support also increases the density of photocleavable groups. This ensures that the same amount of insulin will be photo-released with a much lesser duration of irradiation.
2) Ease of injection: Avoiding the use of polymer to make new generation PAD materials will make the process of injecting easier. Attempts to improve the density of insulin which can easily pass through a 31G needle will also improve the passage of the new generation PAD as the support material will be as low as possible by weight.
3) Elimination after photolysis: Using alternative support materials to create insulin depots will also allow design of new materials that are not retained at

the site of injection, after insulin photo-release. The tag should be biodegradable or highly soluble when it is not conjugated with the protein. Therefore, the new PAD materials are expected to deliver insulin when stimulated with light without leaving any traces at the site of injection.

In this study, attempts will be made to improve the insulin density from 10% to as high as 90%. This implies that the moiety replacing the polymer should only be about 10% by weight of the overall PAD material. Insulin has a molecular weight of 5808 Da. Therefore, the new support material should have a molecular weight of about 600 Da and hence it should be a small molecule. During this study, 'tag' will be used to define a small molecule of approximately 600 Da weight which is conjugated with insulin to modulate the hormone's physicochemical properties.

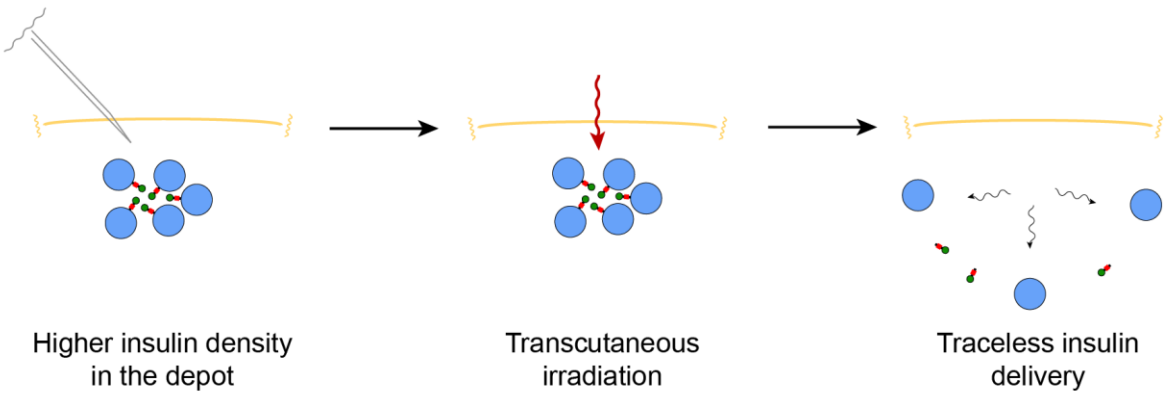

Figure 7 The tag approach showing high insulin density and the idea of traceless delivery

For the PAD approach, tags will be used to lower the protein solubility. This is to allow the creation of depots such that injected hormone stays the site of injection. If the protein is highly soluble, the depot will be easily absorbed into the blood stream

resulting in two unwanted situations - (a) less longevity of the depot, and (b) hypoglycemia of the patient (as large amount of insulin is injected in the form of a depot). Therefore, it is recommended that the insulin tag conjugate is very insoluble at physiological conditions. However, native soluble insulin and the tag should be uncaged and absorbed into the blood upon irradiation (Figure 7).

Factors affecting protein solubility

Physiological conditions in this study will be considered as the water at pH 7.2. The pH of the skin is observed to be buffered at pH 7.2[32]. Therefore, the objective of this study is to lower the solubility of the insulin-tag conjugate at these conditions. Solubility of any type of biomolecule including proteins or nucleic acids under physiological conditions are defined by its interactions with the solvent, i.e. water. A protein with a greater number of polar or charged functional groups will have higher solubility in water. On the other hand, a protein with a greater number of non-polar or uncharged functional groups will have a lower solubility in water. Therefore, protein solubility depends majorly on two factors viz., hydrophobicity and net charge. In this study, insulin solubility will be lowered by conjugating it with different types of photocleavable tags that either increase the hydrophobicity or reduce the net charge at pH 7.2. Since the modification with tag can be removed with light, i.e. these modifications are temporary, the ultimate protein species that is absorbed into the biological system is the native soluble insulin.

Synthesis of photocleavable tags

The common moiety in the construction of any next generation PAD material is the photocleavable group called DMNPE (dimethoxy nitro phenyl ethyl). The DMNPE group itself does not have any functional groups to modify insulin properties. Therefore, DMNPE is modified with a carboxylic acid as discussed previously to provide a handle to link any tags of interest[33]. This is a two-step reaction: (a) alkylation of acetovanillone with tert-butylbromoacetate and (b) followed by the nitration of the product in step (a). Therefore, the first step in the strategy is to condense any small molecule amine with the DMNPE-acid. Then, the ketone is further functionalized for ultimately esterifying insulin on any one of its 6 carboxylates (Figure 8)

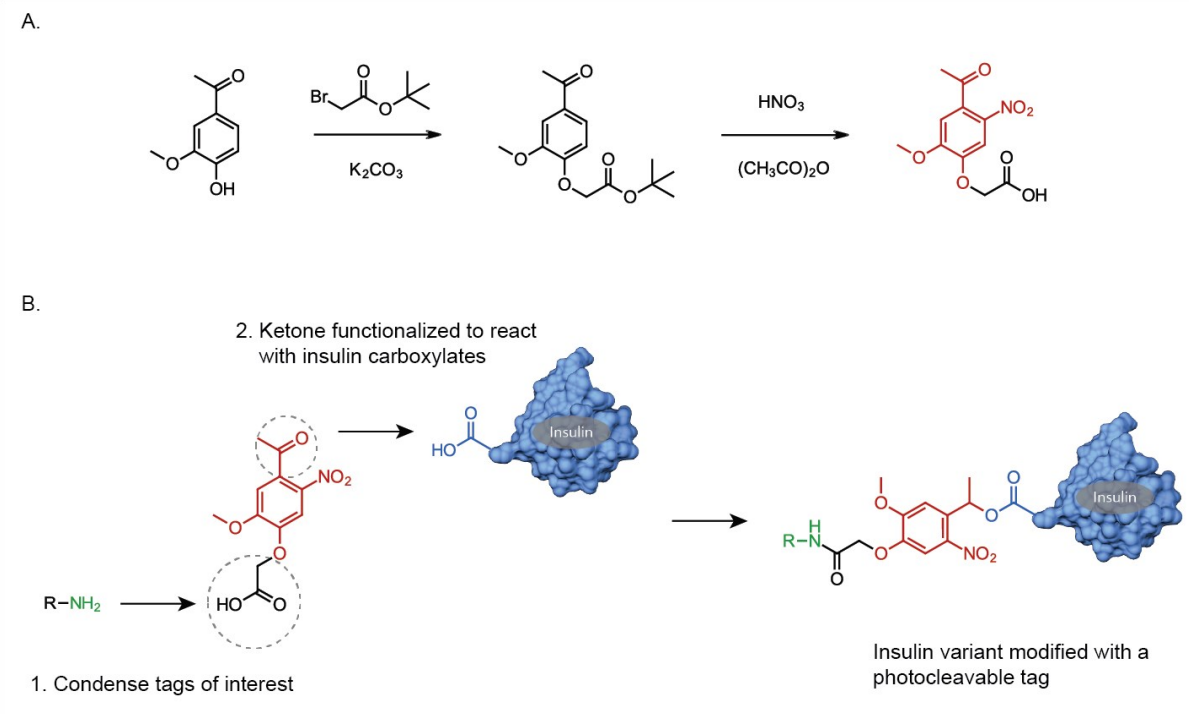

Figure 8 A. DMNPE-acid synthesis, and B. Synthetic strategy

Procedures are discussed below.

Synthesis of tert-butyl (4-acetyl-2-methoxyphenoxy) acetate

63.2 mmol (10.5 g) acetovanillone and 69.2 mmol (13.5 g) tert-butylbromoacetate was dissolved in 75 mL DMF in a 1:1.1 ratio respectively. To this solution, 104 mmol (14.4 g) potassium carbonate was added and stirred at room temperature. Alkylation will be complete by the end of 48 hours. Minimum amount of water was added to the reaction to dissolve the salts. Product was isolated from the reaction by partitioning the mixture between ethyl acetate and water. Pooled ethyl acetate was washed once with saturated sodium chloride to remove any traces of water. The organic layer was then dried in vacuum to obtain the pure product. HPLC and LCMS confirmed the purity of the product (Figure 9). Yield was observed to be 87%.

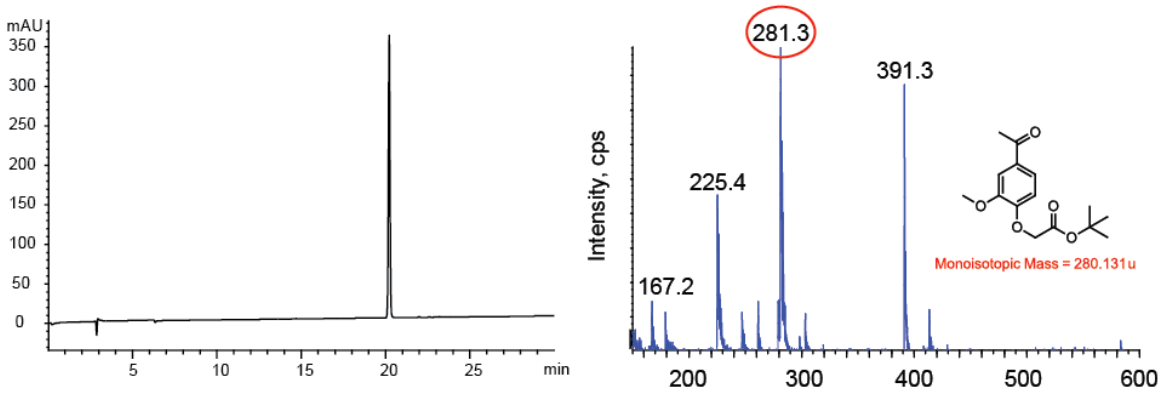

Figure 9 HPLC (280 nm) and MS of tert-butyl (4-acetyl-2-methoxyphenoxy) acetate

Synthesis of (4-acetyl-2-methoxy-5-nitrophenoxy) acetic acid

Nitration mixture was prepared by mixing dropwise 14 mL of acetic anhydride with 20 mL of 70% nitric acid at 0 C in a jacketed beaker. A solution of tert-butyl (4-

acetyl-2-methoxyphenoxy) acetate in acetic anhydride (18 mmol, 5 g in 15 mL prepared at room temperature) was added dropwise to the cooled nitration mixture with stirring. Reaction was stirred for 2 hours at 0 C after the complete addition of solution to nitration mixture. Stirring was continued for an additional 4 hours at room temperature. Reaction mixture was then poured onto crushed ice made with about 75 mL water and allowed to stand at 4 C overnight. The product was obtained as the residue left on the filter after filtration through a glass fritted funnel. It was extensively washed with cold, deionized water. Purity and structure of the product was confirmed using HPLC and MS (Figure 10). Yield of product after purification was observed to be 55%.

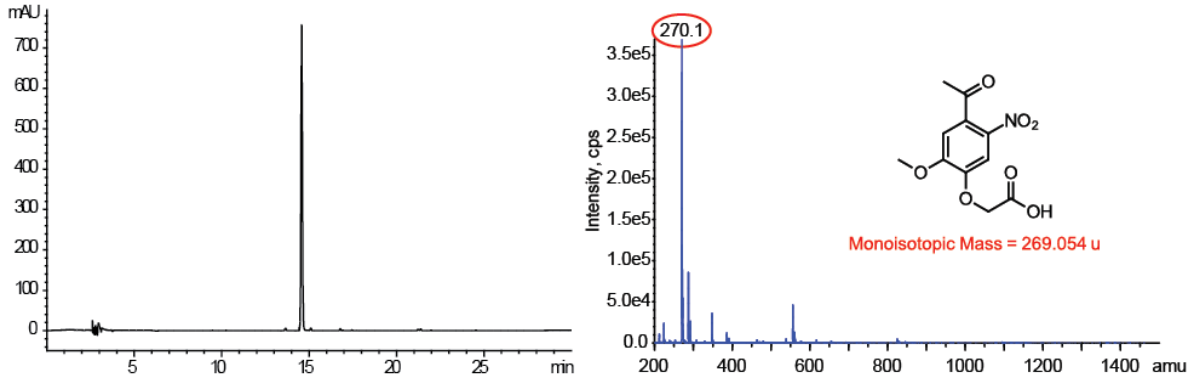

Figure 10 Analysis of DMNPE-acid on HPLC (345 nm, left) and MS (right)

Condensation of tags

In the following chapters, a variety of tags with different properties will be condensed with the carboxylic acid of the photocleavable group. The intention behind the exploring of a variety of tags is to screen for an ideal tag to lower the solubility of the modified insulin by an extent enough to create photoactivated depots at the site

of injection. Design, synthesis and outcomes with the use of both non-polar and charged tags will be explored in the next chapters.

CHAPTER 3

THE HYDROPHOBIC TAGS

The rationale

The goal of this study is to lower insulin solubility by conjugating non-polar photocleavable groups to the protein. Non-polar moieties do not interact well with water and tend to associate with themselves. Moreover, these non-polar – non-polar interactions are relatively stronger in an aqueous environment. This is because interaction of non-polar surfaces with themselves excludes the water interacting with them. This allows water to interact with itself rather than the hydrophobic surfaces, which is favored over the interaction of water with non-polar surfaces. Thus, conjugating non-polar photocleavable groups with insulin will not allow the PAD to interact well with the aqueous physiological fluids at site of injection. On injection, the materials are predicted to precipitate out as a depot.

In this study, four different unnatural and natural (peptide) non-polar photocleavable tags are designed and conjugated with insulin. Unnatural groups have the advantage of being highly insoluble in water. Independently, such molecules may even phase out as they do not interact with water at all and lower the solubility of protein significantly. On the other hand, natural groups such as non-polar peptides can also lower the protein solubility. A variety of peptidic tags can be explored as the sequence can be easily modulated to obtain a protein conjugate with desired properties. Peptides also have the advantage of being biodegradable. The methods discussed in this chapter have been published[34,35].

Cyclododecyl-insulin

Cyclododecyl-insulin (CD-insulin) is a variant designed with an unnatural photocleavable tag. Cyclododecyl group is a compact hydrocarbon which is immiscible in water. Cyclododecyl amine is used in order to condense this hydrocarbon with the DMNPE-acid. Then the CD-DMNPE, i.e. the ketone will be converted into the hydrazone. The hydrazone is oxidized into the diazonium species, which will react specifically with the carboxylic acids on insulin. The obtained product is an insulin ester of CD-DMNPE, or the CD-insulin. Synthetic scheme is shown in the Figure 11.

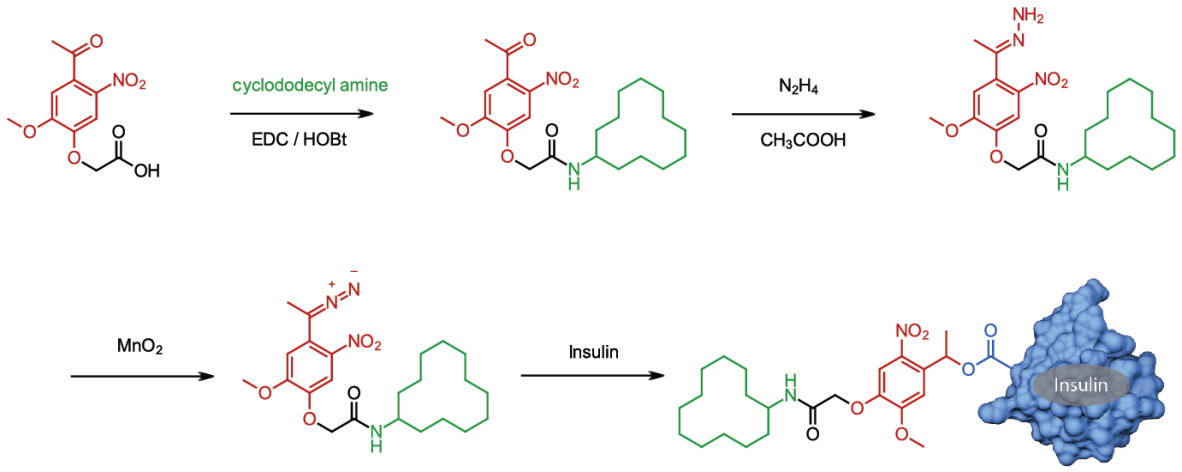

Figure 11 Cyclododecyl-insulin synthesis

All the intermediates in the synthesis of CD-insulin including the CD-DMNPE, CD-hydrazone and the CD-diazo were synthesized and characterized previously[36]. The ultimate reaction of the CD-diazo with CD-insulin is discussed below.

Synthesis of CD-insulin

Freshly prepared CD-diazonium (5.37 µmol) solution in DMSO was directly added to 800 µL dry DMSO solution of insulin (5.37 µmol, 31.2 mg). Additional dry DMSO was added to the mixture to dilute the reaction to a final concentration of 2 mM insulin. Reaction was protected from light for 24 hours. Yield of this reaction is calculated based on the integration of peaks from a chromatogram of the reaction. It was observed to be about 40% for the monoadduct.

Mole ratio of the diazonium:insulin is a critical parameter to be adjusted during this reaction. Excess diazonium may esterify multiple carboxylates on insulin and produce a 'multi-adduct'. The goal in the tag approach is to modulate the properties of the protein with a single tag. Also, having multiple tags on the protein will slow down the insulin photo-release. This is because insulin will not be soluble enough until all the tags are removed. Therefore, it is desirable to have a single tag as a single photolysis event will determine the rate of insulin release.

The reaction can be analyzed using multiple techniques. Firstly, analysis using UV-visible spectroscopy is discussed here. Since insulin is a protein and has tyrosine residues, it has an λ_{max} at 276 nm as shown in Figure 12. Nitrobenzyl groups with their extended conjugations and due to electron donating groups have λ_{max} at 345 nm. When the DNMPE tag reacts with insulin, the UV spectrum of such a monoadduct will be a summation of the spectra of insulin and DMNPE. Insulin has an extinction coefficient of 5128 M^{-1} cm^{-1} at 280 nm. DMNPE has an extinction coefficient of 3272 M^{-1} cm^{-1}.[30] Therefore, insulin monoadduct will have an extinction coefficient of 5128

+ 3272 M^{-1} cm^{-1} = 8400 M^{-1} cm^{-1}. Since insulin does not absorb light at 345 nm, the monoadduct extinction coefficient at this wavelength is same as that of the DMNPE, i.e. 4470 M^{-1} cm^{-1}. The ratio of extinction coefficients at 280 nm and 345 nm for insulin monoadduct is 8400:4470 = 1.9:1. For the diadduct, the ratio of extinction coefficients will be 11672:8940 = 1.3:1.

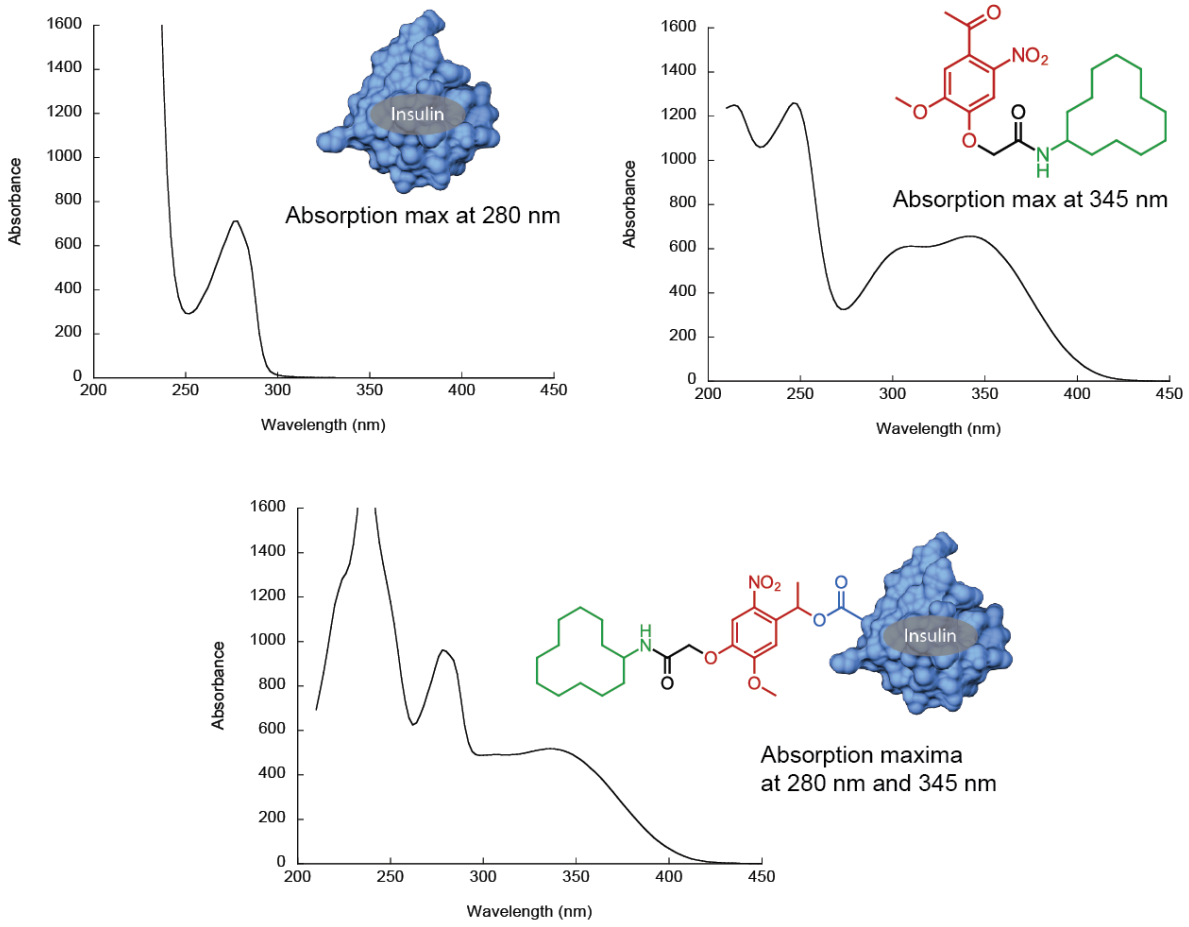

Figure 12 UV absorption spectra of insulin, DMNPE and the protein conjugate

These absorption patterns can also be seen clearly when the reaction is run on a reversed phase column and detected using a diode array detector at 280 nm and 345 nm. Firstly, insulin monoadduct interacts with the C18 silica well due to the addition

of non-polar cyclododecyl group and elutes later than the unreacted insulin. Diadduct is expected to interact better than the monoadduct and thus can be seen eluting after the monoadduct. Finally, the mass spectrometer confirms the mass of these species when these peaks are collected individually for analysis (Figure 13).

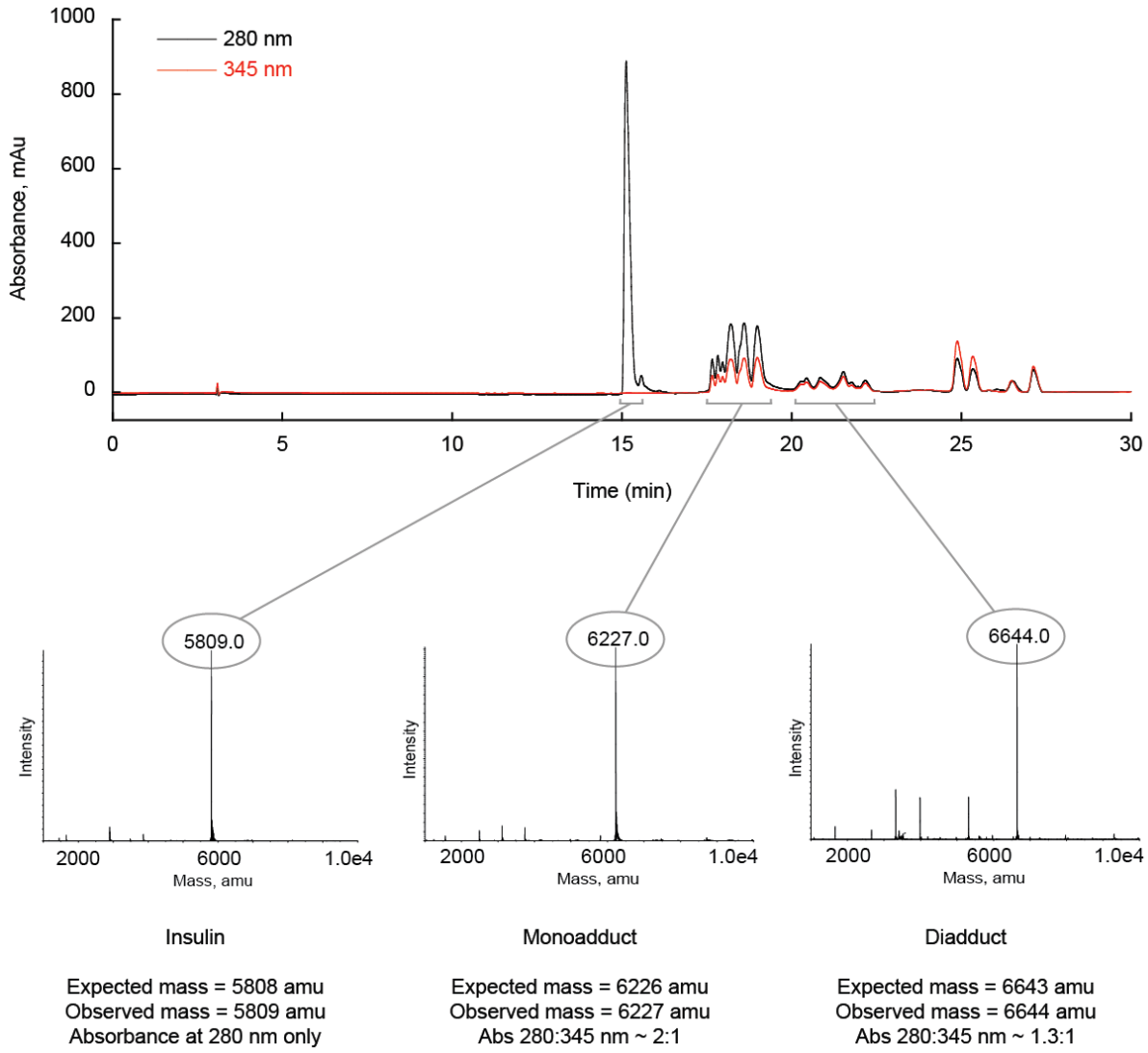

Figure 13 CD-insulin HPLC and MS analysis

CD-insulin was purified by injecting the reaction mixture on a 250 X 21.2 mm 10 µm C18 column. Fraction was collected from 19.25-22.50 minutes when run on 25-

100% acetonitrile gradient over 40 minutes, at 8 ml/min. Mobile phases contained 0.1% trifluoroacetic acid (Figure 14).

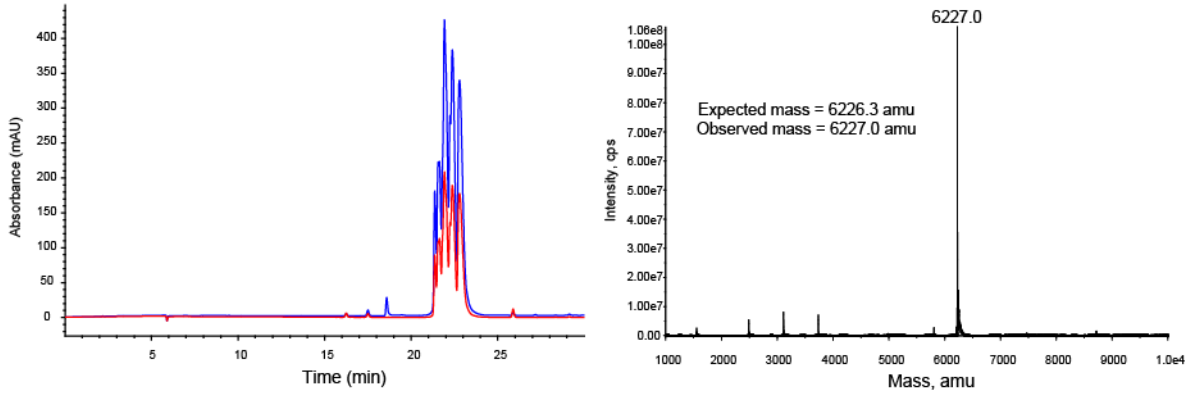

Figure 14 Pure CD-insulin, HPLC (blue = 280 nm, red = 345 nm; left) and MS (right)

Peptidic non-polar tags

Long chain fatty acids and similar molecules have already been conjugated with insulin. The number of such unnatural non-polar molecules available for protein conjugation is limited. Moreover, not all unnatural non-polar molecules are can be easily eliminated from the body. Some compounds may have adverse reactions and result in local or systemic toxicities. Therefore, peptidic tags are also explored in this study. Since peptides are natural, they are easily tolerated and biodegradable. Most importantly, peptides offer variability in the types of conjugations. By varying the sequence of the peptide, a variety of tags may be created to modulate the properties of the protein as desired. This study requires that the solubility of the insulin-tag conjugate to be as low as possible to allow the formation of depots at the site of injection. Hence, a family of non-polar tags were designed and conjugated with insulin.

In this study, the size of tag is limited to three amino acids. Since amino acids have an average molecular weight of 110 g/mol, a tag consisting of three amino acids and DMNPE should have a molecular weight of about 600 Da. Such tripeptidic tags should maintain insulin density at about 90% w/w. It should also be noted if when these amino acids are incorporated genetically on the backbone of the peptide, the solubility may not be as lowered as with chemical conjugation. Genetic incorporation may direct the protein to fold in a way to minimize interactions between non-polar amino acids and the solvent. Whereas chemical conjugation 'grafts' the peptide on polar side chains, which are exposed to the solvent. This approach ensures that the protein solubility is lowered due to hydrophobic effect. The rationale for the design of each tag and the methods for synthesis are discussed below.

Ile-Ile-Ile-insulin

The rational for the selection of isoleucine for the design of tripeptidic tag than any other amino acid is the hydrophobicity of the side chain. Isoleucine is the least soluble amino acid at any pH, excluding amino acids with aromatic side chains. Aromatic residues may change the UV-absorbance and hence the extinction coefficient of the protein conjugate or the tag and hence make quantitation difficult. Moreover, a similar amount of reduction in solubility can be brought with amino acids containing both aromatic and non-aromatic hydrophobic side chains. Therefore, it is atom-efficient to use non-aromatic amino acids to maintain a higher density of insulin in the material.

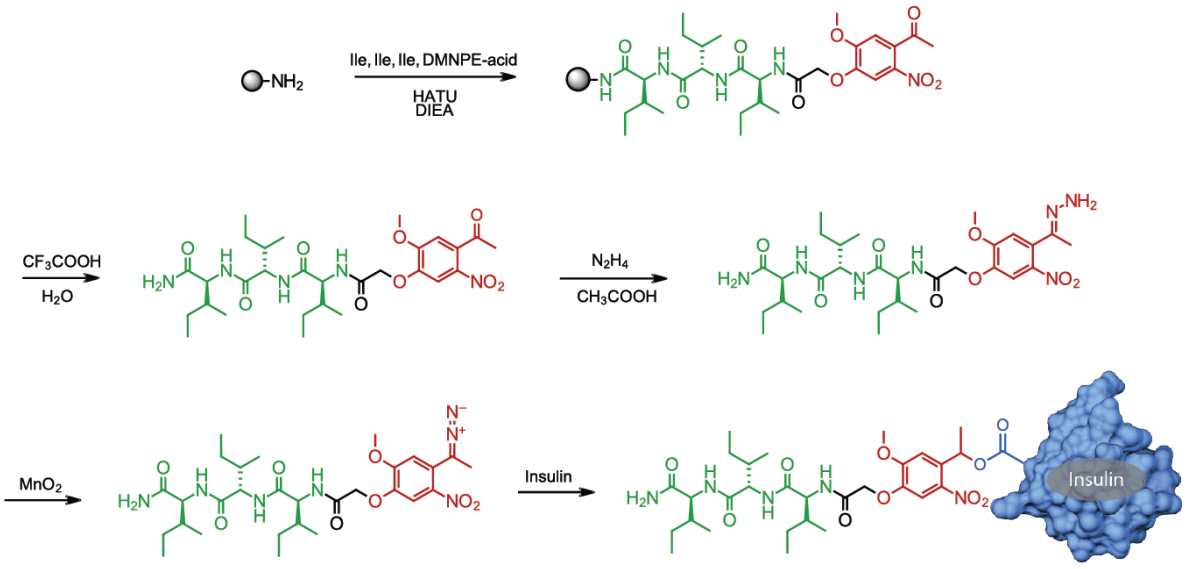

Figure 15 Synthesis of Ile-Ile-Ile-insulin

Synthesis of Ile-Ile-Ile-insulin is shown in the Figure 15. Solid phase synthesis on a Rink amide resin will be employed to construct the peptide. Subsequently, the photocleavable group DMNPE-acid will be condensed on the solid phase. This peptidic ketone will then be cleaved off the resin. Purified ketone will be converted into hydrazone in solution, then oxidized to diazonium and ultimately reacted with insulin.

A peptide with C-terminal amide is beneficial in this study as it will be neutral during the successive reactions. For instance, if a peptide with C-terminal carboxylate is synthesized on a Wang resin, the diazonium in the ultimate step may react with the carboxylic acid of the tag instead of the carboxylates on insulin.

Synthesis of Ile-Ile-Ile-DMNPE

(2S,3S)-2-[(2S,3S)-2-{(2S,3S)-2-[2-(4-Acetyl-2-methoxy-5-nitrophenoxy)acetylamino]-3-methylvalerylamino}-3-methylvalerylamino]-3-methylvaleramide

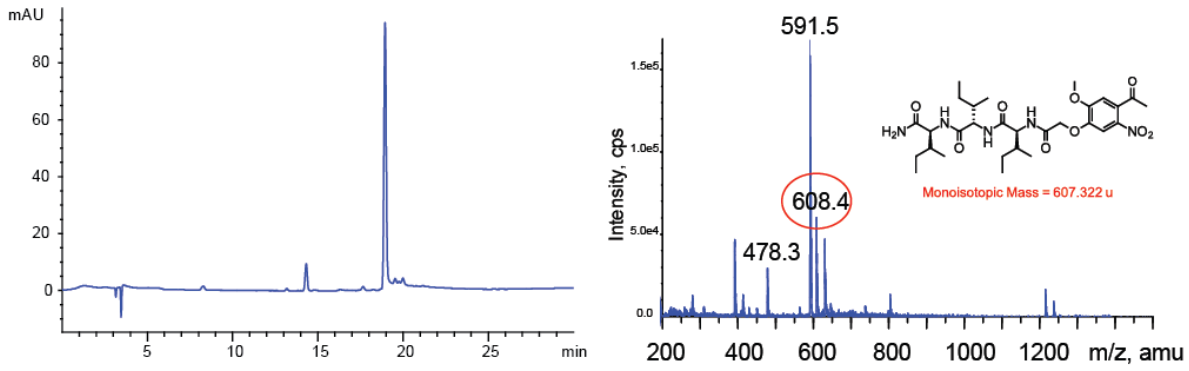

Figure 16 Ile-Ile-Ile-DNMPE HPLC (345 nm, left) and MS (right)

Ile-Ile-Ile-DMNPE was synthesized using Fmoc-solid phase peptide synthesis. 0.5 g (235 µmol) of Chemmatrix Rink amide resin (PEG) was suspended in NMP at a concentration of 60 mM. 10% piperidine, 2% DBU solution was used to deprotect amines. Coupling was carried out with 300 mM Fmoc-isoleucine/DMNPE-acid, 300 mM HATU and 600 mM DIEA. Unreacted amines were capped with 10% acetic anhydride, 5% DIEA solution in NMP, before Fmoc-deprotection in each cycle. After the synthesis was completed, resin was extensively washed with dichloromethane and dried. Ile-Ile-Ile-DMNPE was then cleaved off the resin with 95% TFA, 5% water solution for 1 hour. TFA was evaporated and the dried peptide crude was purified on preparative HPLC (Yield = 79%). Analysis of the pure product was performed using HPLC and mass spectrometry (Figure 16).

Synthesis of Ile-Ile-Ile-hydrazone

(2S,3S)-2-[(2S,3S)-2-{(2S,3S)-2-[2-(4-Acetohydrazonoyl-2-methoxy-5-nitrophenoxy)acetylamino]-3-methylvalerylamino}-3-methylvalerylamino]-3-methylvaleramide

The conversion of ketone to the hydrazone was attempted in solution under similar conditions used for CD-hydrazone synthesis. Ile-Ile-Ile-DMNPE was suspended in 50% acetonitrile 50% ethanol for dissolution. However, the ketone was observed to be insoluble in this solvent mixture. Proteins and peptides are generally insoluble in non-polar solvents including ethyl acetate, dichloromethane and hexane. Protic solvents such as methanol and ethanol assist in proton transfers during the reaction. A variety of mixtures of different non-polar/polar aprotic (like acetonitrile) and protic solvents were also prepared to attempt dissolution; however, the peptide was still insoluble.

Acids can promote dissolution of the peptide by protonating the amide function and providing charge. Stronger acids such as TFA and hydrochloric acid dissolve the peptide for sure, as the peptide is known to elute on a C18 column in TFA containing solvents. However, stronger acids will convert the hydrazone back into ketone as it is a reversible carbonyl addition. Therefore, a weak acid such as acetic acid can only be used in this reaction for both dissolution and catalysis. Acetic acid failed to protonate and promote dissolution of Ile-Ile-Ile-DMNPE as the pKa of amide (-0.5) is much below the acidity of acetic acid (~4).

Hypothesis: why is Ile-Ile-Ile-DMNPE insoluble?

Dissolution of any species is either driven by the interactions of the solvent with the solute. The stronger these interactions, higher is the solubility of the solute. In addition, interactions of solute with solute themselves also plays a key role in this process. If the solute-solute interactions are stronger than the solvent-solute

interactions, then the solute remains insoluble and cannot go into the solution. In the case of Ile-Ile-Ile-DMNPE, it can be hypothesized that the interactions between the peptide molecules are extremely strong. This may be due to the ability of linear peptides to stack up on one another with strong intermolecular hydrogen bonds. In the amide bond, the nitrogen has a partial positive charge and the oxygen, a partial negative charge. Therefore, a hydrogen bond can be easily formed when two amide bonds are stacked over one another, specifically between the nitrogen and the oxygen by the acidic proton. Many hydrogen bonds, in addition to the hydrophobic effect of the interacting side chains, can make the Ile-Ile-Ile-DMNPE very insoluble as the water-peptide interactions are way weaker than these interactions.

Val-Pro-Ile-insulin

Val-Pro-Ile tripeptide is chosen as a tag to overcome the dissolution problem as in the case of linear peptides. Proline is the only amino acid that consists of a secondary amine as the side chain makes an intramolecular 5 membered cyclic ring with the nitrogen. This conformationally restricts the amine at a direction away from the carboxylic acid. Consequently, a kink is introduced the peptide wherever proline is located. The goal of designing sequence is to introduce a kink in the peptide such that it prevents the intermolecular hydrogen bonds between the peptides. Since the side chain of proline does not any polar functional groups, it is expected to lower the solubility of insulin significantly after conjugation. Synthesis is shown in the Figure 17.

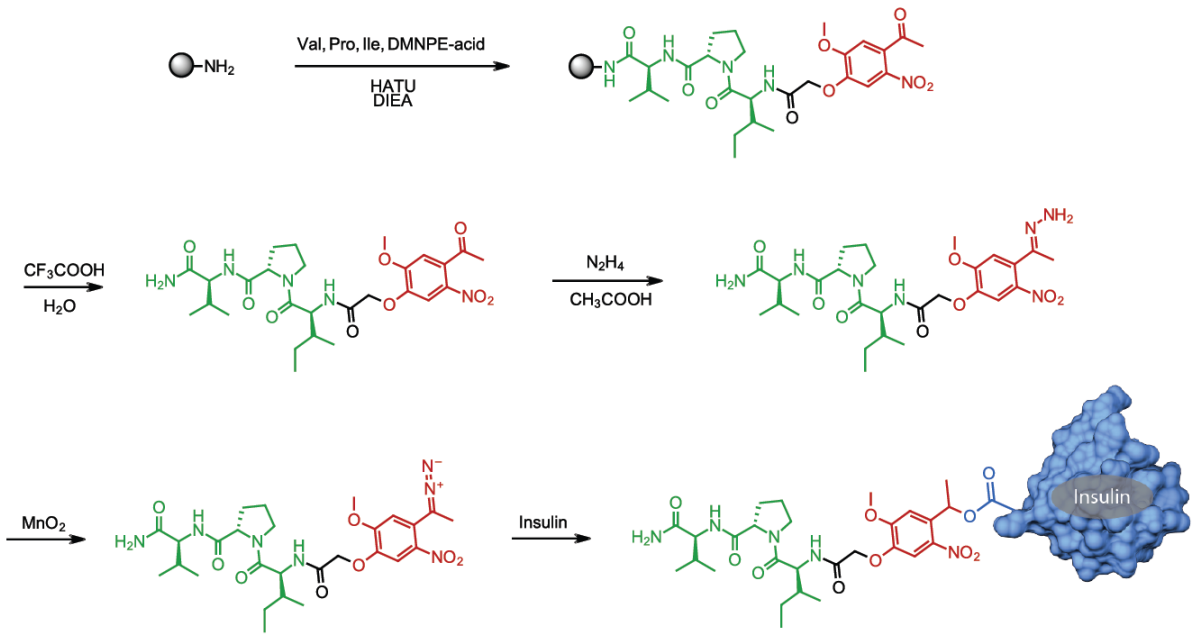

Figure 17 Val-Pro-Ile-insulin synthesis

Synthesis of Val-Pro-Ile-DMNPE

(S)-2-{[(S)-1-{(2S,3S)-2-[2-(4-Acetyl-2-methoxy-5-nitrophenoxy)acetylamino]-3-methylvaleryl}-2-pyrrolidinyl]carbonylamino}-3-methylbutyramide

Val-Pro-Ile-DMNPE was synthesized using Fmoc solid phase peptide synthesis. Briefly, 0.65 g (0.306 mmol) Chemmatrix Rink amide resin that has 0.47 mmol/g loading capacity was suspended in NMP at a concentration of 60 mM. Fmoc deprotection was carried out with 10% piperidine, 2% DBU in NMP. Carboxylic acids were coupled to free amine on solid phase with 300 mM Fmoc-amino acid (or DMNPE-acid), 300 mM HATU and 600 mM DIEA. This was done by pre-activating amino acids (or NKA) with HATU each at 300 mM concentrations in NMP, and then adding this activated mixture and DIEA to the resin. Capping was performed with

10% acetic anhydride, 5% DIEA in NMP after each coupling. Resin was washed thoroughly with excess NMP before and after each step.

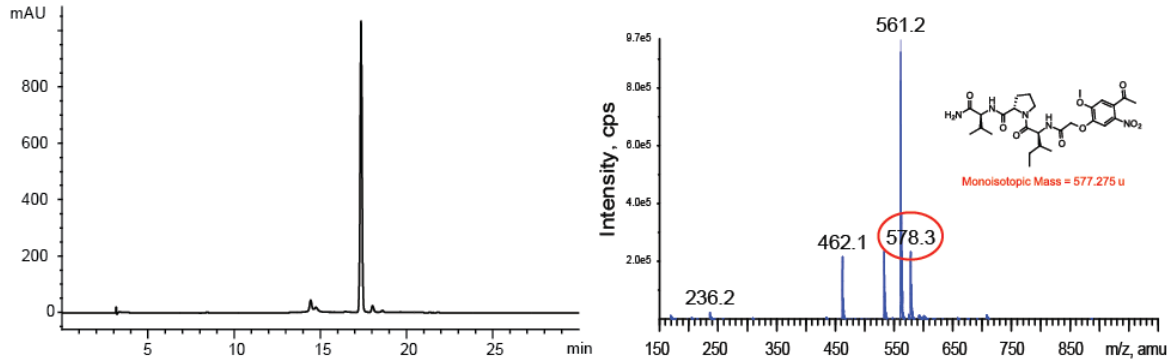

Figure 18 Val-Pro-Ile-DNMPE HPLC (345 nm, left) and MS (right)

After the completion of synthesis, the resin was washed thoroughly with DCM and dried. Val-Pro-Ile-DMNPE was cleaved off resin with 95% TFA solution (1 hour). TFA containing the peptide was collected by filtration and evaporated by blowing nitrogen. The peptide was purified on a C18 column using an acetonitrile gradient and the fraction was dried in vacuum (Figure 18). The yield of this reaction, after purification was observed to be 74%.

Synthesis of Val-Pro-Ile-hydrazone

(S)-2-{[(S)-1-{(2S,3S)-2-[2-(4-Acetohydrazonoyl-2-methoxy-5-nitrophenoxy)acetylamino]-3-methylvaleryl}-2-pyrrolidinyl]carbonylamino}-3-methylbutyramide

Purified peptide was dissolved in DMSO for quantitation using UV absorbance (ϵ_{345} = 4470 M^{-1} cm^{-1}). DMSO solutions were transferred into Eppendorf tubes and dried in speed vac. 18.1 µmol dry Val-Pro-Ile-DMNPE was dissolved in 240 µL 50%

acetonitrile 50% ethanol mixture. To this solution, 1.62 µL acetic acid and 17.48 µL (360.1 µmol) hydrazine monohydrate were added. Reaction was performed in sealed tube at 90 C for 4 hours. Reaction was analyzed on HPLC using a C18 column. Complete conversion of ketone to hydrazone was observed (100% yield). Pure hydrazone was collected by repeated injections of the crude reaction on C18 column. Two peaks corresponding to E/Z isomers were observed. LCMS analysis of the species also revealed that the hydrazone was formed (Figure 19).

Conclusions can be made from this experiment that the introduction of proline in the sequence improved the solubility of peptide significantly. Hydrazone was made successfully and thus the next reactions were attempted.

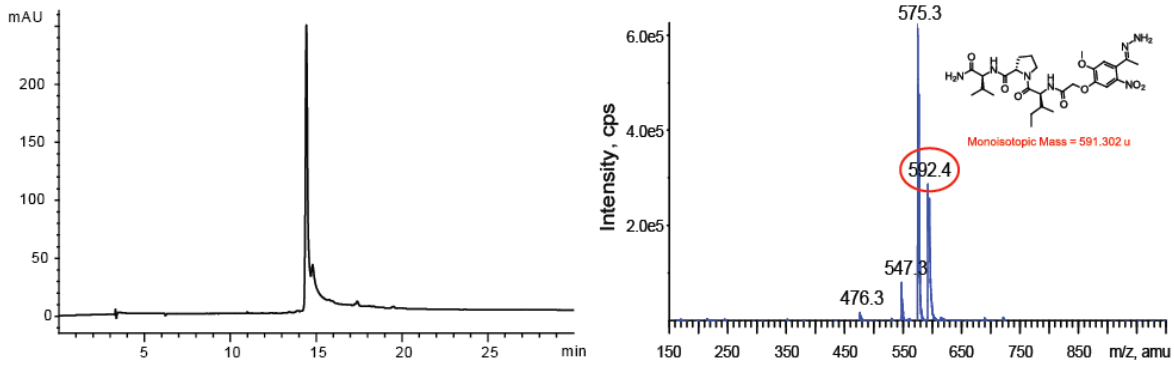

Figure 19 Val-Pro-Ile-hydrazone HPLC (345 nm, left) and MS (right)

Synthesis of Val-Pro-Ile-diazo and reaction with insulin

The method described for the synthesis of diazo-DMNPE-azide was adopted since the conditions were previously optimized[30]. Val-Pro-Ile-hydrazone was dissolved in least amount of dry DMSO and quantitated using UV spectroscopy (ϵ_{345} = 4470 M^{-1} cm^{-1}). Additional DMSO was added to have a final concentration of 165.6

mM hydrazone. To a solution containing 10 µmoles of Val-Pro-Ile-hydrazone (60 µL), 277.7 µmol (24.1 mg) manganese (IV) oxide was added. Reaction was shaken vigorously for 45 minutes at room temperature in dark. After the reaction was completed, it was centrifuged at 15000 g for 5 minutes to separate manganese oxide from the reaction. Clear supernatant containing the diazo species was collected and added to 10 µmol insulin in dry DMSO. Final concentration of insulin in the reaction was adjusted to 2 mM by dilution with dry DMSO. After 24 hours, reaction was analyzed on HPLC. However, it was observed that the insulin ester, i.e. the product was not formed (Figure 20).

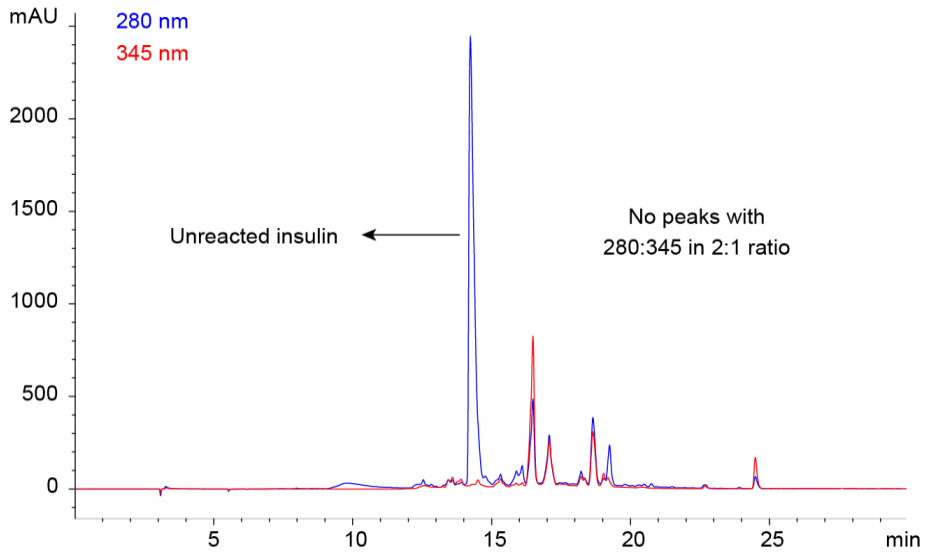

Figure 20 Failed Val-Pro-Ile-insulin reaction on HPLC. Expected mono-adduct should have an absorbance at 280:345 with 2:1 ratio.

Investigation of failure of diazotization and insulin esterification

The oxidation reaction was performed by maintaining the concentration of hydrazone at 165.6 mM. At these conditions, it was interpreted that the diazonium

species was not formed as any amount was not trapped by insulin as an ester. In this reaction, manganese dioxide can be easily removed from the reaction by centrifugation. The reaction therefore does not contain any by products that will interact with insulin. Other methods of diazotization of the hydrazone were also explored. Firstly, the oxidation reaction was attempted using peroxyacetic acid as the oxidant, instead of the manganese dioxide. It should be noted that the hydrazone was again maintained at a concentration of 165.6 mM. This approach too did not yield the ester. Alternatively, the ketone can be converted to an imine using tosyl-hydrazine and subsequently converted to diazo using triethylamine (acid-base reaction); however, this method was not attempted as it will be easier to optimize the already known conditions rather than establishing new conditions with new reagents in the laboratory. Also, both the peroxyacetic acid and tosyl-hydrazone based diazotization will leave by products in the reaction mixture (acetic acid and p-toluenesulfonic acid), which may interact with the protein in an undesirable way. For instance, p-toluenesulfonic acid has a pKa of -2.8 and insulin may lose its activity in the presence of such highly acidic molecules.

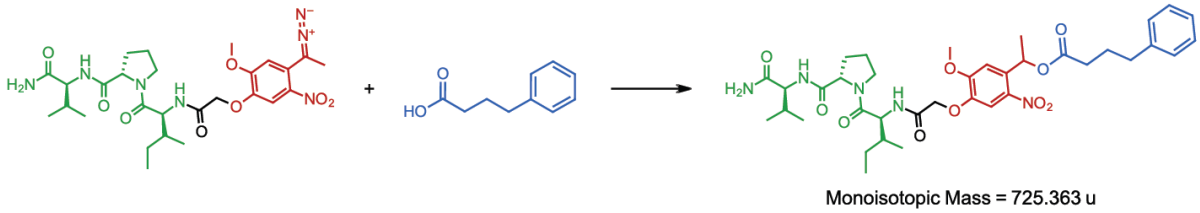

Figure 21 Val-Pro-Ile-diazo trapped with a model carboxylic acid (4-phenylbutyric acid, blue) in optimization studies

To investigate why the reaction failed, the oxidation reactions with Val-Pro-Ile-hydrazone were set up on a small scale and analyzed on the LC-MS. The diazonium is an unstable species and will be converted to alcohol when run on the LC with acidic solvents. Therefore, after the oxidation reaction, manganese oxide was removed by centrifugation and the diazonium is trapped as an ester with a model carboxylic acid. The model compound used in this study is 4-phenylbutyric acid (Figure 21).

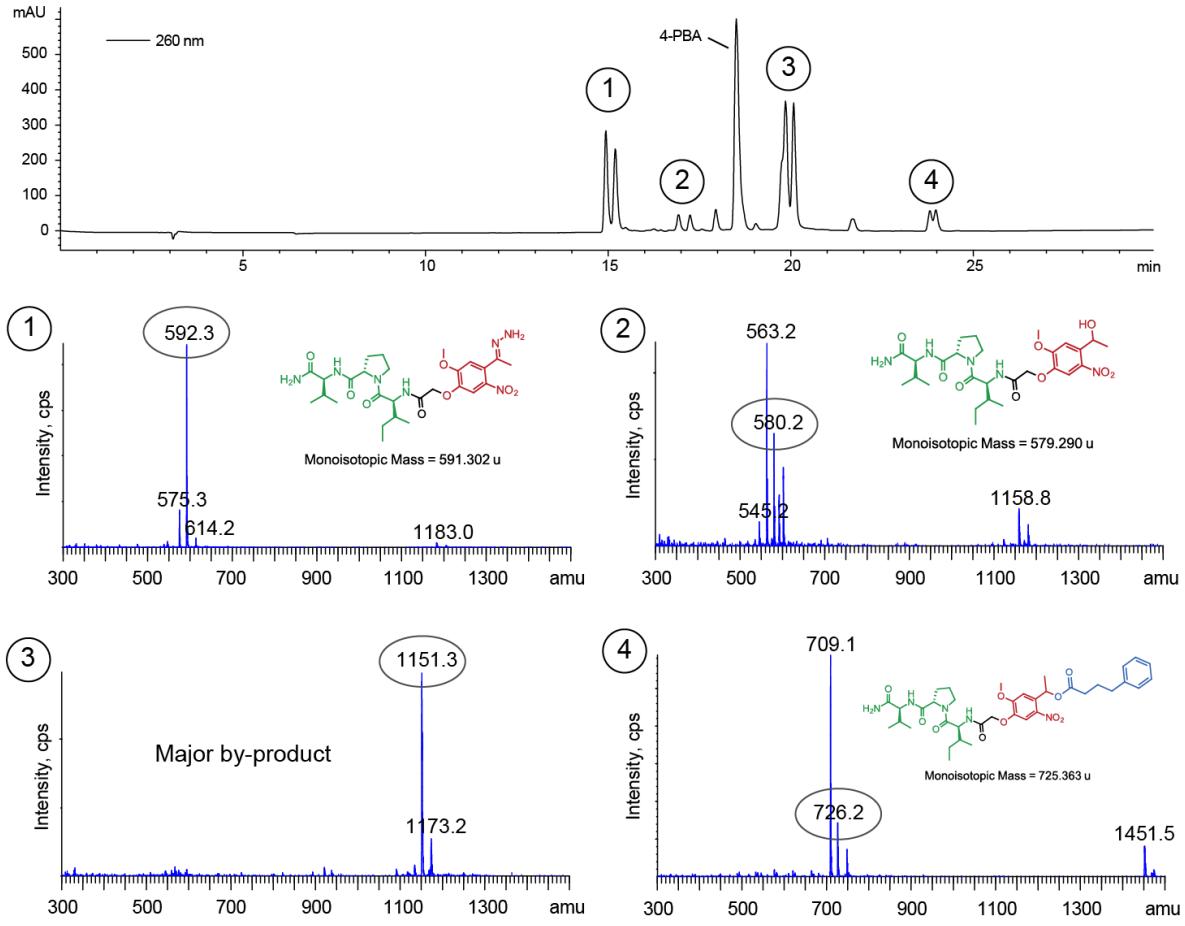

Figure 22 Val-Pro-Ile-diazo reaction with 4-PBA analysis on HPLC. Hydrazone left over from previous reaction (1), hydrolyzed diazo i.e. alcohol (2), major by-product (3) and 4-PBA ester (4) are labelled

The major by-product is actually two closely eluting peaks having 345 nm absorbance were observed at ~20 minutes (Figure 22). Since the retention of the by product is also greater than the hydrazone, these species should be more non-polar than the reactant hydrazone itself. This mass 1151.3 amu is also about 2x the mass of Val-Pro-Ile-hydrazone (591.3 amu). So, the byproduct might have formed due the reaction between two reactant molecules. Most chemical functional groups on the Val-Pro-Ile-hydrazone are inert under normal conditions, the only plausible site for such 'dimerization' reaction is the imine. The free amine on one molecule of Val-Pro-Ile-hydrazone can attack the electrophilic carbon of the imine on another hydrazone species and kick out the hydrazine to form a new imine called azine (Figure 23).

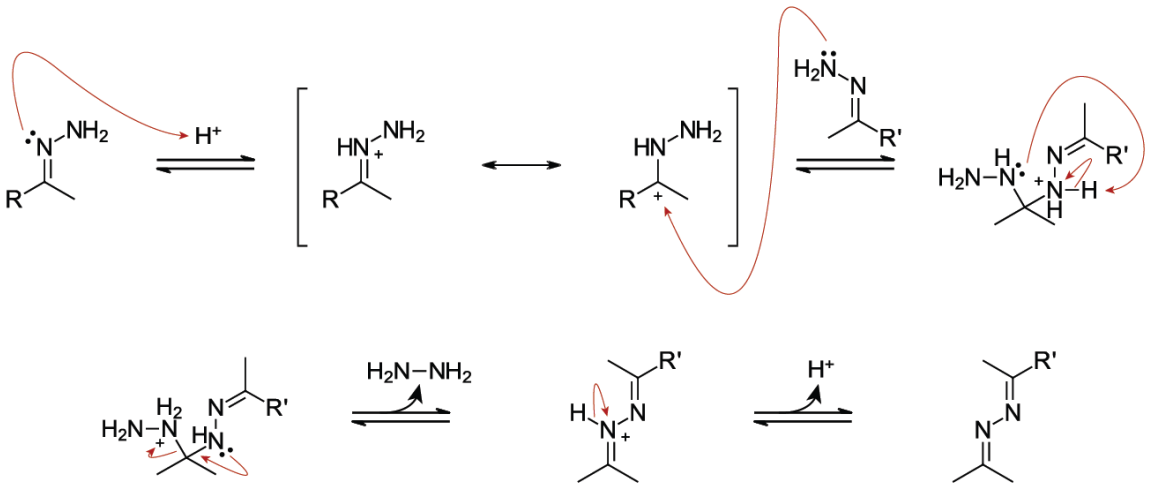

Figure 23 Mechanism of azine formation. Mass of the azine is consistent with the mass spectrum.

Precedence on the formation of azines from diazo compounds corroborates this hypothesis, along with the mass seen on the LCMS which is consistent with the mass of an azine[37]. Moreover, it was also observed that the azines are formed in stored Val-

Pro-Ile-hydrazone stock solutions prior to the diazotization reaction. Since these peptidic hydrazones are purified using reversed phase chromatography with TFA containing mobile phases, these acids can catalyze the conversion of hydrazones to azines[38]. In addition to these problems, it was also observed that azines are rapidly formed while drying the purified HPLC fractions of hydrazones. Removal of solvent from the solution increases the concentration of hydrazones, thereby increasing the rate of formation of azines especially in the presence of acids. To summarize, azines are formed due to the intermolecular reaction between two hydrazone compounds.

This does not occur during the *synthesis* of hydrazones because the hydrazine is used in excess (20x) in the reaction. As soon as the hydrazone is purified from the reaction mixture using acidic mobile phases on a reversed phase chromatography, azines tend to accumulate in the solution. Azine formation is also accelerated during the drying process due to concentration of hydrazone. Azines are also formed after the diazotization as loss of gaseous nitrogen promotes the rate of reaction between two diazo compounds.

Why azines were observed only with the peptidic hydrazones

Azines were observed only with Val-Pro-Ile-hydrazone. But they were not observed during the storage, drying and the diazotization of CD-hydrazone. CD-diazo compounds are easy to synthesize and yield insulin esters at high yields. Though the photocleavable group bearing the hydrazone function is the same for both compounds, the only structural difference is the tag.

Firstly, CD-hydrazone is purified from the reaction by normal phase chromatography with solvents that do not contain acids. Therefore, the rate of formation of azine (CD-azine) is lower in the absence of acids. Second, the cyclododecyl group is highly non-polar and does not have any functional groups for strong polar interactions. Since the reaction is performed in dry DMSO where CD-compounds are highly soluble, hydrophobic interactions are also not strong enough. Therefore, it is not easy for two hydrazone or diazo species to chemically interact to form azines.

But Val-Pro-Ile-hydrazone is firstly purified using acidic solvents. Thus, acids assist in the formation of azines during the concentration of purified hydrazone HPLC fractions. Also, when Val-Pro-Ile-hydrazone was maintained at the same concentration (165.6 mM) during diazotization reaction as CD-hydrazone, only the former forms azines probably due to the way peptides interact. Peptidic tags have amide functions in addition to non-polar side chains. Therefore, polar-polar interactions as well as hydrophobic interactions bring two hydrazone molecules closer in solution. This increases the local concentration of hydrazones, thus forming azines at a significantly higher rate.

Approaches to prevent the formation of azines

In a pure hydrazone solution, the amount of hydrazone goes down as the azines form. Azines cannot be oxidized to diazo compounds as they lack the protons and hence cannot play role of reductant in the oxidation reaction. In such cases, the amount of tag available for insulin esterification, and thus the yield of the ultimate

reaction goes down significantly. Therefore, it is critical to minimize the formation of azines, specifically at these three steps.

1) *Purification*: Since there is no alternative approach the purification of peptides, C18 chromatography with acidic solvents cannot be avoided. However, measures were taken to drastically slow down the rate of azine production. It is preferred that the hydrazone is purified at a preparative scale versus analytical scale as the reaction can be purified as bulk. If purification is performed by repeated injections on an analytical C18, hydrazone fractions should be stored at -80 C until the purification is completed. Or else, storage at room temperature gives ample time for the hydrazones to be converted to azines. Additionally, each fraction may be pooled into multiple containers in the freezer to avoid repeated freeze-thawing of the sample. Some reactions are known to be accelerated due to freeze thawing as the chemical compounds are excluded from the solvent crystals, thus increasing effective concentration of the species in the unfrozen solvent. The solution may not freeze if stored at -20 C due to the presence of acetonitrile in the HPLC fraction. After purification, it is suggested that the drying is performed in a large round bottom flask in a rotavapor as it improves the rate of drying due to larger surface area. Application of heat during the drying process is not recommended. Drying should be performed in as less time as possible. The hydrazone should be stable in a dried state, as the azine reactions proceed only in solution. Dried hydrazone samples should be stored in a desiccated condition at -80 C as moisture can redissolve the pure material.

2) *Quantitation*: Dried HPLC puridied hydrazone material should be dissolved in DMSO to be utilized for the subsequent diazotization reaction. The process of dissolution initiates the formation of azines. Therefore, UV spectroscopic quantitation and volume adjustment should be done as quickly as possible.
3) *Diazotization*: A model was developed for the conversion of hydrazones to azines during the diazotization reaction using the principles of chemical kinetics. In this bimolecular reaction, the rate is dependent on the concentration of the reactants i.e. two molecules of hydrazone. Higher concentration of hydrazone results in a higher rate of formation of azines during the reaction. Similarly, to address the issue and improve the diazotization yields, the concentration of hydrazone in the reaction was lowered to reduce the rate of formation of azines. For instance, lowering the concentration of hydrazone by 5x reduces the rate of azine production by 25x.

Effect of concentration on azine of formation – experimental evidence

To test the hypothesis discussed above, a series of reactions were set up with varying concentrations of Val-Pro-Ile-hydrazone. The concentration used for DMNPE-diazo-azide species, i.e. 165.6 mM, was used as the reference concentration. Five reactions were set up in which the hydrazone concentration was lowered 2x, 10x, 15x, 20x and 25x respectively. Reactions were initiated by the addition of manganese oxide. The manganese oxide mole ratio was maintained at 20 times the hydrazone amount in all reactions. Reactions were shaken for 45 minutes in dark at room temperature. Reactions were then centrifuged at 15000 g for 5 minutes, and the clear

supernatant from each tube containing Val-Pro-Ile-diazo was pipetted into respective tubes containing 4-phenylbutyric acid solutions. The amount of 4-phenylbutyric acid is taken in a 1:1 ratio with the hydrazone (or diazo assuming 100% oxidation). Volume of the reactions were adjusted such that the final concentration of 4-phenylbutyric acid or diazo is 2 mM. Reactions were incubated in dark at room temperature for 4 hours and analyzed on C18 HPLC and LCMS.

Table 2 Amounts of each species formed during the diazotization and esterification reactions. Amount determined based on integrations of each peaks at 345 nm

Concentration (hydrazone, mM)	Times reduction (from 165.6 mM)	Hydrazone %	Alcohol %	Azine %	Ester %
82.80	2	4.8	14.7	37.3	43.2
16.56	10	8.1	9.8	34.5	47.6
11.08	15	8.3	11.0	33.4	47.3
8.28	20	7.6	8.7	35.4	48.2
6.62	25	7.6	13.8	38.9	39.8

Four major species including the cages species were identified in each reaction based on mass spectrometry, viz., caged carboxylate, azine, hydrolyzed diazo (i.e. alcohol) and unreacted hydrazone as seen in Figure 22. The percentage of each species formed in each reaction was estimated using the area under the respective peaks. Table 2 shows the amounts of azine and the desired caged 4-phenylbutyric acid in

respective reactions. From these experiments, it was concluded that the right approach was chosen to solve the azine issue. Reaction yield was improved from 0% to about 48% by lowering the concentration of hydrazone by 20x. Therefore, this optimized method was adopted for the synthesis of Val-Pro-Ile-diazo to esterify insulin.

Successful synthesis of Val-Pro-Ile-diazo

(S)-2-{[(S)-1-[(2S,3S)-2-{2-[4-(1-Diazoethyl)-2-methoxy-5-nitrophenoxy]acetylamino}-3-methylvaleryl]-2-pyrrolidinyl]carbonylamino}-3-methylbutyramide

Dried Val-Pro-Ile-hydrazone was dissolved in minimal volume of dry DMSO and quantitated using UV spectroscopy *quickly*. Additional DMSO was added to dilute the solution to 8.28 mM concentration. Stock solution containing 43.5 µmol of the hydrazone (5.25 mL) was transferred into a glass reaction vial, and 2.1 g (24.18 mmol) of manganese dioxide was added. The mixture was shaken vigorously for 45 minutes. Manganese dioxide was then removed by centrifugation at 15000 g for 5 minutes. Supernatant containing Val-Pro-Ile-diazo, with a characteristic red color, was used immediately for the reaction with insulin.

Manganese dioxide pellet was washed with additional 1 mL DMSO and pooled with the supernatant after centrifugation. The diazo compound being unstable is characterized by UV-visible spectroscopy only (Figure 24). Yield of the reaction was not estimated due to instability of the diazo. It was assumed that 100% hydrazone is oxidized.

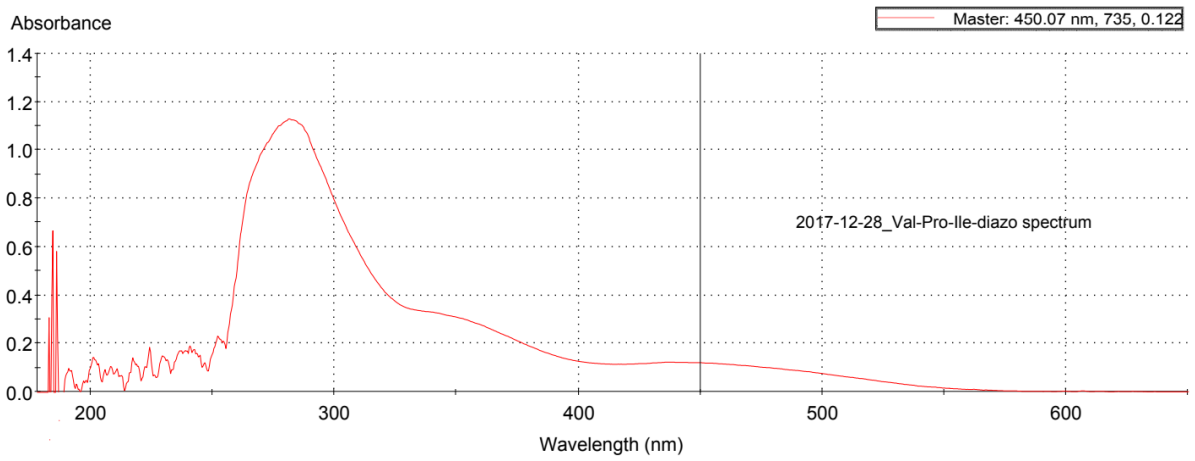

Figure 24 Val-Pro-Ile-diazo spectrum in DMSO

Synthesis of Val-Pro-Ile-insulin

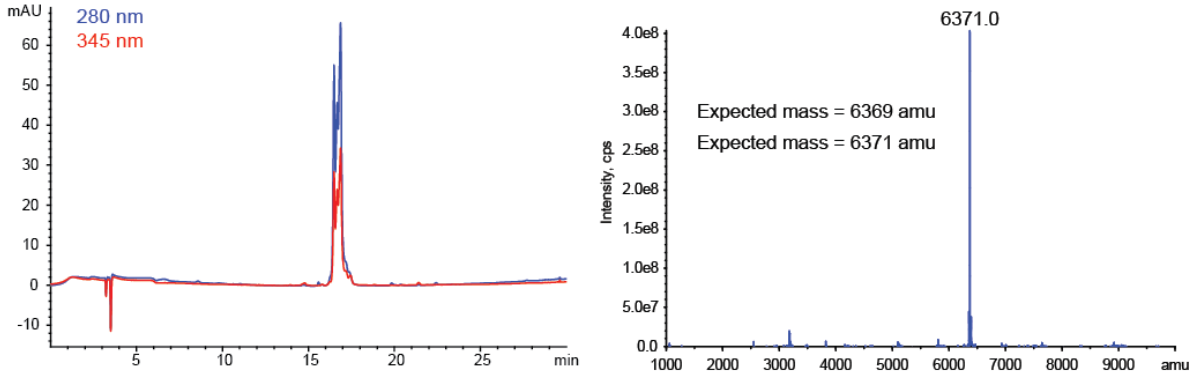

Figure 25 Val-Pro-Ile-insulin (pure) HPLC and MS

43.5 µmol (252.7 mg) insulin was dissolved in 6.6 mL anhydrous DMSO. To this solution, 43.5 µmol of freshly prepared Val-Pro-Ile-diazo was added and vortexed briefly. Additional DMSO was added to make up the volume to 21.7 mL to adjust insulin concentration to 2 mM. Reaction was left overnight, protected from light for 24 hours (Yield = 21%). Val-Pro-Ile-insulin was purified by injecting the reaction mixture on a 250 X 4.6 mm 5 µm C18 column. Mobile phases contained 0.1%

trifluoroacetic acid. Fraction was collected from 15.6-17.2 minutes when run on 0-100% acetonitrile gradient over 28 minutes, at 0.8 mL/min (Figure 25).

Synthesis of peptidic hydrazones on solid phase

Synthesis of insulin variants with peptidic photocleavable tags was a challenging task. Previously, a proline was incorporated in the tag to introduce a kink and resolve the solubility issue for the synthesis of peptidic hydrazones. Though this was an effective approach, it may be difficult to make use of proline and still make new insulin variants with a variety of properties. Therefore, development of alternative strategies to get past the solubility issue was critical to enable the design and synthesis of a wider variety of tags and insulin variants.

In the previous synthetic route, the DMNPE-acid was condensed with the tripeptide on solid phase resulting in a DMNPE-peptide with a ketone group. This peptidic ketone was cleaved off the resin and converted into the hydrazone in solution. Only with the introduction of a kink in the peptide, dissolution of ketone was possible. Therefore, this approach allows the synthesis of a limited variety of peptides with a common central proline moiety.

In this new approach, attempts were made to synthesize the hydrazone on solid phase. It will be advantageous in the following ways to make hydrazones on solid phase:

1) Since ketone is not cleaved off and converted into hydrazone on the solid phase, the solubility issue of linear peptides is completely avoided.

2) Linear hydrazones are more polar than ketones. Moreover, the subsequent oxidation of hydrazones is performed in DMSO in which peptides (including linear ones) are highly soluble. Therefore, cleaved linear hydrazones can be purified and oxidized in DMSO.
3) Hydrazones of peptides with any sequence can be synthesized. Since the side chains are protected before TFA cleavage on solid phase, peptidic structures are preserved. For instance, treatment of arginine with hydrazine will convert the arginine into ornithine. But since the guanidine side chains are protected, this side reaction is prevented in this approach.

Earlier, methods were developed to convert non-peptidic ketones into p-toluenesulfonylhydrazones. Since a reversible carbonyl addition is possible on a solid phase, methods were slightly modified and the synthesis with hydrazine monohydrate was attempted. Briefly, 235 µmol of Val-Pro-Ile-DMNPE on 0.5g ChemMatrix (PEG) rink amide resin was suspended in 8 mL NMP:ethanol (9:1) ratio. 2.35 mmol (135 µL) acetic acid and 23.5 mmol (1.14 mL) 65% hydrazine monohydrate were added to this suspension. Reaction vessel was sealed tightly to prevent evaporation of hydrazine and shaken at 65 ºC. It was observed that 50% of ketone was converted to hydrazone by the end of 6 hours. 100% conversion of ketone to hydrazone was observed at the end of 18 hours. Resin was extensively washed with NMP, DCM and dried. Hydrazone was cleaved off solid phase with 95% TFA 5% water mixture (1 hour). It is critical to note that the reaction did not go to completion

when the peptide was synthesized on a polystyrene solid support. The peptides on PEG resin were only converted into hydrazone completely.

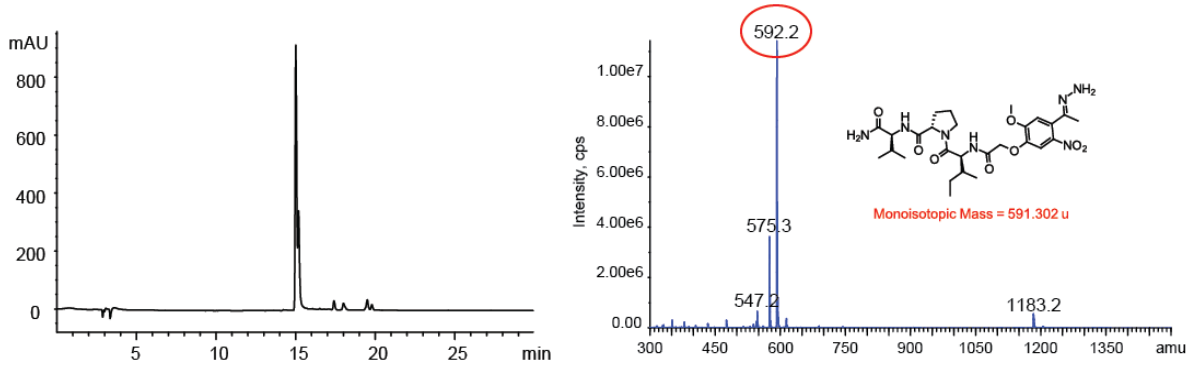

Figure 26 Pure Val-Pro-Ile-hydrazone synthesized on solid phase. HPLC (345 nm, left) and MS (right) analysis

Val-Pro-Ile-hydrazone crude was dissolved in DMSO and purified by injecting it on a 250 X 21.2 mm 10 µm C18 column. Mobile phases contained 0.1% trifluoroacetic acid. Fraction was collected from 26.3-29.5 minutes when run on 0-100% acetonitrile gradient over 35 minutes, at 5 mL/min. Analysis was performed on HPLC and LCMS (Figure 26).

The reaction is high yielding and the TFA cleavage results in a ~90-95% pure peptidic hydrazone. This is because all the impurities and by products of the reaction are washed off prior to the cleavage and only the hydrazone is retained on solid phase. The hydrazone can also be stored on the solid phase after drying at -20 C. The compound was observed to be stable for months after synthesis under these storage conditions. Thus, a convenient universal approach for the synthesis of peptidic-DMNPE-hydrazones was developed which allowed the design of a wider variety of tags in this study.

Val-Val-Val-insulin

Synthesis of peptidic hydrazones on solid phase enabled the design of newer photocleavable tags. Since solubility of the peptide is not an issue in the reaction anymore, synthesis of hydrazone derivatives of linear peptides were attempted. The first linear peptidic tag which was made using this synthetic approach is Val-Val-Val-DMNPE. Valine consists of an aliphatic non-polar side chain and is very insoluble in water. A valine tripeptide grafted onto insulin's carboxylate side chain or termini increases the non-polar surface area exposed to the aqueous environment. This conjugation lowers the solubility of the protein conjugate due to hydrophobic effect. Also, the solubility of the Val-Val-Val-insulin variant is expected to be lower than the Val-Pro-Ile-insulin due to its structure and higher non-polarity.

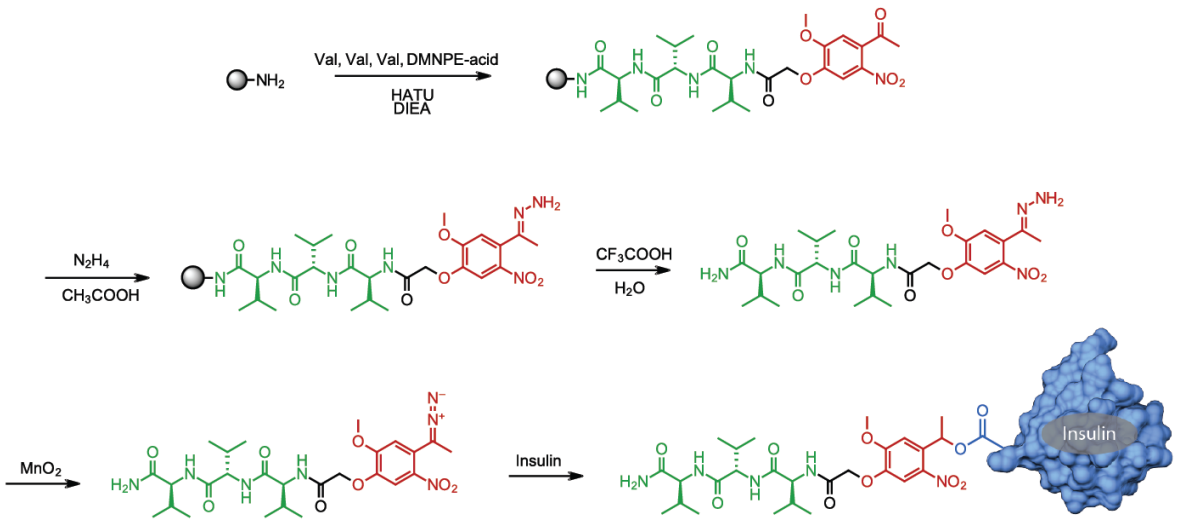

Figure 27 Val-Val-Val-insulin synthesis

Synthesis is shown in Figure 27. The same strategy used for the synthesis of Val-Pro-Ile-insulin is used here. The ketone is converted into hydrazone on the solid

phase and cleaved off. Diazotization can be easily performed as the peptide should be highly soluble in DMSO.

Synthesis of Val-Val-Val-DMNPE

(S)-2-[(S)-2-{(S)-2-[2-(4-Acetyl-2-methoxy-5-nitrophenoxy)acetylamino]-3-methylbutyrylamino}-3-methylbutyrylamino]-3-methylbutyramide

Val-Val-Val-DMNPE was synthesized by Fmoc-solid phase peptide synthesis. 0.5 g of Chemmatrix Rink amide resin (PEG), equivalent to 0.235 mmol, was suspended in NMP at a concentration of 60 mM. Fmoc was removed with 10% piperidine 2% DBU mixture. Coupling with the resin bound amine was performed with 300 mM of either Fmoc-valine or DMNPE-acid using 300 mM HATU and 600 mM DIEA. Capping was performed after each coupling with 10% acetic anhydride and 5% DIEA. Solid phase was washed extensively (~5x) with NMP after each step. For HPLC and mass spectrometric analysis, a small amount of resin was sampled, and peptide was brought into solution with 95% TFA 5% water mixture (Figure 28). Yield = 92% (based on Fmoc quantitation in piperidine solution).

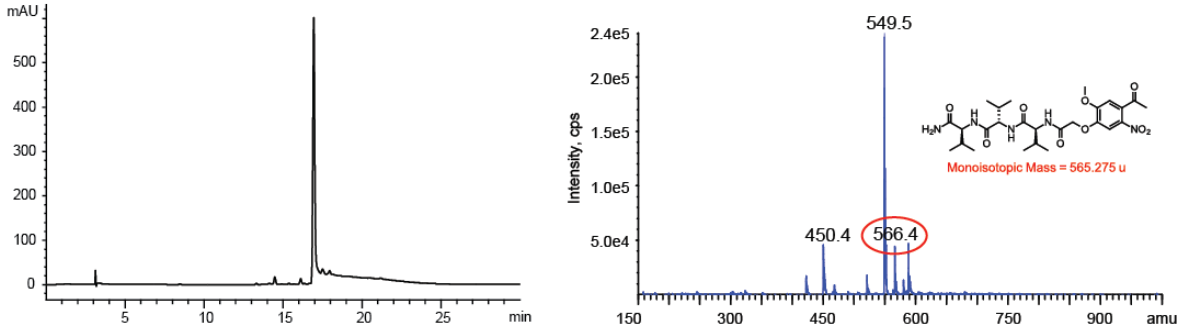

Figure 28 Val-Val-Val-DMNPE analysis by HPLC (left) and MS (right)

Synthesis of Val-Val-Val-hydrazone

(S)-2-[(S)-2-{(S)-2-[2-(4-Acetohydrazonoyl-2-methoxy-5-nitrophenoxy)acetylamino]-3-methylbutyrylamino}-3-methylbutyrylamino]-3-methylbutyramide

235 µmol of Val-Val-Val-DMNPE on 0.5 g Chemmatrix (PEG) rink amide resin was suspended in 8 mL NMP:ethanol (9:1) ratio. To this suspension, 2.35 mmol (135 µL) acetic acid and 23.5 mmol (1.14 mL) 65% hydrazine monohydrate were added and vortexed. Reaction was shaken at 65 ºC for 24 hours (Yield = 100% conversion). Val-Val-Val-hydrazone was brought into the solution by treating the solid phase with 95% TFA 5% water for 1 hour. Resin was removed by filtration and TFA solution containing the product was collected and evaporated. The crude hydrazone was dissolved in DMSO and purified on a 250 X 21.2 mm 10 µm C18 column. Val-Val-Val-hydrazone was collected from 26-33 minutes when run on a 0-100% acetonitrile gradient for 35 minutes at 5 mL/min. Mobile phases contained 0.1% TFA (Figure 29). Injections can be repeated if it is necessary to collect higher amount of material, keeping in mind that the fractions should be stored at lower temperatures temporarily to prevent azine formation.

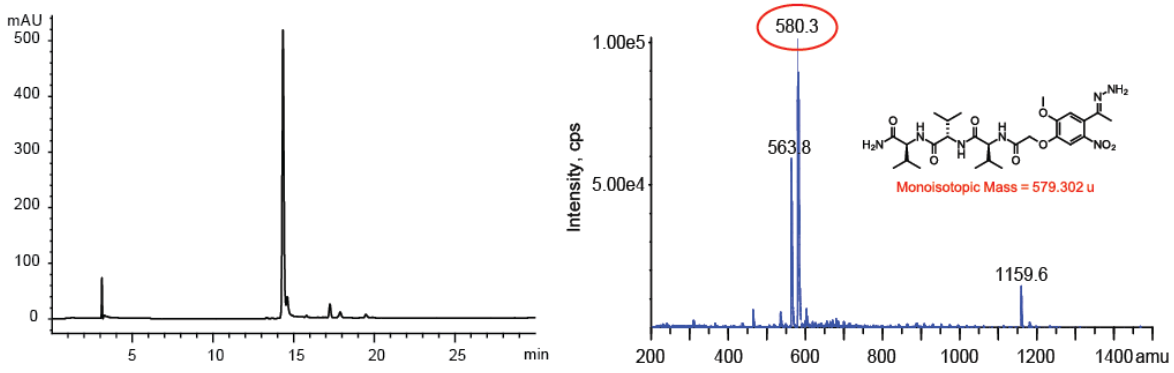

Figure 29 Val-Val-Val-hydrazone analysis by HPLC (345 nm, left) and MS (right)

Synthesis of Val-Val-Val-diazo

(S)-2-[(S)-2-[(S)-2-{2-[4-(1-Diazoethyl)-2-methoxy-5-nitrophenoxy]acetylamino}-3-methylbutyrylamino]-3-methylbutyrylamino]-3-methylbutyramide

Dried Val-Val-Val-hydrazone was dissolved in minimal volume of anhydrous DMSO and quantitated using UV spectroscopy quickly. Additional DMSO was added to dilute to a concentration of 11 mM. Volume containing 19.2 µmol hydrazone (1741.7 µL) was transferred into a glass reaction vial. 8 mmol (699.7 mg) manganese (IV) oxide was added and shaken vigorously for 30 minutes. Manganese dioxide was removed by centrifugation (15000 g, 5 minutes) and the supernatant containing Val-Val-Val-diazo was used for the next reaction immediately. Manganese dioxide pellet was washed with additional 3 mL DMSO to extract maximum amounts. Each time, suspension was centrifuged, and all the supernatants were pooled. Since diazo compounds are unstable, it is only analyzed using UV-visible spectroscopy. Formation of the diazo compound can be identified by a characteristic absorbance (λ_{max}) 450 nm (Figure 30). Yield of the reaction was not estimated.

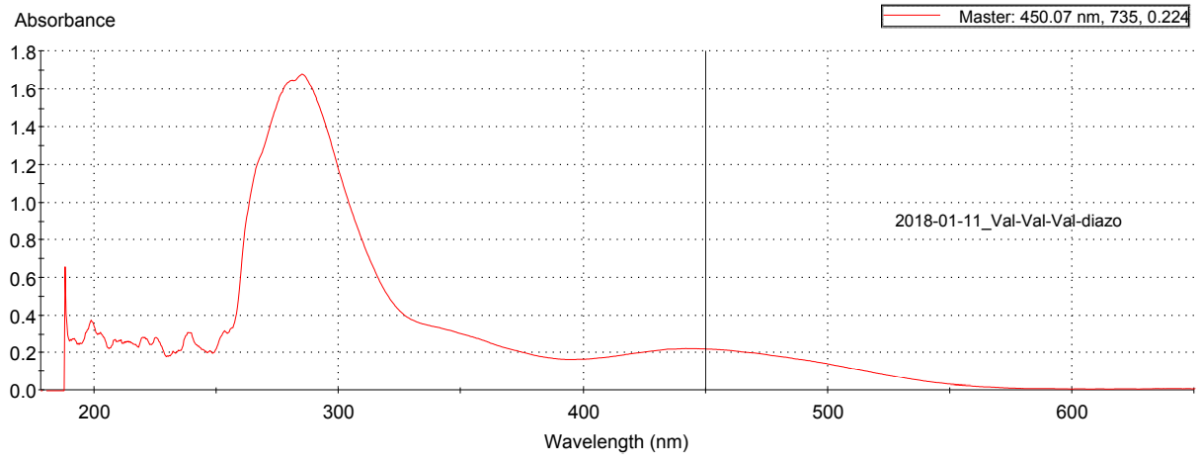

Figure 30 Val-Val-Val-diazo UV-visible absorption spectrum

Synthesis of Val-Val-Val-insulin

19.2 µmol (113.6 mg) human recombinant insulin was dissolved in 4.5 mL dry DMSO. 19.2 µmol (4.74 mL) of freshly synthesized Val-Val-Val-diazo was added to insulin solution. Total volume was made up to 9.2 mL with DMSO to have insulin at a concentration of 2 mM. Reaction was vortexed and allowed to stand in dark for 24 hours. Yield = 17%.

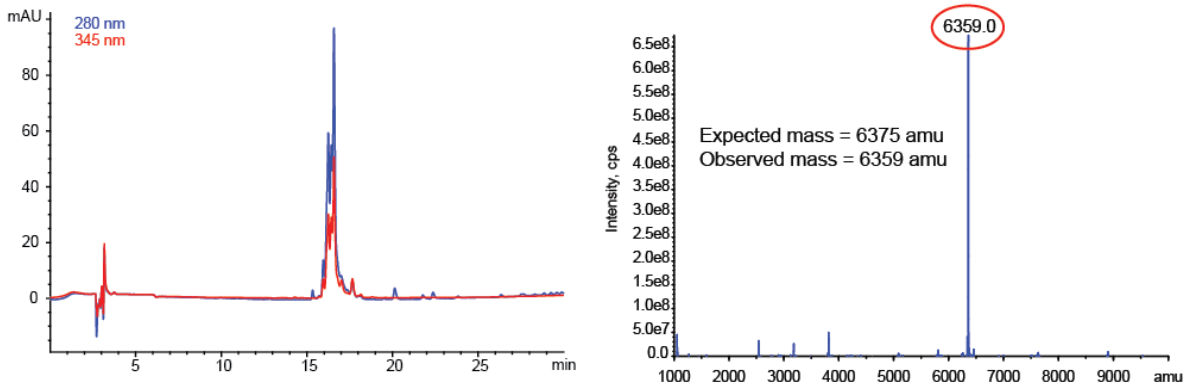

Figure 31 Val-Val-Val-insulin analysis on HPLC (left) and MS (right)

Val-Val-Val-insulin was purified by injecting the reaction mixture on a 250 X 4.6 mm 5 µm C18 column. It was collected from 21.3-23.3 minutes when run on 10-65% acetonitrile gradient over 35 minutes, at 1 mL/min. Mobile phases contained 0.1% trifluoroacetic acid (Figure 31).

Ile-Ile-Ile-insulin

Ile-Ile-Ile-insulin was the first peptidic insulin variant attempted. Since the insolubility of the ketone has been addressed by following an alternative synthetic route on solid phase, synthesis of this variant was re-attempted. Moreover, synthesis of this specific variant validates that the approach developed earlier is ideal and can

be used for constructing a variety of peptidic sequences. Isoleucine consists of an aliphatic non-polar side chain and is the least soluble amino acid. A tri-isoleucine tag will be the most insoluble biodegradable tag and will lower the insulin solubility even further, relative to a tri-valine peptidic tag. Synthetic approach is similar and is shown in Figure 32.

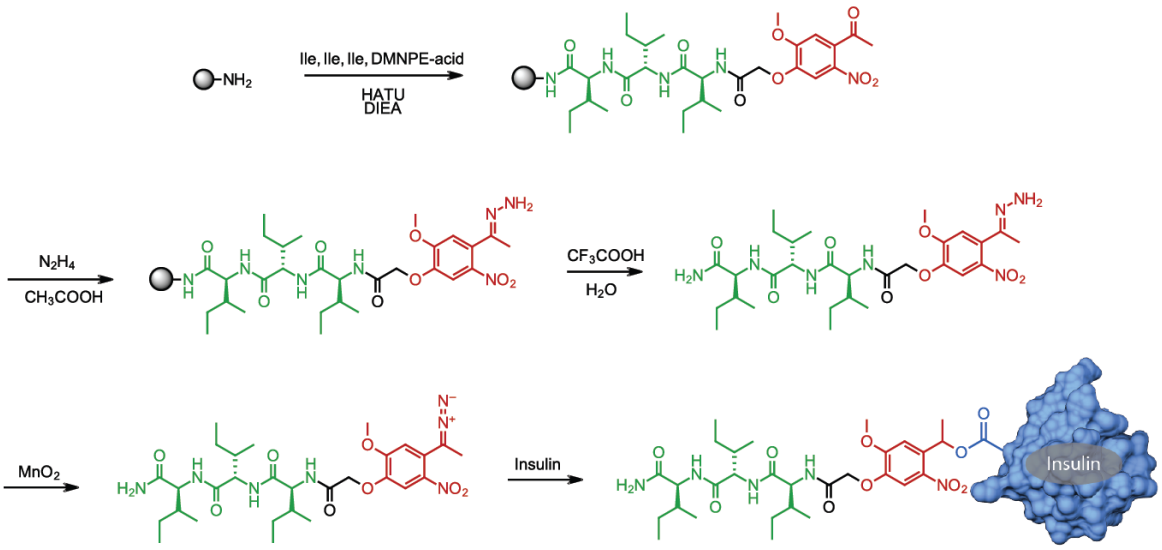

Figure 32 Ile-Ile-Ile-insulin synthesis

Synthesis of Ile-Ile-Ile-DMNPE

(2S,3S)-2-[(2S,3S)-2-{(2S,3S)-2-[2-(4-Acetyl-2-methoxy-5-nitrophenoxy)acetylamino]-3-methylvalerylamino}-3-methylvalerylamino]-3-methylvaleramide

Synthesis and characterization of Ile-Ile-Ile-DMNPE was shown earlier. Previously, this species was synthesized and cleaved off the solid phase. Conversion of the ketone to hydrazone was unsuccessful in solution due to solubility issues. Therefore, the ketone is not cleaved from the solid phase in this approach but converted to hydrazone. The method is discussed below.

Synthesis of Ile-Ile-Ile-hydrazone

(2S,3S)-2-[(2S,3S)-2-{(2S,3S)-2-[2-(4-Acetohydrazonoyl-2-methoxy-5-nitrophenoxy)acetylamino]-3-methylvalerylamino}-3-methylvalerylamino]-3-methylvaleramide

235 µmol of Ile-Ile-Ile-DMNPE on 0.5 g Chemmatrix (PEG) rink amide resin was suspended in 8 mL NMP:ethanol (9:1) ratio. To this suspension, 2.35 mmol (135 µL) acetic acid and 23.5 mmol (1.14 mL) 65% hydrazine monohydrate were added and mixed. Reaction was shaken at 65 ºC for 24 hours. Ile-Ile-Ile-hydrazone was cleaved off the resin with 95% TFA 5% water (1 hour). Solid phase was removed by filtration and TFA solution was collected and evaporated. Ile-Ile-Ile-hydrazone was purified on a 250 X 10 mm 5 µm C18 column by injecting DMSO solution of the crude material. It was collected from 34.85-36.8 minutes when run on a 0-100% acetonitrile gradient for 40 minutes at 1 mL/min. Mobile phases contain 0.1% TFA (Figure 33).

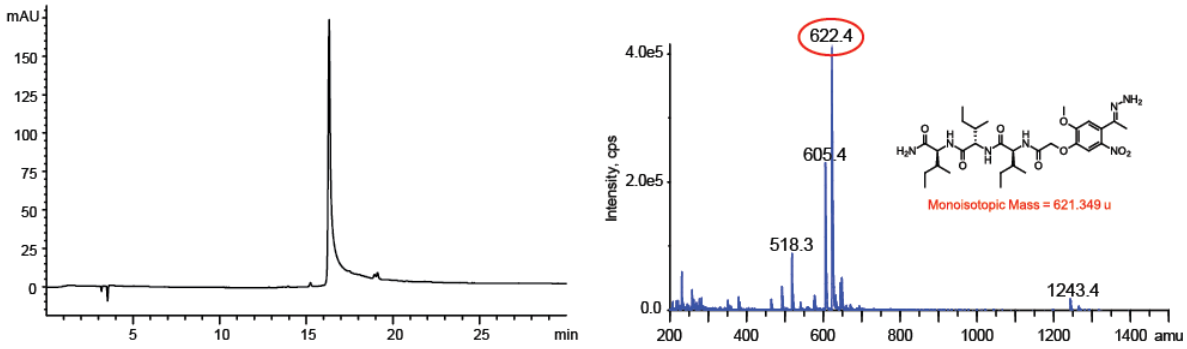

Figure 33 Ile-Ile-Ile-hydrazone analysis on HPLC (345 nm, left) and MS (right)

It was observed that Ile-Ile-Ile-hydrazone crashes out of water-acetonitrile solution immediately after fraction was collected from HPLC. This conclusion is made from the observation that the fraction becomes cloudy, probably due to aggregation

of the peptide. This precipitation may protect the hydrazone from reacting with itself to form azines, as it will no more be in the solution.

Synthesis of Ile-Ile-Ile-diazo

(2S,3S)-2-[(2S,3S)-2-[(2S,3S)-2-{2-[4-(1-Diazoethyl)-2-methoxy-5-nitrophenoxy]acetylamino}-3-methylvalerylamino]-3-methylvalerylamino]-3-methylvaleramide

Dried Ile-Ile-Ile-hydrazone was dissolved in minimal dry DMSO and quantitated using UV spectroscopy quickly (Note: Ile-Ile-Ile-hydrazone does not dissolve immediately in DMSO). Solution was diluted to a final concentration of 11 mM. 5.77 µmol hydrazone (552.5 µL) was transferred into a glass reaction vial. 2.4 mmol (209 mg) manganese (IV) oxide was added and shaken vigorously for 45 minutes. Manganese dioxide was removed by centrifugation (15000 g, 5 minutes) and the supernatant containing Ile-Ile-Ile-diazo was collected. Manganese dioxide pellet was washed with additional 552.5 µL DMSO to extract maximum amounts. This wash solvent was extracted from the oxidant by centrifugation. Clear wash solvent was collected and pooled with the reaction. Pooled diazo containing DMSO solution was used immediately for the reaction with insulin. Solution was also diluted with DMSO and analyzed using UV spectroscopy to monitor the 450 nm absorbance (Figure 34). Yield of the reaction was not estimated due to instability of the diazo. It was assumed that 100% hydrazone is oxidized, and therefore reacted with insulin in a 1:1 mole ratio relative to the hydrazone.

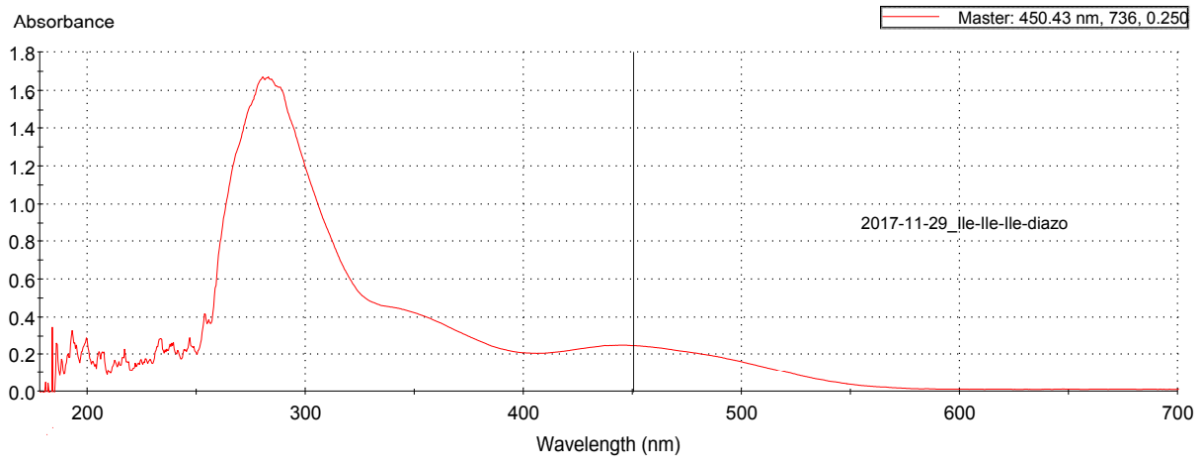

Figure 34 Ile-Ile-Ile-diazo UV-visible spectrum

Synthesis of Ile-Ile-Ile-insulin

5.77 µmol (33.5 mg) human recombinant insulin was dissolved in 1800 µL dry DMSO. 5.77 µmol (1105 µL) of freshly synthesized Ile-Ile-Ile-diazo was added to insulin solution, and the total volume was made up to 3050 µL with DMSO (2 mM). Reaction was vortexed and allowed to stand in dark for 24 hours (Yield = 19%).

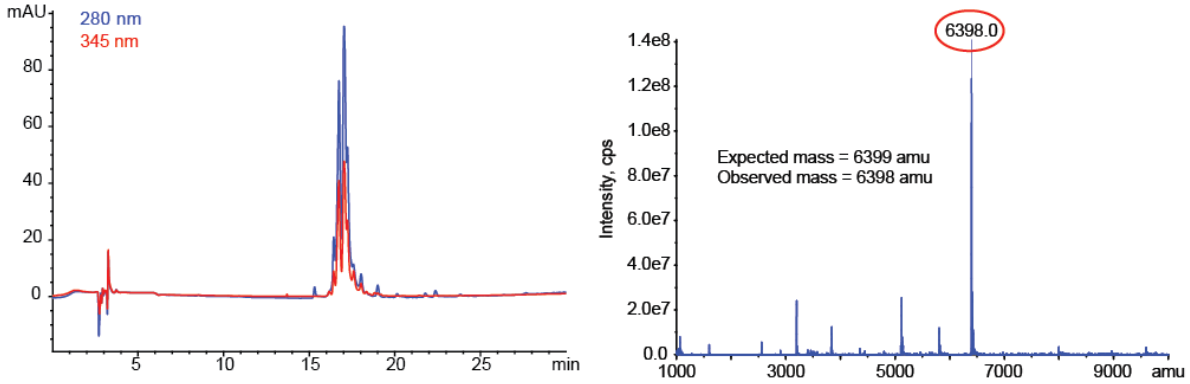

Figure 35 Ile-Ile-Ile-insulin analysis on HPLC (left) and MS (right)

Ile-Ile-Ile-insulin was purified on a 250 X 4.6 mm 5 µm C18 column. Mobile phases contained 0.1% trifluoroacetic acid. Ile-Ile-Ile-insulin was collected from 15.2-

17.2 minutes when run on 20-80% acetonitrile gradient over 30 minutes, at 0.75 mL/min (Figure 35).

Determination of isoelectric point of non-polar insulin variants

Diazo chemistry was utilized in this study in order to conjugate the photocleavable tag with insulin as an ester. All the non-polar insulin variants were characterized using chromatography and mass spectrometry, but these techniques do not reveal the nature of the residue on which the reaction occurred.

Conjugation is expected to occur on the carboxylates of the protein. The negatively charged functional groups on insulin are the carboxylic acids (aspartates, glutamates and C-termini) and phenols (tyrosines). However, tyrosine usually exists in the neutral protonated form at physiological conditions and does not affect the charge of the protein. Hence, it can be assumed that the negative charges on insulin are majorly contributed by carboxylic acids. Reaction of the photocleavable tag with insulin converts the acid into an ester, thereby quenching a negative charge on the protein. Therefore, the protein loses a unit negative charge and the isoelectric point is expected to increase.

If the photocleavable tag reacts on any positively charge groups like amines or guanidines, it is possible that the isoelectric point will decrease or remains the same. The pI decreases if the amine or guanidine are converted into other functional groups such as carbamates or ureas. It will not be effect if lysines or guanidines are just alkylated into secondary amines or guanidines, but still have their basic nature

preserved. Therefore, isoelectric points of these insulin variants were determined on an isoelectric focusing gel.

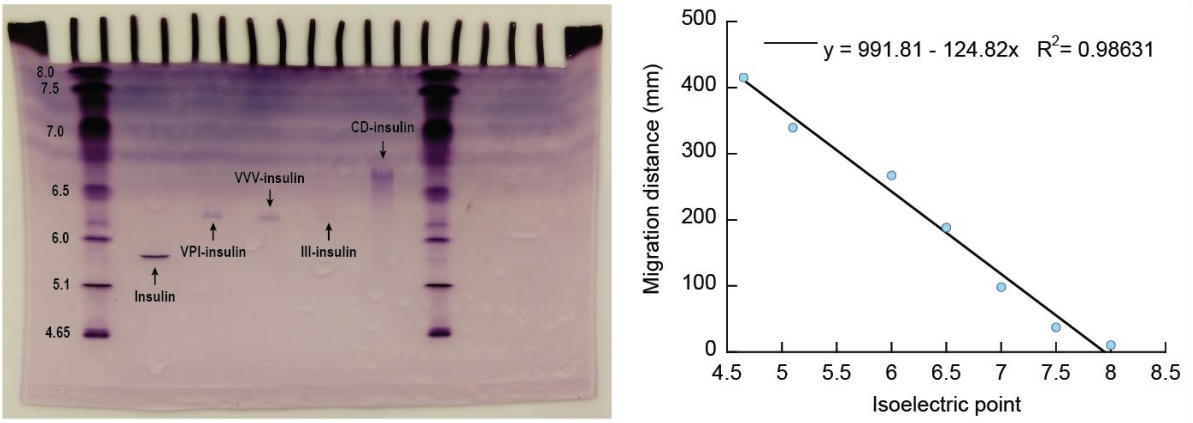

Figure 36 Hydrophobic tag insulin variants - isoelectric focusing

Briefly, 1 nmol of each of the non-polar insulin variant (8 µL) each were diluted to 10 µL with IEF sample buffer. Samples and IEF standards were loaded on the IEF gel. 1x cathode and anode buffers were added in cathode and anode chambers, respectively. Gel was run for one hour at 100 V, another one hour at 250 V and an additional 30 minutes at 500 V. Gel was then fixed with 15% glutaraldehyde in 30% methanol for 2 hours. Since insulin is a small protein, bands were fixed by crosslinking with glutaraldehyde (methanol-based fixing did not work for either insulin, or its variants). The gel was then washed with 27% isopropanol, 10% acetic acid solution to remove any traces of glutaraldehyde. Staining was performed for 45 minutes with a 0.1x staining solution (1x composition: 0.04% w/v Coomassie Blue R-250, 0.05% w/v Crocein Scarlet in 27% isopropanol, 10% acetic acid). It was observed that the staining of the bands was non-uniform between different species, which may depend on the nature of the protein itself. The gel was destained with 40% methanol, 10% acetic acid

solution. Images of the gel were captured, and migration distance was analyzed on Adobe Photoshop to determine isoelectric point (Figure 36).

Table 3 Protein isoelectric points and distances migrated

Protein	Isoelectric point	Distance (mm)	Determined pI
Phycocyanin	4.65	415.6	
B-Lactoglobulin B	5.1	339.4	
Bovine carbonic anhydrase	6.0	267.4	
Human carbonic anhydrase	6.5	188.4	
Equine myoglobin	7.0	98.3	
Human Hb C	7.5	37.4	
Lentil Lectin	8.0	10.6	
Insulin		293.5	5.6
Val-Pro-Ile-insulin		232.8	6.1
Val-Val-Val-insulin		231.1	6.1
Ile-Ile-Ile-insulin		227.0	6.1
CD-insulin		243.8 – 161.9	6.0 – 6.6

Native insulin has an isoelectric point of 5.4[39]. It was seen on the IEF gel that insulin band is focused at 5.6 pH (Table 3). As predicted, the pI of insulin variants was raised from 5.4 to ~6.1 due to the quenching of a negative charge. The final material is also a mixture of regioisomers – in which the photocleavable tag reacted at different sites on different insulin molecules. All the isomers seem to have the same pI, indicating that the difference in pI is caused due to reaction on only one type of the negatively charged amino acids.

CD-insulin being a very hydrophobic tag, did not run well and can only be seen as a smear[40]. Since the pI shifted by a significant amount, i.e. about 0.6 units, it can be concluded that a strong negative charge such as a carboxylate was quenched by the photocleavable tag.

Preparation and study of injectable non-polar insulin variants

In this study, unnatural and peptidic photocleavable tags were conjugated with insulin with the aim of lowering insulin solubility in aqueous conditions. Therefore, these insulin variants will be insoluble in physiological buffers at pH 7. Due to the presence of non-polar groups, these materials will also have a lower solubility at both acidic and basic pHs. Purified dried materials are at least required to be suspended, if not dissolved, in buffers (vehicle) for injection. Insulin suspensions (NPH insulin) have been previously approved by the FDA for injection. But the crude suspensions of photoactivated insulins may not have a uniform particle size and hence clog the needle during injection. This may complicate the delivery process. Therefore, it is critical to address this problem and optimize an ideal and reproducible delivery method.

A simple, yet reliable approach was developed to deliver such non-polar proteins. It was observed that these non-polar insulin variants form particles of roughly uniform size when they are ground with a tissue homogenizer in PBS. Briefly, dried hydrophobic insulins in Eppendorf tubes were suspended in 10 mM PBS pH 7.2 at a concentration of 1 mM (150 nmol/150 µL). Materials were milled with Argos Motorized Pestle Mixer for 1 minute on ice. pH was adjusted to 7.2 with minute

volumes of sodium hydroxide and milled again for 4 minutes. This process resulted homogenous milky suspensions of each material. These suspensions were studied for their ability to pass through a 31G needle of a typical insulin syringe. Studies were also performed to know how concentrated these suspensions can be made, to determine the amount of insulin that can be injected as a depot.

Particle size analysis

It is important to study the size of the particles formed with this method to know if they can pass through the syringe, or if they will be retained at the site of injection. Malvern Zetasizer Nano was used to determine the size of these particles. 40 µL of the 1 mM suspension was diluted to 1 mL in 10 mM PBS 7.2. Particle size was determined using the Zetasizer. The observations show that the size of particles of any non-polar insulin variant lies in the higher micron range (Table 4).

Table 4 Size of non-polar insulin particles determined with Zetasizer Nano

Protein	Particle size, z average (d. nm)
VPI-insulin	673.9 ± 129.5
VVV-insulin	456.8 ± 191.1
III-insulin	629.1 ± 11.2
CD-insulin	1540 ± 123.9

This is ideal in two ways – (a) particles of this size easily pass through a 31G needle as the needle's internal diameter is larger, and (b) particles of this size are ideal to be injected as a depot[41]. Sizes above this range may result in immune responses,

and below this range may easily diffuse through the matrix of skin and not retain at the site of injection.

Injectability

Since the size of the milled particles lie in an ideal range, an experiment was carried out to know if these particles pass through a 31 G needle. In this study, CD-insulin was used due to the ease of synthesis in large amounts. Moreover, the size of CD-insulin particles was observed to be the highest – if CD-insulin can pass through the needle, rest of the materials can also be easily injected.

2 µmol CD-insulin was suspended in 80 µL 10 mM PBS pH 7.2. pH of the suspension was adjusted with minimal quantity of NaOH. Final volume of the suspension was adjusted to 100 µL to achieve a concentration of 20 mM. Suspension was milled with a motorized homogenizer for 4 minutes on ice. The tube was centrifuged at 1000 g for 2 minutes to remove froth. Particles in the pellet were re-suspended in the supernatant with the help of a pipettor, taking care that froth was not regenerated. The suspension was loaded into a glass syringe with a 31 G needle with a pipettor. It was passed through the needle into a HPLC glass insert by pushing the plunger (Figure 37). Amount of CD-insulin that passed through the 31 G needle was quantitated by diluting the suspension in DMSO and quantitated by UV spectroscopy (ϵ_{max} = 4470 M^{-1} cm^{-1}). Additional PBS was used to wash the syringe and extract traces of CD-insulin particles left in the syringe. Buffer was collected in another HPLC glass insert and quantitated by UV spectroscopy (345 nm), by diluting

it in DMSO. This wash step was repeated until no more CD-insulin was seen in the buffer.

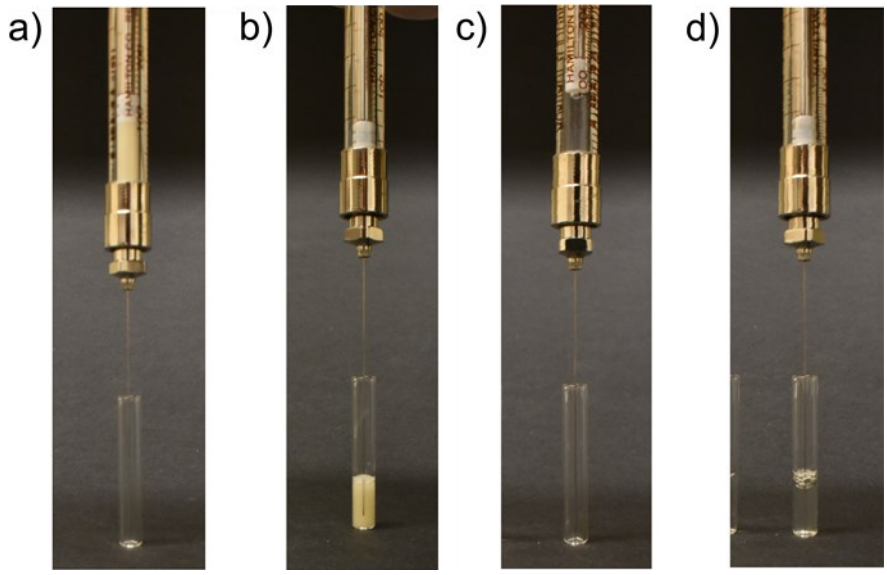

Figure 37 Pictorial demonstration of non-polar tagged insulin injectability through a 31 G needle. a) Material in syringe prior to injection. b) Material after injection into tube. c) Rinse buffer in syringe prior to injection. d) Rinse buffer after injection

It should be noted that the highest concentration achievable was about 20 mM. Acidity of the final insulin variant lowers the pH of the buffer. Addition of sodium hydroxide solution to lower the pH dilutes the solution and lowers the concentration. Also, CD-insulin was no longer a suspension at higher concentrations - the material behaved as a paste and hence could not be loaded into the syringe.

This experiment revealed that with the replacement of polymer with the tags, significant developments were made in two ways over the first-generation PAD material. Firstly, it demonstrated that the next generation materials such as CD-insulin can be milled into particles at a concentration of 20 mM. This is a significant

advancement over the first-generation PAD, as 120 µL of this suspension contains hormone that is enough for about a week for a T1D patient. Second, it was observed that >99% of the 20 mM suspension passed through the 31 G needle in the first injection. In comparison, a larger diameter needle (27 G) was used to inject the first-generation material in rodent models[31].

Solubility of non-polar insulin variants

The goal of this study is to lower insulin solubility by conjugation of non-polar photocleavable tags. To understand the effect of this chemical modification, solubility of insulin and the non-polar variants were determined at physiological pH. Since a 10 mM phosphate buffer pH 7.2 is the best buffer that is closest to physiological conditions, solubility was determined by saturating this buffer with the respective insulin species.

100 nmol of insulin particles were suspended in 100 µL 10 mM PBS 7.2, in Eppendorf tubes. pH was adjusted to 7.2 with small amounts of 0.1 N sodium hydroxide. Tubes were shaken for 2 hours at 300 RPM. Tubes were then centrifuged (15000 g, 5 minutes) and the amount of protein in the clear supernatant was analyzed by HPLC. Pellet left in tubes after centrifugation was also dissolved in DMSO and analyzed on HPLC to know that saturation was achieved and quantitate the amount undissolved. Solubility of the 4 non-polar insulin variants was compared with that of native insulin.

Table 5 and the Figure 38 show the solubility of each species in PBS. A clear trend in the solubility reduction can be seen with an increase in the non-polarity of

the tag. Peptidic tags lowered the solubility to low μM range. Cyclododecyl modification, being the most non-polar among all the tags, lowered insulin solubility by ~1300x to sub-μM range. This reduction in solubility is enough for the creation of depots, as it is known that commercially available long acting insulin that form subcutaneous depots have solubility in low μM ranges.

Table 5 Solubility of insulin and non-polar insulin variants

Species	Solubility (μM) ± S.D.	Reduction
Insulin	1053.0 ± 158.1	-
VPI-insulin	54.4 ± 1.9	20x
VVV-insulin	10.7 ± 1.3	100x
III-insulin	3.0 ± 0.7	350x
CD-insulin	0.81 ± 0.06	1300x

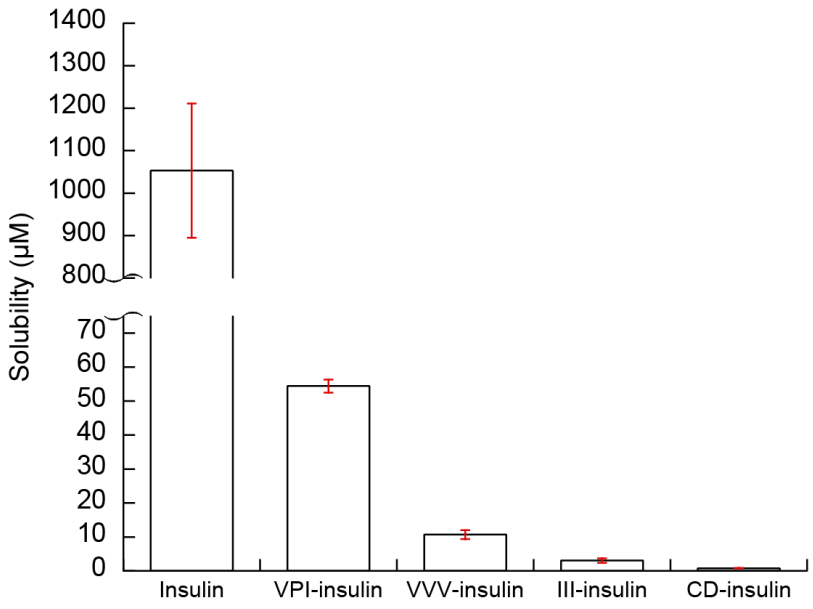

Figure 38 Solubility of insulin versus non-polar insulins (Mean ± SD)

Insulin photorelease in PBS

Chemical modifications were performed on insulin to lower the solubility of insulin to sub-μM range. Thus, the non-polar insulin variants stay as insoluble particles in solid state, i.e. they may not be solvated when injected under the skin. Therefore, it is critical to study if the photochemical reaction occurs with the materials that are out of the solution phase to release of native soluble insulin into the solution. It will also be beneficial to know at what rate this insulin release will occur. This is to predict the amount of insulin photoreleased and ultimately develop an automated insulin delivery system. An *in vitro* experiment was designed to study this phenomenon.

1 mM suspension of the non-polar insulins, 100 nmol in 100 μL were taken in 1 mL HPLC glass inserts. The tube (bottom) was placed 5 cm away from a Nichia 200 mW 365 nm LED (absolute irradiance = 1.95 mW/cm^2). Materials were exposed to light for specific time intervals. The tubes were centrifuged at 15000 g for 5 minutes and the total clear supernatant was collected from the tubes for analysis. The pellet was resuspended in 100 μL fresh buffer and the irradiation was continued till the next time point. A control tube containing 100 nmol was also used for each hydrophobic insulin, which was not exposed to light. The amount of insulin released into the supernatant was analyzed by IEF gel. Insulin in these supernatant samples was estimated using an insulin standard curve, run on the same gel. Band intensity was determined by analyzing the pictures using Adobe Photoshop. See Figure 39.

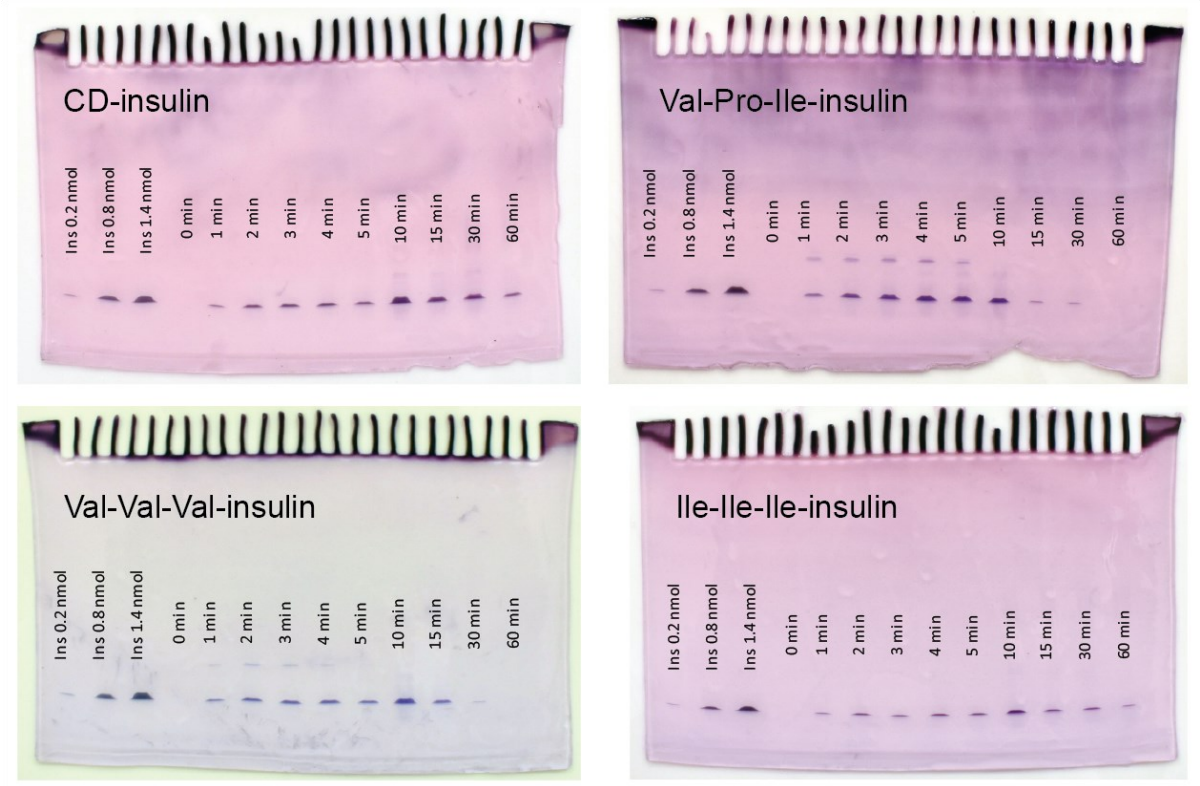

Figure 39 Photolytic release of native soluble insulin from non-polar tag materials. IEF gel showing insulin released into supernatant upon different periods of irradiation

These gels showed that the native insulin was photo-released from all the non-polar insulins into the supernatants. The reaction is expected to be a second order reaction as the rate should depend on the concentration of both the reactants, viz., photons and the modified insulins. But since the number of photons is very large in number relative to the number of molecules of modified insulins, an apparent rate is observed that is dependent only on the concentration of the modified insulin. Therefore, this is a pseudo first order reaction. Insulin release was plotted as a function of time and fitted using the following first order equation in Kaliedagraph,

Insulin = Non-polar-insulin$_{t=0}$ [1 – exp^{-kt}]. Following results were obtained (Figure 40, Table 6).

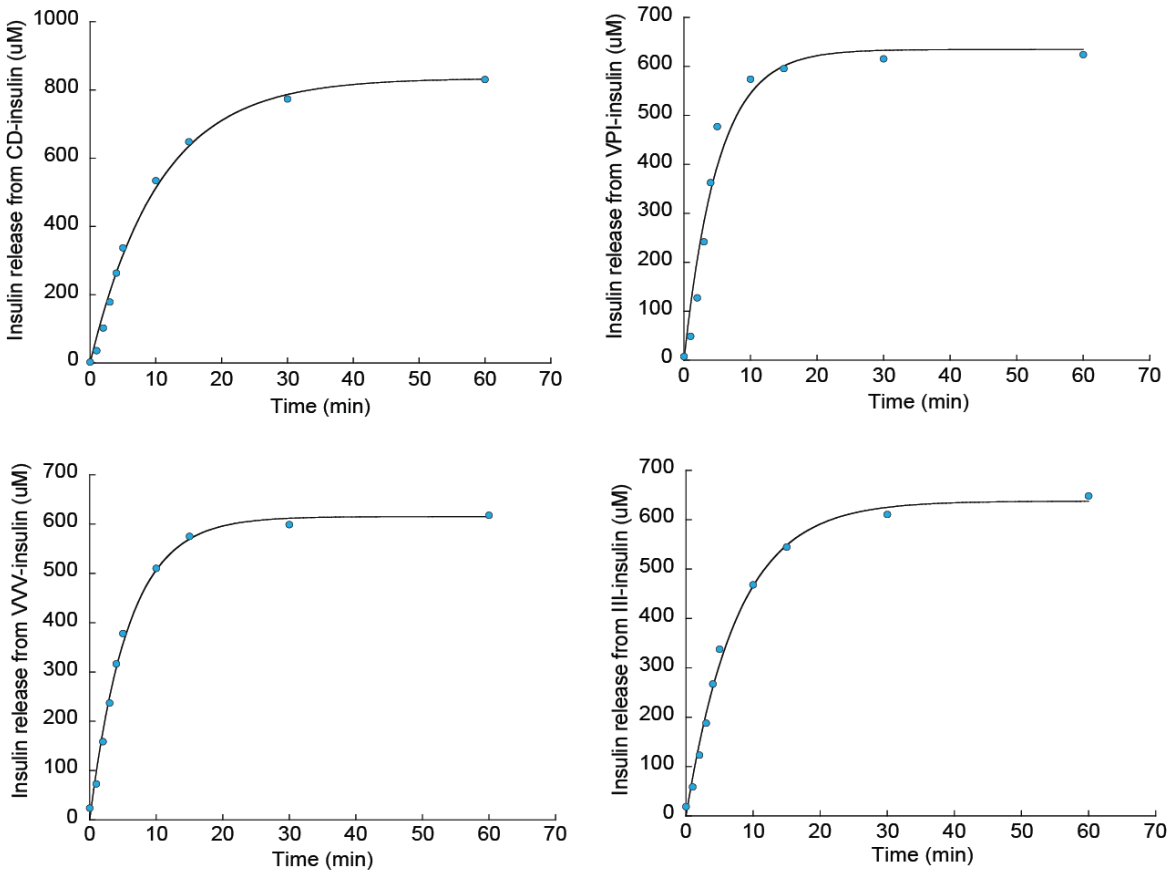

Figure 40 Insulin photorelease from non-polar tag variants in PBS. Cumulative insulin concentration in the buffer over time is plotted for all 4 species

The rates of insulin photorelease from all 4 non-polar insulins lie in the range of ~0.1 – 0.2 min^{-1}. These results matched with prediction as all variants have the same photocleavable group. A trend can also be noticed with the rate of insulin release. More the non-polarity of the tag, the slower is the insulin release. This may be due to the physical nature of the particles. As the non-polarity of the particle increases, it

may be harder for insulin to get into the buffer and be solvated. Therefore, a slow release may be observed for more non-polar tags.

Table 6 Kinetic rate constants for the photolytic release of insulin from all non-polar insulins.

Species	Photolysis yield (%)	k (min^{-1})	Error of k (from the fit)
CD-insulin	83.4	0.095	0.006
VPI-insulin	63.5	0.19	0.029
VVV-insulin	61.5	0.17	0.009
III-insulin	63.8	0.13	0.008

Summary

Firstly, the tag approach established here has a wider applicability for the development of photoactivated depots of many proteins. Also, the methods developed in this study can be applied to conjugate a wide variety of peptidic photocleavable tags with proteins. The tag approach made significant advancements in photoactivated delivery of insulin. By replacing the polymer with tags, the density of insulin as well as the photocleavable groups improved significantly. The PAD materials consisted ~90% insulin w/w. These new generation PAD insulins can also easily pass through a 31 G needle, which was possible only due to use of photocleavable tags.

In this study, insulin solubility was lowered by conjugating different non-polar photocleavable tags with the protein. Peptidic tags offer variety in terms of design. But aliphatic unnatural compounds lower the solubility drastically and can make efficient PAD materials. Solubility of insulin was lowered by ~1300x with the cyclododecyl tag. These insoluble materials behaved as ideal PAD materials as native soluble insulin was released in a predictable manner when they are exposed to light.

CHAPTER 4

THE CHARGE TAGS

Introduction

In the previous chapter, insulin solubility was lowered by making use of the principles of hydrophobic effect. Different non-polar photocleavable tags were conjugated with insulin, and thus an increase in the area of non-polar protein surface conferred insolubility to the protein. This chapter discusses an alternative approach to lower solubility, i.e. by the manipulation of total charge on protein.

A trend is generally observed with the solubility in biological molecules – the higher the net charge, the higher is its solubility in aqueous environment. This is because the charged functional groups associate well with water with charge-charge interactions and hydrogen bonds. For instance, nucleic acids such as DNA and RNA have a negatively charged phosphodiester backbone. Proteins also fold in such way that minimize exposure of hydrophobic domains to water, and hence maximize exposure of hydrophilic charged functional groups and their interactions with water.

Effect of pH on protein charge

Chemical properties of a protein can be described by the properties of the amino acids with which it is made of. The sequence of amino acids in the protein determines the way they fold and what net charge they have. A protein can be considered acidic and has a net negative charge if it contains more aspartates/glutamates than the lysines/arginines and vice versa. Individually at the level of amino acids, the side chains contain chemical functional groups whose

behavior is nevertheless determined by the principles of chemical equilibria and their acid-base properties. Therefore, it is necessary to understand the nature of charges and how they are affected by the environmental pH. Based on the knowledge available on pKas of all biochemical functional groups, we can predict if a specific group on a protein, and hence the protein, will be charged or uncharged at a given pH.

Acid-base properties of these functional groups can be described with the help of pKas. At a lower acidic pH (below pKa), all the side chains of amino acids are in their protonated states as the excess protons in environment tend to bind with the functional groups. In this case, carboxylates gain protons and lose their negative charge and amines/guanidines gain their positive charges. Likewise, at a pH above their pKas, the functional groups are deprotonated. Here, carboxylates are deprotonated and gain negative charges and amines/guanidines lose their positive charges. The Henderson-Hasselbach equation tells us the fraction of molecules that remain charged or uncharged at any given pH.

Proteins are polymers of amino acids, i.e. they have multiple positive and negative charges. In general, a protein cannot be 'uncharged' at any pH. The protein will have a net positive charge at lower pH as the carboxylates lose their charge, and the basic functional groups are protonated. At higher pH, the carboxylates are deprotonated and charged while the basic residues are deprotonated – imparting a net negative charge to the protein. Due to the combined effect of acidic and basic functions, the Henderson-Hasselbach equation alone cannot be applied to study the

charge on proteins. The total charge on a protein at a given pH is an approximation of the sum of charges of individual amino acids. The fraction of each functional group on proteins that remains charged at any given pH is first determined by the Henderson-Hasselbach equation. Then, the total charge on the protein is estimated by calculating the sum of all the charges at that specific pH. Several online tools can predict the pH at which net charge on proteins is zero, though their calculations are not always reliable.

pH dependent protein solubility and insulin isoelectric point

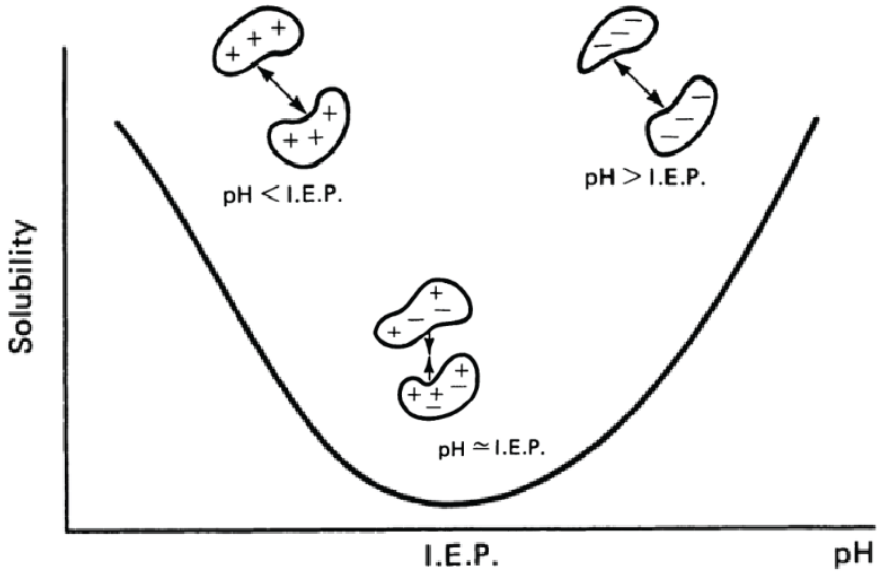

Figure 41 The effect of pH on protein solubility. Image taken from[42]

We have seen how environmental pH affects the charge on protein. Also, protein solubility increases with an increase in net charge, as charged groups interact well with water and solvated. At lower pH, there is an excess of positive charge on a protein and hence has a net positive charge. Similarly, protein loses protons at higher pH to have an excess of negative charges. During the transition from a low pH to high

pH, the amount of positive and negative charges on protein vary in an opposite way. At a point on the pH scale, the 'amount' of positive charges will be equal to the 'amount' of negative charges, i.e. the net charge on protein is zero. This pH is termed as the isoelectric point (pI) of the protein. At the isoelectric point in any buffer, the protein also has the lowest solubility because of the lack of a net charge. The protein interacts weakly with water at this point, but aggregates with the neighboring protein molecules and crashes out of the solution. Isoelectric points vary between protein to protein and depends on the sequence of amino acids. Figure 41 shows a plot of how a protein's solubility is modulated by the pH of environment.

Structure of human insulin is discussed earlier. Briefly, it consists of A (21 amino acids) and B (30 amino acids) chains connects with two disulfide linkages. Insulin has six negative charges, contributed by four glutamates along with two C-termini of A and B chains. On the other hand, insulin only has four positive charges from a lysine, an arginine and the two N-termini. Therefore, there are an excess of two negative charges on the hormone at pH 7. Insulin is thus an acidic protein and its isoelectric point is observed to be 5.4[39]. It has the lowest charge and solubility at pH 5.4 and precipitates out of solution.

The charge tag approach

The rationale for this alternative approach is to make use of the isoelectric point of the protein to create photoactivated depots. The goal of this study is to raise the isoelectric point of insulin to ~7.2 by chemical modification with a charged tag, so that

the modified insulin will be least soluble at skin pH[43]. This allows precipitation of the protein at the site of injection (Figure 42).

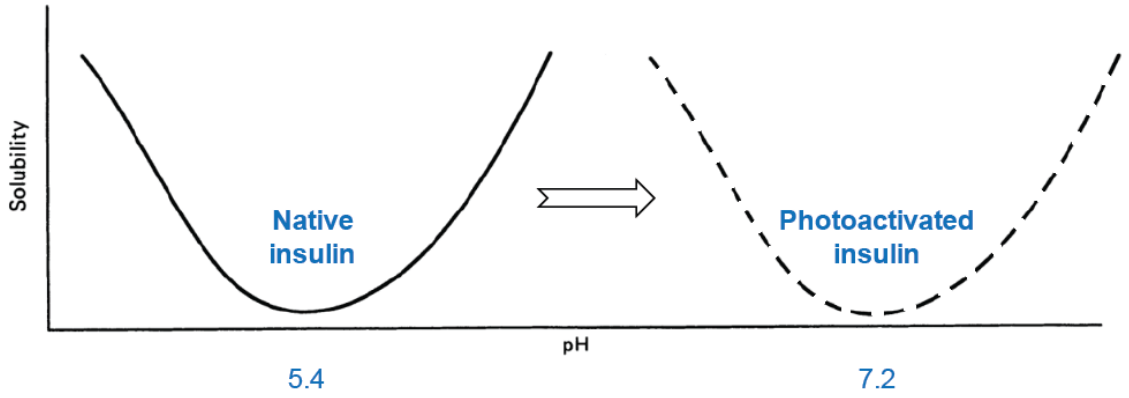

Figure 42 Goal of the charge-tag approach in PAD

Upon photolysis, the charged tag will be cleaved off the protein and native, soluble insulin will be absorbed into the blood from the depot. An additional advantage with the charge tags is that, after photolysis the tag is cleared faster than the non-polar tags are the tag itself will have charges and will be polar.

Design of the tags is critical in this approach as it varies from protein to protein. So, the design in this study is discussed only for insulin. Firstly, tags are required to be basic to provide positive charges to the protein on conjugation to raise the pH. However, the second step, i.e. to estimate the number of basic functions to raise the pI from 5.4 to 7.2, is a major challenge in this approach. Though the charge on protein at pH 7.2 can be calculated mathematically, these calculators do not predict accurately for chemically modified proteins. Therefore, prior literature was pursued to design the tags appropriately.

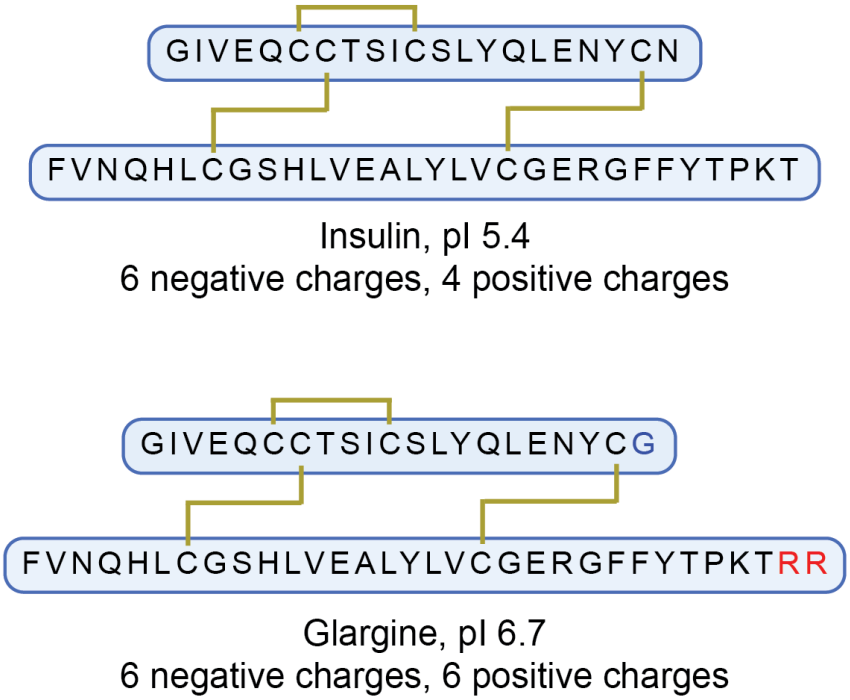

Figure 43 Primary structures, isoelectric points, and number of charges on insulin and glargine

Glargine (Lantus ®) is a long acting insulin marketed by Sanofi. This protein is designed to have lower solubility at physiological pH in comparison to native insulin. This was achieved by making use of the concept of protein charge and isoelectric point. This designer insulin is genetically modified to have two additional arginines at the C terminus of the B chain (Figure 43). This adds two positive charges to insulin and the observed isoelectric point of this protein is 6.7. Since the isoelectric point of designer insulin is closer to the physiological pH, it is less soluble in the skin tissue. Therefore, the protein precipitates at the site of injection and is very slowly absorbed into the blood to act like a long acting insulin. For ease of injection, the protein is solubilized in a formulation maintained at pH 4. The C terminal asparagine of A chain

is also modified to glycine in glargine; this is to maintain stability of the protein in the acidic formulation by preventing deamidation of the side chain.

Based on this information, a model was developed for raising the isoelectric point of insulin to 7.2. Since addition of two positive charges resulted in a shift of isoelectric point from 5.4 to 6.7 in glargine, i.e. by 1.3 units, it was assumed that a single positive charge would raise the pI by 0.65 units. Based on this calculation, addition of three positive charges should raise the isoelectric point of insulin by 0.65 x 3 times to approximately 7.2.

However, photoactivated insulin will not be developed by genetic incorporation of positive charges. Chemical reactions will be performed to link the photocleavable tag with insulin. Specifically, diazo chemistry will be applied to esterify a carboxylic acid on the protein. It should be noted from the hydrophobic tag approach that esterification of the protein with a photocleavable tag will raise the pI of insulin from 5.4 to ~6. This reaction resulted in 0.65 units increase in pI of protein. Therefore, it was also concluded that the quenching of one of the negative charges on the protein by chemical reaction is equivalent to the addition of a positive charge. Based on this knowledge, charge tags were designed according to the model discussed in the Table 7. Neutral tags, tags with a single positive charge and two positive charges should be explored systematically to prove this hypothesis. However, all the non-polar tags are neutral, and we have seen that their isoelectric pint is ~6. Therefore, neutral tags are not further explored in this study. Two versions

of a singly charged and doubly charged tags each will be designed. Both unnatural and peptidic tags are explored in this study.

It should be noted that this addition is limited by the pKa of the modifying functional group. For example, modifying insulin with 'n' guanidine moieties will not raise the pI by n x 0.65 units. But the it can raise until the pI of the protein equals the pKa of guanidine and may not any further.

Table 7 Model showing the expected raise in isoelectric point of insulin for each modification

Species	#charges added	Model	Observed / Expected pI
Insulin	--	--	5.4
Lantus	2	5.4 + (2x0.65)	6.7
Chemical modification quenches one carboxylate, and raises the pI of protein from by 0.65 units from 5.4 to 6.05			
	0	6.05 + (0x0.65)	6.05
Variants	1	6.05 + (1x0.65)	6.7
	2	6.05 + (2x0.65)	7.35

P-insulin

P-insulin is a variant with a tag containing a single positive charge. Positive charges can be conferred with amines or guanidines. However, primary or secondary amines may not be neutral as they can potentially form by products during the reactions of hydrazone synthesis and diazotization. Therefore, the first tag is designed

with a 5-membered cyclic tertiary amine (pyrrolidine) and is condensed with the photocleavable group and conjugated with insulin. Since a pyrrolidine moiety is used in the construction of the tag, this insulin variant is named P-insulin. Conjugation raises the isoelectric point of insulin by 0.65 units in addition to the 0.65 units provided by positive charge on the tag. Therefore, the isoelectric point of this protein is predicted to be ~6.7. Synthesis was carried out using the same approach as shown in Figure 44.

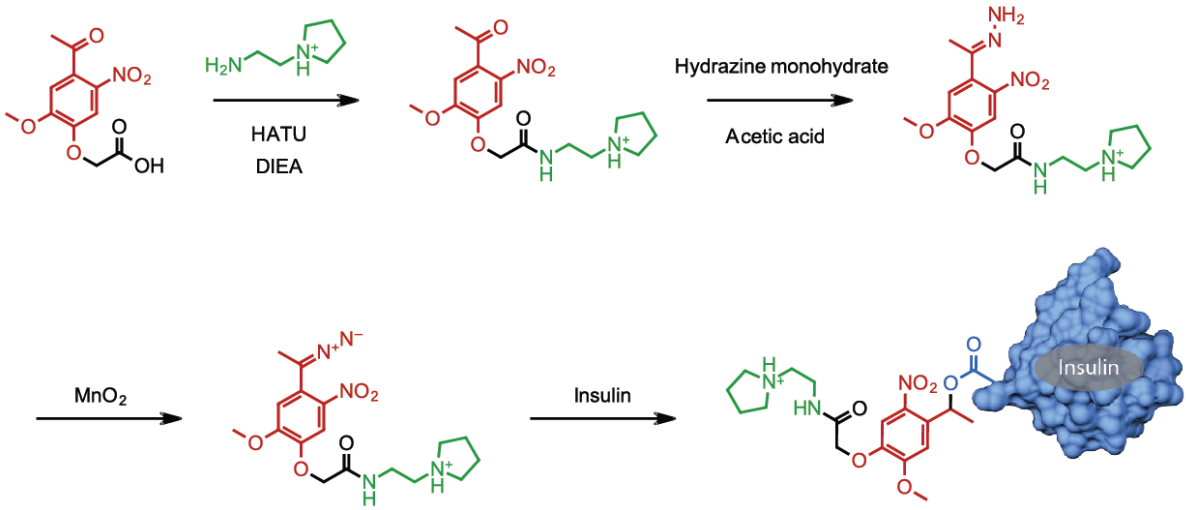

Figure 44 Synthesis of P-insulin

Synthesis of P-DMNPE

2-(4-acetyl-2-methoxy-5-nitro-phenoxy)-N-(2-pyrrolidin-1-yl-ethyl)-acetamide

106 mg of DMNPE-acid (394 µmoles, 65.6 mM) was dissolved in 6 mL of anhydrous N,N-dimethylformamide. 141 mg of HATU (372 µmoles, 60 mM) was added to the solution and allowed to stand for 5 minutes. 123 µL of N,N-diisopropylethylamine (744 µmol, 120 mM) was added, followed by addition of 47 µL of 1-(2-aminoethyl)pyrrolidine (372 µmoles, 60 mM) to the reaction mixture. Contents

were stirred and allowed to react for 3 hours. P-DMNPE was purified by partitioning the reaction between ethyl acetate and 0.5 N sodium hydroxide, followed by dehydration of organic layer with saturated sodium chloride. The solvent was evaporated to obtain the pure product (Yield = 94%). It was analyzed using HPLC and MS (Figure 45).

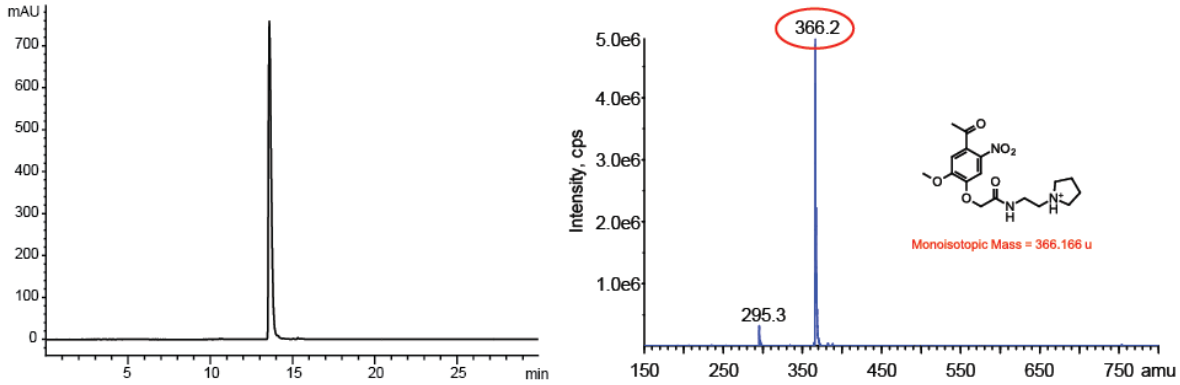

Figure 45 P-DMNPE analysis on HPLC (345 nm, left) and MS (right)

Synthesis of P-hydrazone

2-[4-(1-hydrazono-ethyl)-2-methoxy-5-nitro-phenoxy]-N-(2-pyrrolidin-1-yl-ethyl)-acetamide

Purified P-DMNPE was dissolved in 4 mL of ethanol:acetonitrile (1:1) solution. Concentration of P-DMNPE was quantified using UV spectroscopy (ϵ_{345} = 4470 M^{-1} cm^{-1}). Solution containing 524 µmol of P-DMNPE (36.8 mM, 14.24 mL) was transferred into a reaction vessel. 94 µL of glacial acetic acid (524.1 µmol) and 507 µL of hydrazine monohydrate (10.47 mmoles) were added and the reaction vessel was sealed. Contents were mixed and reaction was incubated for 4 hours at 90 C (Yield = 100% conversion). Reaction mixture was cooled, and P-hydrazone was purified on a

preparative HPLC C18 column using a 0-100% acetonitrile gradient. The pure product was analyzed using HPLC and LCMS (Figure 46).

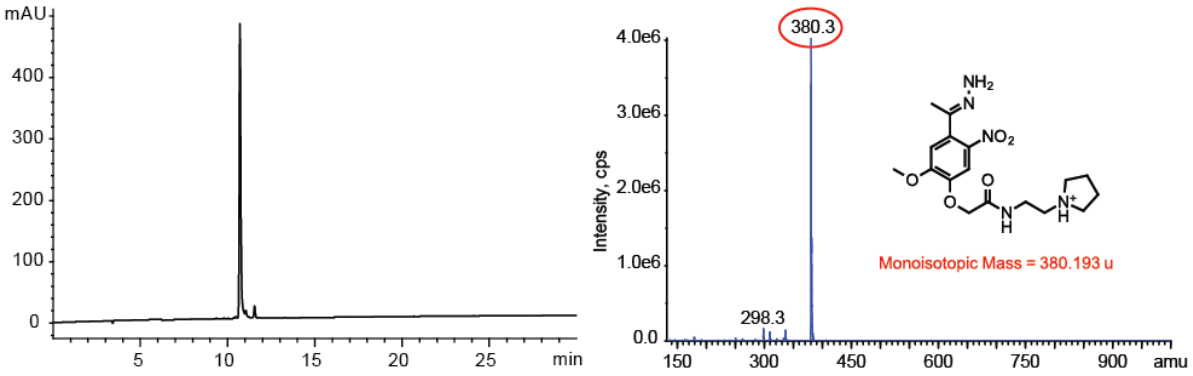

Figure 46 P-hydrazone HPLC (345 nm, left) and MS (right) analysis

Synthesis of P-diazo

2-[4-(1-diazo-ethyl)-2-methoxy-5-nitro-phenoxy]-N-(2-pyrrolidin-1-yl-ethyl)-acetamide

P-hydrazone was dissolved in anhydrous DMSO and quantified using UV spectroscopy (ϵ_{345} = 4470 M^{-1} cm^{-1}). Solution containing 6.4 µmol of P-hydrazone was diluted with anhydrous DMSO (to 383.8 µL) to a final concentration of 16.56 mM. The reaction was shaken vigorously with 120 mg of manganese (IV) oxide for 45 minutes. It was then centrifuged at 15000 g for 5 minutes to remove manganese oxide. The manganese oxide pellet was washed with additional DMSO to recover any trapped P-diazo. DMSO solution containing P-diazo was immediately used for reaction with insulin. P-diazo can be identified by its characteristic red color and absorbance at 450 nm (Figure 47). Yield of the diazotization is estimated from the successive esterification reaction (as any diazo formed will be trapped by insulin).

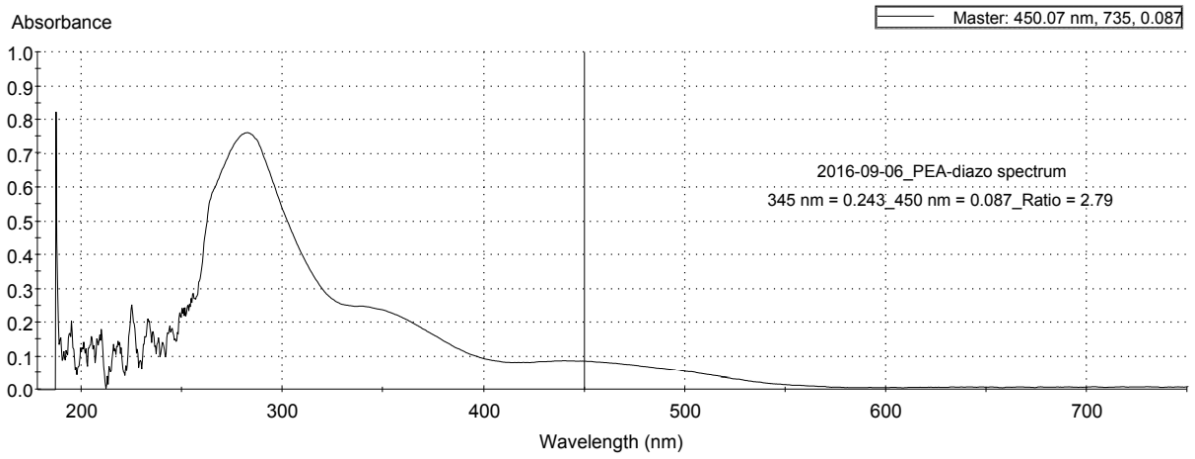

Figure 47 P-diazo UV-visible spectrum

Synthesis of P-insulin

6.4 µmol of insulin (36.9 mg) was dissolved in 383.8 µL of anhydrous DMSO. DMSO solution containing 6.4 µmol of P-diazo (assuming 100% conversion) was added to insulin solution. The reaction was incubated in dark for 24 hours (Yield = 16%).

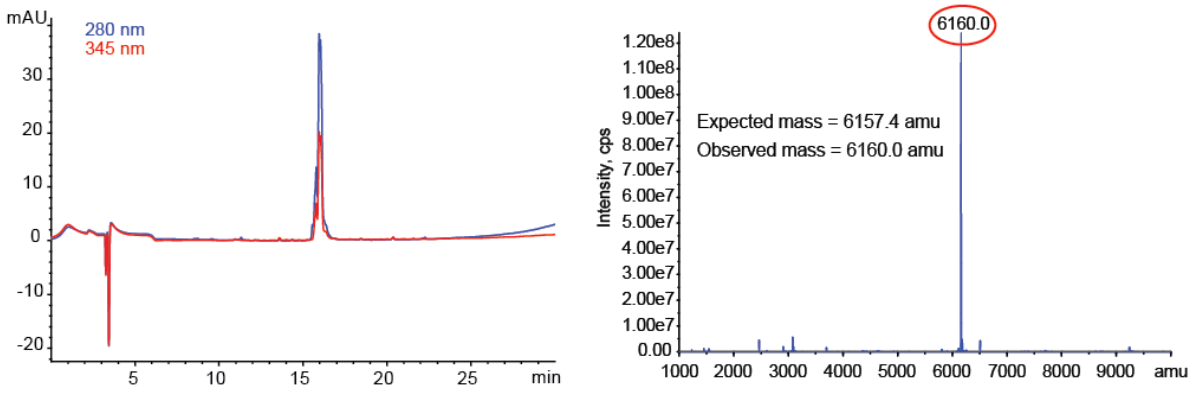

Figure 48 P-insulin analysis on HPLC (left) and MS (right)

P-insulin was purified by repeated injections on RP-HPLC using 250 x 4.6 mm, 5 µm, C18 column. Flow rate was adjusted to 1 mL/min on a 24% acetonitrile to 38%

acetonitrile gradient over 35 minutes. Compound 6 was collected from 26.0 – 32.0 minutes. Solvents contained 0.1% trifluoroacetic acid. Purified P-insulin was characterized using HPLC and MS (Figure 48).

Determination of P-insulin isoelectric point

0.5 nmol/μL solutions of insulin, Glargine (diluted from Lantus formulation, (ϵ_{280} = 5128 M^{-1} cm^{-1}), and P-insulin (ϵ_{345} = 4470 M^{-1} cm^{-1}) were prepared in DMSO. 1 nmol of each of the proteins, along with the standards were loaded on an IEF gel.

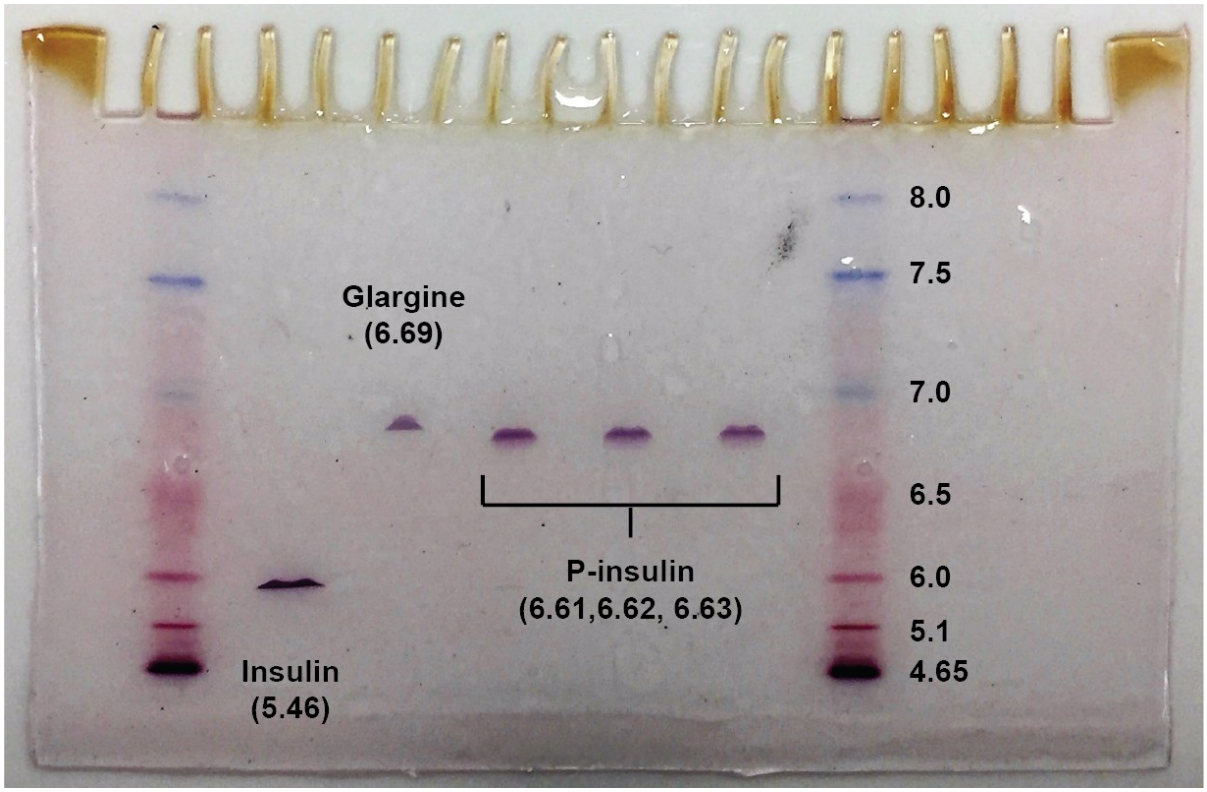

Figure 49 Isoelectric focusing gel electrophoresis of insulin, glargine and P-insulin

Electrophoresis was performed as described for the non-polar tag variants by varying the voltage at respective time intervals. Protein bands were fixed with glutaraldehyde and stained with a Crocein Scarlet-Coomassie Blue R-250 mixture.

The gel was then destained with 40% methanol, 10% acetic acid solution. After the gel image was captured on a white background, the distance migrated by proteins in the gel was analyzed using Adobe Illustrator. pI of P-insulin was estimated by comparing its migration distance with the distances of protein standards (Figure 49). It is clearly understood from the IEF gel that the isoelectric point of P-insulin was raised to ~6.7. This was the first experimental evidence that the developed model was accurate in predicting the isoelectric point shifts.

Q-insulin

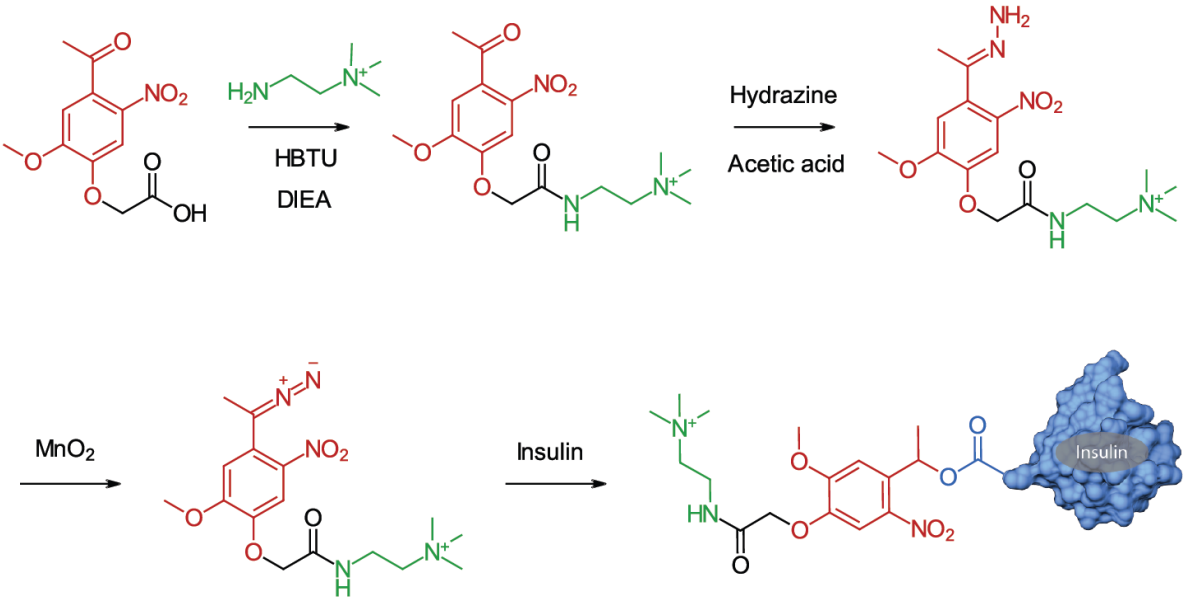

Figure 50 Synthesis of Q-insulin

Q-insulin is also another insulin variant modified with a tag containing a single positive charge. Like P-insulin, the predicted raise in isoelectric point will be by 1.3 units, i.e. from 5.4 to 6.7. The charge on tertiary amines can be affected by the pH of the environment as the amine has a pKa of ~10. However, the positive charge provided by the quaternary ammonium species is independent of the pH. Therefore,

in this study a tag with a quaternary ammonium group is used. Thus, this insulin variant is named Q-insulin. Synthetic route is discussed in the Figure 50.

Synthesis of Q-DMNPE

{2-[2-(4-acetyl-2-methoxy-5-nitro-phenoxy)-acetylamino]-ethyl}-trimethyl-ammonium trifluoroacetate

0.77 g of DMNPE-acid (2.86 mmol, 120 mM) was dissolved in 23.8 mL of anhydrous NMP. 2.17 g of HBTU (5.7 mmol, 240 mM) was dissolved in this solution and allowed to stand for 5 minutes. 2.4 mL of N,N-diisopropylethylamine (14.3 mmol, 600 mM) and 0.25 g of (2-aminoethyl)trimethylammonium chloride hydrochloride (372 µmol, 60 mM) were added to the reaction mixture. Contents were dissolved and allowed to stand for 12 hours. Q-DMNPE was purified on a 250 x 21.2 mm, 10 µm, C18 reverse phase HPLC. 3 mL of reaction was directly injected on each run. Pure product was collected from 32.0-36.0 minutes when run on a 0% to 100% acetonitrile gradient over 70 minutes with a flow rate of 5 mL/min. Solvents contained 0.1% TFA. Product was analyzed using HPLC and LCMS (Figure 51). Yield = 77%.

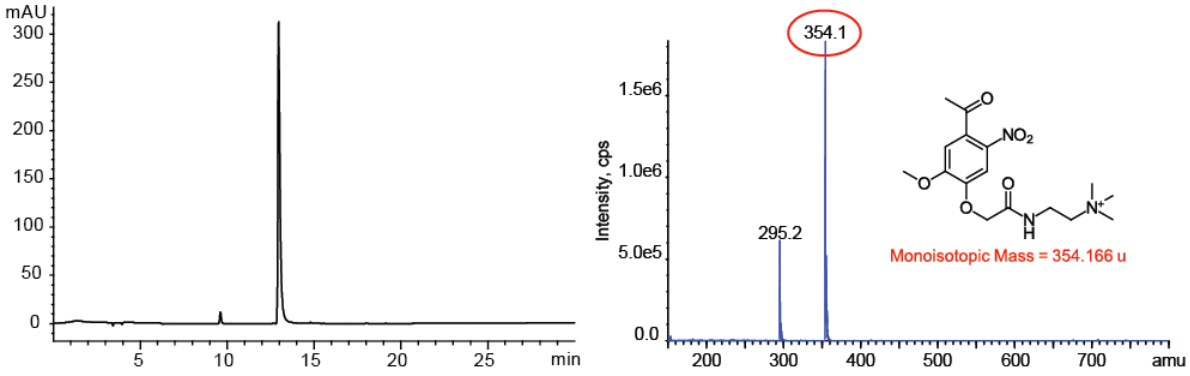

Figure 51 Q-DMNPE analysis on HPLC (345 nm, left) and MS (right)

Synthesis of Q-hydrazone

2-{2-[4-(1-hydrazono-ethyl)-2-methoxy-5-nitro-phenoxy]-acetylamino}-ethyl)-trimethyl-ammonium hydrochloride

Q-DMNPE was quantified using UV spectroscopy (ϵ_{345} = 4470 M^{-1} cm^{-1}) in DMSO. Stock solution containing 29.45 µmol of Q-DMNPE was transferred into an Eppendorf tube and solvent dried in vacuum. Dried Q-DMNPE was dissolved in 772 µL of ethanol:acetonitrile solution 80:20 (38.15 mM). 2.64 µL of glacial acetic acid (44.2 µmol) and 100 µL of hydrazine monohydrate (2 mmol) were added and reaction vessel was sealed. Contents were mixed and allowed to react for 36 hours at 60 C (Yield = 100% conversion). Q-hydrazone was observed to be highly unstable. It converts to Q-DMNPE soon after the reaction is dried. Therefore, Q-hydrazone is precipitated out of the reaction mixture using excess cold ether. The suspension was then centrifuged to collect the precipitated Q-hydrazone and the impure ether was discarded. The pellet was dried in vacuum thoroughly to remove any traces of ether and immediately used for the oxidation reaction. Pure Q-hydrazone was analyzed using HPLC and LCMS (Figure 52).

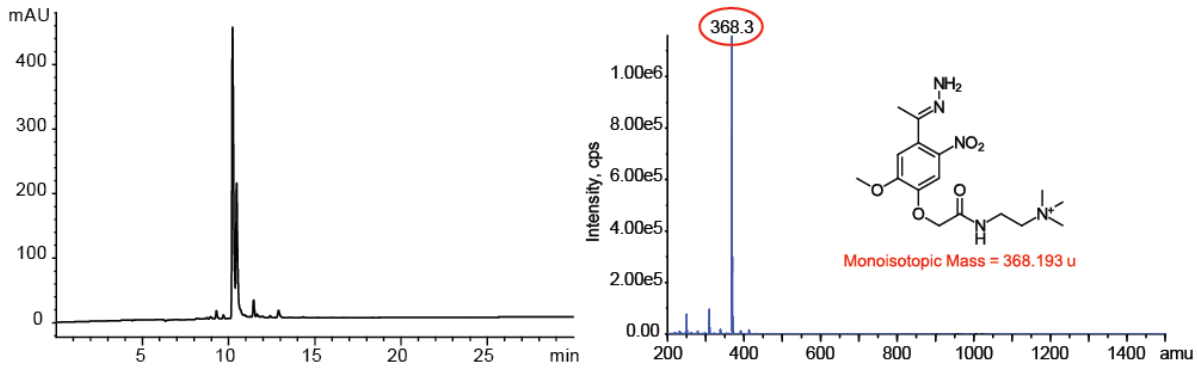

Figure 52 Q-hydrazone analysis on HPLC (345 nm, left) and MS (right)

Synthesis of Q-diazo

(2-{2-[4-(1-diazo-ethyl)-2-methoxy-5-nitro-phenoxy]-acetylamino}-ethyl)-trimethyl-ammonium

Q-hydrazone was dissolved in least quantity of anhydrous DMSO and quantified using UV spectroscopy ((ϵ_{345} = 4470 M^{-1} cm^{-1}). Solution containing 20.8 µmol of Q-hydrazone was adjusted to a concentration of 11.04 mM with 1880 µL with anhydrous DMSO. To this solution, 400 mg of manganese (IV) oxide was added and shaken vigorously for 45 minutes. The reaction was then centrifuged at 15000 g for 4 minutes to remove manganese oxide. DMSO containing Q-diazo was collected into another reaction vial for reaction with insulin. The manganese oxide pellet was washed with additional DMSO (1000 µL) to recover any trapped diazo. DMSO solutions of Q-diazo were pooled and used for insulin reaction immediately. Q-diazo has a characteristic red color and an absorbance at 450 nm (Figure 53).

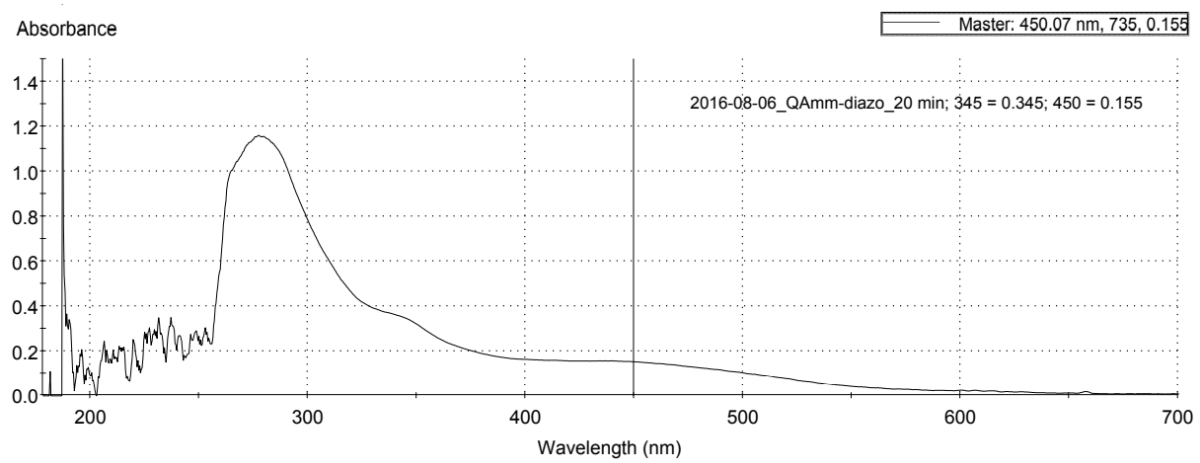

Figure 53 Q-diazo UV-visible spectrum

Synthesis of Q-insulin

20.8 µmol of insulin (120.5 mg) was dissolved in 500 µL of anhydrous DMSO. DMSO solution containing 20.8 µmoles of Q-diazo (assuming 100% conversion) was mixed homogenously with the insulin solution. Reaction was incubated in dark for 24 hours (Yield = 14%). Q-insulin reaction was directly injected on a 250 x 4.6 mm, 5 µm, C18 column for purification. Pure Q-insulin is collected from 26.0 – 29.0 minutes when run on a 24% - 38% acetonitrile gradient at a flow rate of 1 mL/min. HPLC and MS analysis of the pure product is shown (Figure 54).

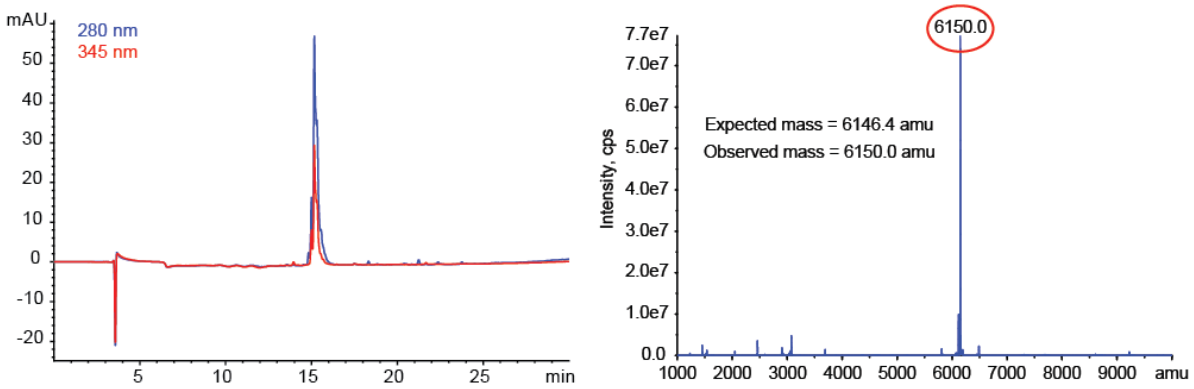

Figure 54 Q-insulin characterization on HPLC (left) and MS (right)

Determination of Q-insulin isoelectric point

0.5 nmol/µL solutions of insulin, Glargine (diluted from Lantus formulation, (ϵ_{280} = 5128 M^{-1} cm^{-1}), and Q-insulin (ϵ_{345} = 4470 M^{-1} cm^{-1}) were prepared in DMSO. 1 nmol of each of the proteins, along with the standards were loaded on an IEF gel. Electrophoresis was performed as described for the non-polar tag insulins by varying the voltage at respective time intervals. Protein bands were fixed with glutaraldehyde and stained with a Crocein Scarlet-Coomassie Blue R-250 mixture. The gel was then

destained with 40% methanol, 10% acetic acid solution. After the gel image was captured on a white background, the distance migrated by proteins in the gel was analyzed using Adobe Illustrator. pI of Q-insulin was estimated by comparing its migration distance with the distances of protein standards. IEF shows that the pI of Q-insulin is also similar to P-insulin, i.e. ~6.7 (Figure 55). This again proves that the prediction for charges of insulin is precise. Though quaternary ammonium function is inherently positively charge and is independent of the pH of the environment, it did not affect the way charges are shifted for insulin upon conjugation.

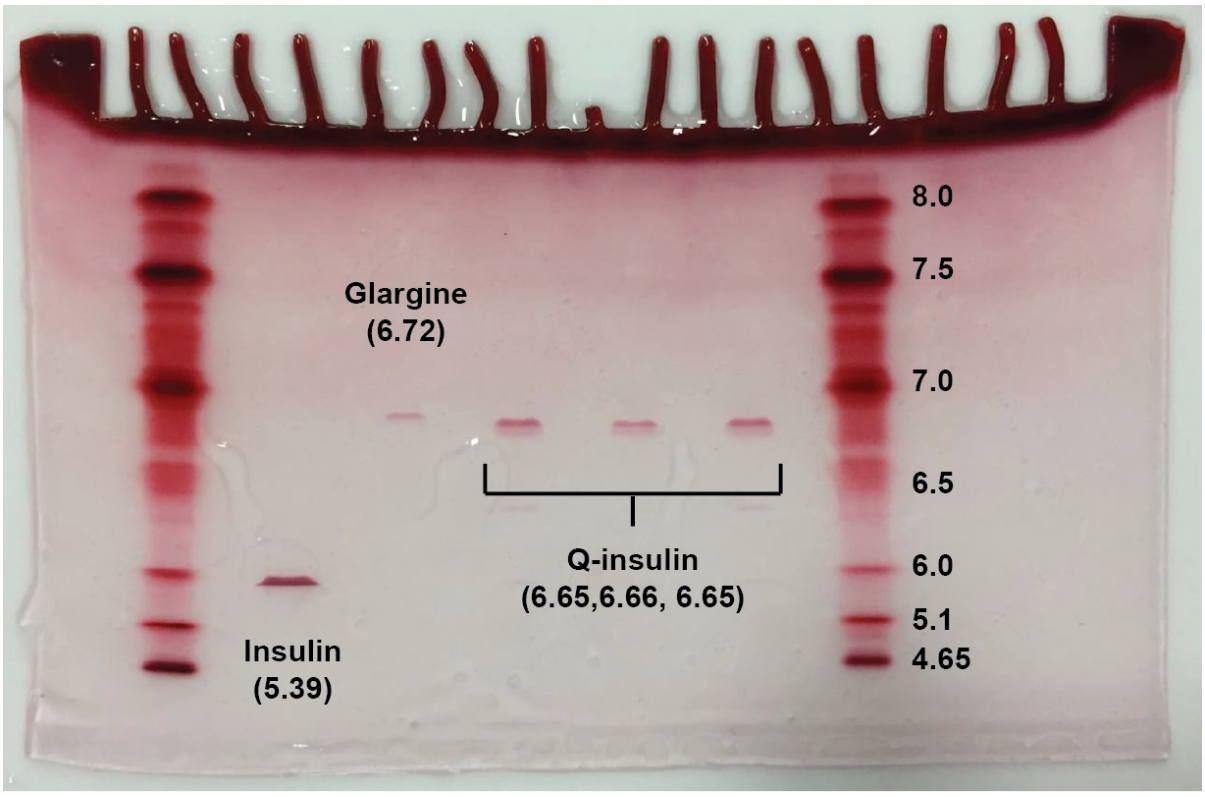

Figure 55 Isoelectric focussing gel electrophoresis of insulin, glargine and Q-insulin

With the addition of a single positive charge, whether as an amine or a quaternary amine, the isoelectric point of insulin was raised to 6.7. Though the

quaternary ammonium tag is better in terms of providing charge, due to the following reasons they were not pursued to make more materials:

(a) The shift caused with quaternary ammonium group is same as that of the tertiary amine.

(b) Intermediates made with quaternary ammonium tags are highly unstable, probably due to the strong inductive effects of the functional group.

Arg-Arg-insulin

Since the tags with single positive charged raised the isoelectric point as predicted, new tags with two positive charges were designed to raise the isoelectric point to ~7.2, i.e. the physiological pH. To recap, conjugation raises the pI by 0.65 units. Two positive charges contribute to an additional 0.65 units each. This will lead to a total shift from 5.4 by 0.65 x 3, i.e. by ~1.95 units, to ~7.35. Studies were started with peptidic tags containing two arginine residues. Arginines, in addition to being biocompatible, are stronger bases than amines and can contribute to the pI shifts effectively. Scheme for the synthesis of Arg-Arg-insulin is discussed in the Figure 56.

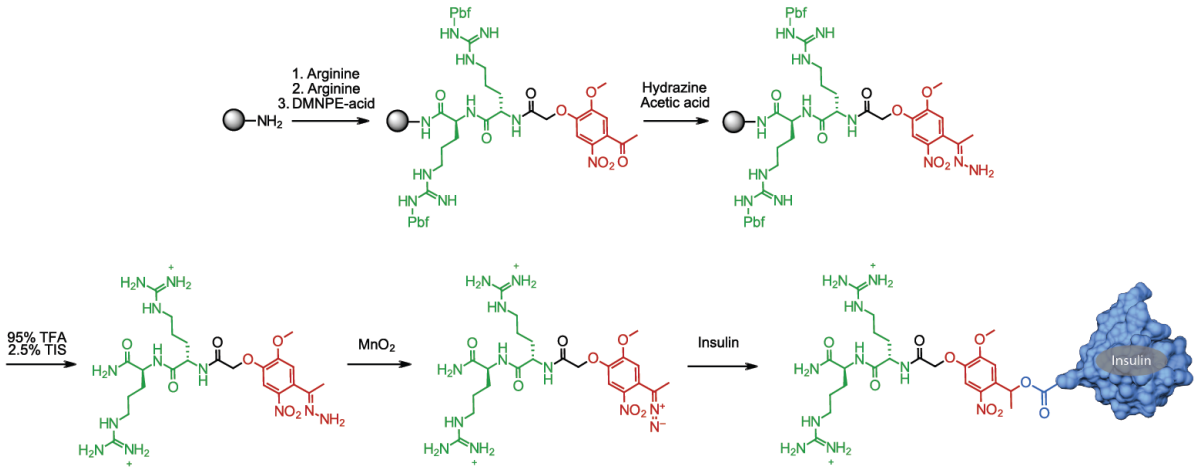

Figure 56 Synthesis of Arg-Arg-insulin

Synthesis of Arg-Arg-DMNPE

2-{2-[2-(4-acetyl-2-methoxy-5-nitro-phenoxy)-acetylamino]-5-guanidino-pentanoylamino}-5-guanidino-pentanoic acid amide

Arg-Arg-DMNPE was synthesized using Fmoc-solid phase peptide synthesis. 0.5 g (235 µmol) of Chemmatrix Rink amide resin (PEG) was suspended in NMP at a concentration of 60 mM. 10% piperidine, 2% DBU solution was used to deprotect amines. Coupling was carried out with 300 mM Fmoc-Arg-(Pbf)/DMNPE-acid, 300 mM HATU and 600 mM DIEA. Unreacted amines after each coupling (before Fmoc removal) were capped with 10% acetic anhydride, 5% DIEA solution in NMP. The solid phase was extensively washed between each step. A small amount of resin was sampled, and the peptide was cleaved (95% TFA, 5% water for 1 hour) for analysis (Figure 57). Yield (~94%) was determined based on the Fmoc removed after each deprotection. Condensation of the DMNPE-acid was assumed to be ~100% as the yield cannot be determined due to the lack of an Fmoc group and a deprotection step here.

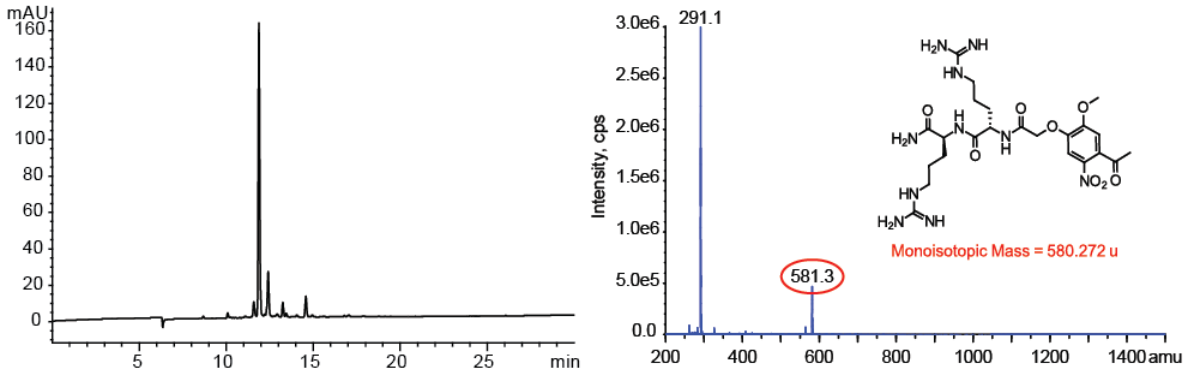

Figure 57 Arg-Arg-DMNPE analysis on HPLC (345 nm, left) and MS (right)

Synthesis of Arg-Arg-hydrazone

5-guanidino-2-(5-guanidino-2-{2-[4-(1-hydrazono-ethyl)-2-methoxy-5-nitro-phenoxy]-acetylamino}-pentanoylamino)-pentanoic acid amide

The advantage of synthesizing hydrazones on solid phase can be seen here. It is known that hydrazine converts the arginine into ornithine due to its reactivity with guanidine groups[44]. Since the side chains are protected while performing the hydrazone synthesis here, the desired hydrazone was easily obtained in high yields (100% conversion of ketone to hydrazone). 235 µmol of Arg-Arg-DMNPE (assuming 100% coupling on resin, 235 µmol of resin, 0.5 g) was suspended in 7 mL of 1:1 NMP:ethanol solvent mixture in a siliconized glass reaction vial. 352.5 µmol (20.2 µL) glacial acetic acid was added and mixed gently. 9.4 mmol hydrazine monohydrate (456.4 µL) was added and reaction vessel was sealed tightly. Reaction mixture was shaken at 800 RPM overnight in an Eppendorf Thermomixer at 60 C. Resin was washed (5X) with NMP and DCM and dried. Arg-Arg-hydrazone was cleaved off resin by treating the resin with 95% TFA 5% water solution for 1 hour.

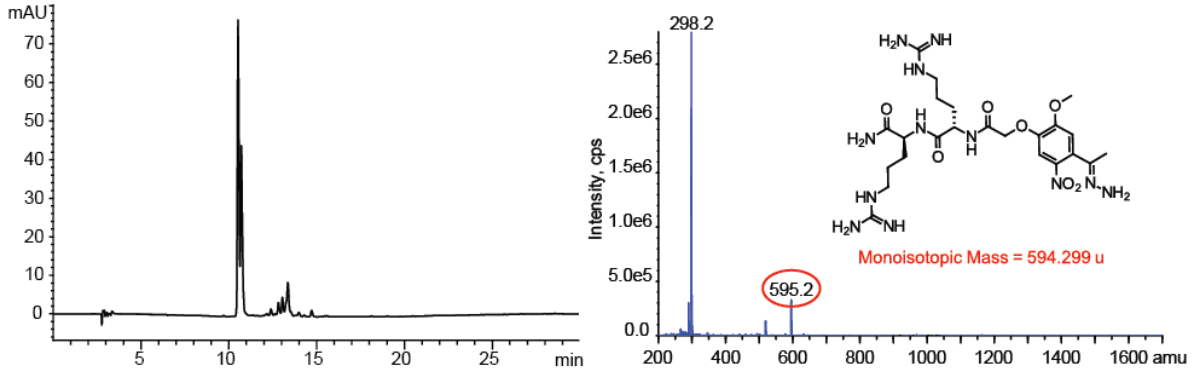

Figure 58 Arg-Arg-hydrazone analysis on HPLC (345 nm, left) and MS (right)

TFA was evaporated as quickly as possible to avoid formation of azines, until a small volume of the solution is left. Cold ether (10x volume) was added to this concentrated TFA solution to precipitate the hydrazone out. Solution was centrifuged to obtain Arg-Arg-hydrazone and the ether was discarded. The pellet was dried in vacuum to remove any traces of ether and was immediately used for the diazotization reaction. Analysis of the material was carried out with HPLC and LCMS (Figure 58).

Synthesis of Arg-Arg-diazo

2-(2-{2-[4-(1-diazo-ethyl)-2-methoxy-5-nitro-phenoxy]-acetylamino}-5-guanidino-pentanoylamino)-5-guanidino-pentanoic acid amide

Arg-Arg-hydrazone was dissolved in minimal amount of anhydrous DMSO and quantified using UV spectroscopy (ϵ_{345} = 4470 M^{-1} cm^{-1}). Final concentration of the solution was adjusted to 11.04 mM (1.66 µmol) with additional DMSO. 690 µmol (60 mg) of MnO_2 was added to solution containing 1.66 µmol Arg-Arg-hydrazone. Reaction mixture was shaken vigorously for 45 minutes. It was then centrifuged at 15000 g for 4 minutes to remove manganese oxide. The orange/red supernatant containing Arg-Arg-diazo was collected and the manganese oxide pellet was washed with additional DMSO. DMSO solutions were pooled and used for esterifying insulin immediately. Arg-Arg-diazo has a characteristic red color and an absorbance at 450 nm (Figure 59). Yield of the reaction was not estimated due to instability of the diazo. It was assumed that 100% hydrazone is oxidized, and therefore reacted with insulin in a 1:1 mole ratio relative to the hydrazone.

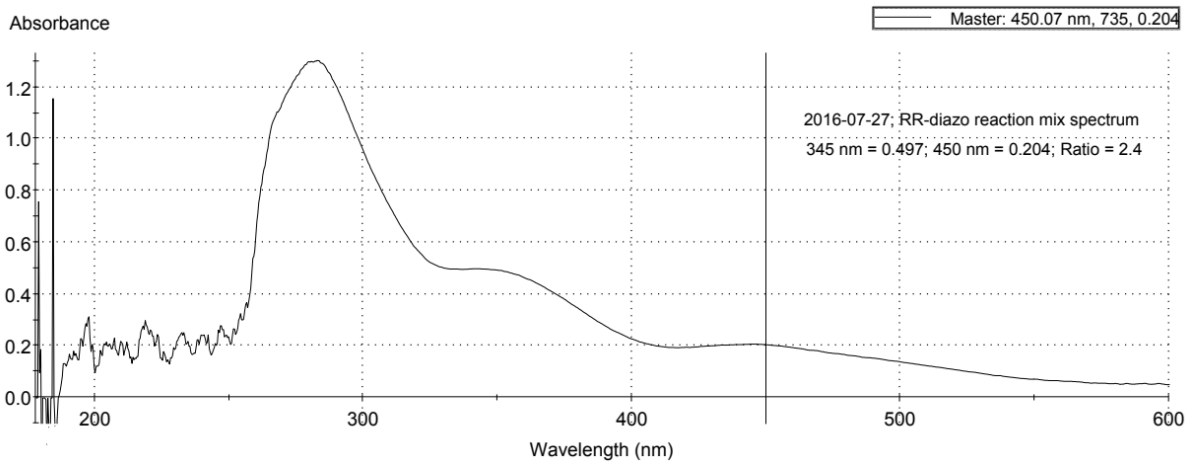

Figure 59 Arg-Arg-diazo UV-visible spectrum

Synthesis of Arg-Arg-insulin

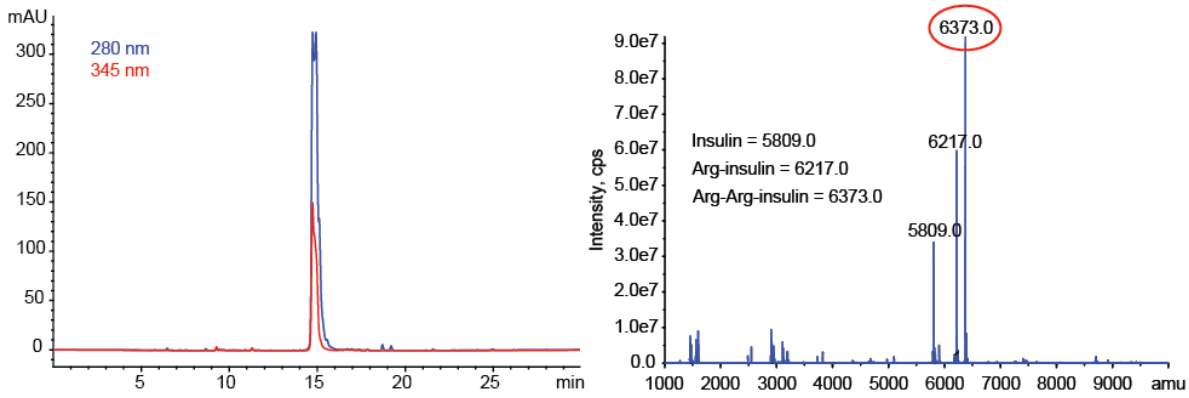

Figure 60 Arg-Arg-insulin analysis on HPLC (left) and MS (right). Pure variant could not be isolated due to chromatographic issues

1.66 µmol (9.6 mg) of insulin was dissolved in 150 µL of dry DMSO. To this solution, Arg-Arg-diazo solution from previous reaction was added, mixed and allowed to react for 24 hours in dark (Yield = 9% monoadduct, with respect to insulin). Arg-Arg-insulin was purified by RP-HPLC using 250 x 4.6 mm, 5 µm, C18 column. The method was developed with a flow rate of 1 mL/min. The pure product was

collected from 25.0 – 27.0 minutes on a 20% acetonitrile to 40% acetonitrile over 28 minutes. The column was washed with 100% acetonitrile after the gradient in each run. Arg-Arg-insulin was analyzed on HPLC and MS (Figure 60).

It can be observed from the chromatogram and mass spectra that Arg-Arg-insulin was impure. The difficulty with the purification of this insulin variant was that the product has the same retention time as of insulin. Therefore, it was impossible to resolve the proteins on a C18 column. Purification with C8 and RP-CN columns was also attempted, however the protein was still impure after purification. Ion exchange chromatography should result in a good separation. However, it was difficult to isolate the species since the yield of this reaction was ~10%. Moreover, insulin weakly acidic. To bind insulin well with the stationary phase, a strong anion exchanger would work at pH 7. However, due to unavailability of a strong anion exchanger and lack of time, Arg-Arg-insulin could not be purified in the laboratory. Purification by isoelectric focusing could be the best method if gel extraction procedures are developed.

Another observation was made with the di-arginine peptide that it was hydrolyzing during the esterification reaction with insulin. A reason for why this phenomenon happens is understood yet. This impurity of insulin with a single arginine tag is consistent with the mass seen on the mass spectrum. Due to these issues, it will be difficult to scale up Arg-Arg-insulin synthesis for future studies including *in vitro* and *in vivo* experiments.

Determination of Arg-Arg-insulin isoelectric point

0.5 nmoles/μL solutions of insulin, Glargine (diluted from Lantus formulation, (ϵ_{280} = 5128 M^{-1} cm^{-1}), and Arg-Arg-insulin (ϵ_{345} = 4470 M^{-1} cm^{-1}) were prepared in DMSO. 1 nmol of each of the proteins, along with the standards were loaded on an IEF gel. Electrophoresis was performed as described earlier by varying the voltage at respective time intervals. Protein bands were fixed with glutaraldehyde and stained with a Crocein Scarlet-Coomassie Blue R-250 mixture. The gel was then destained with 40% methanol, 10% acetic acid solution.

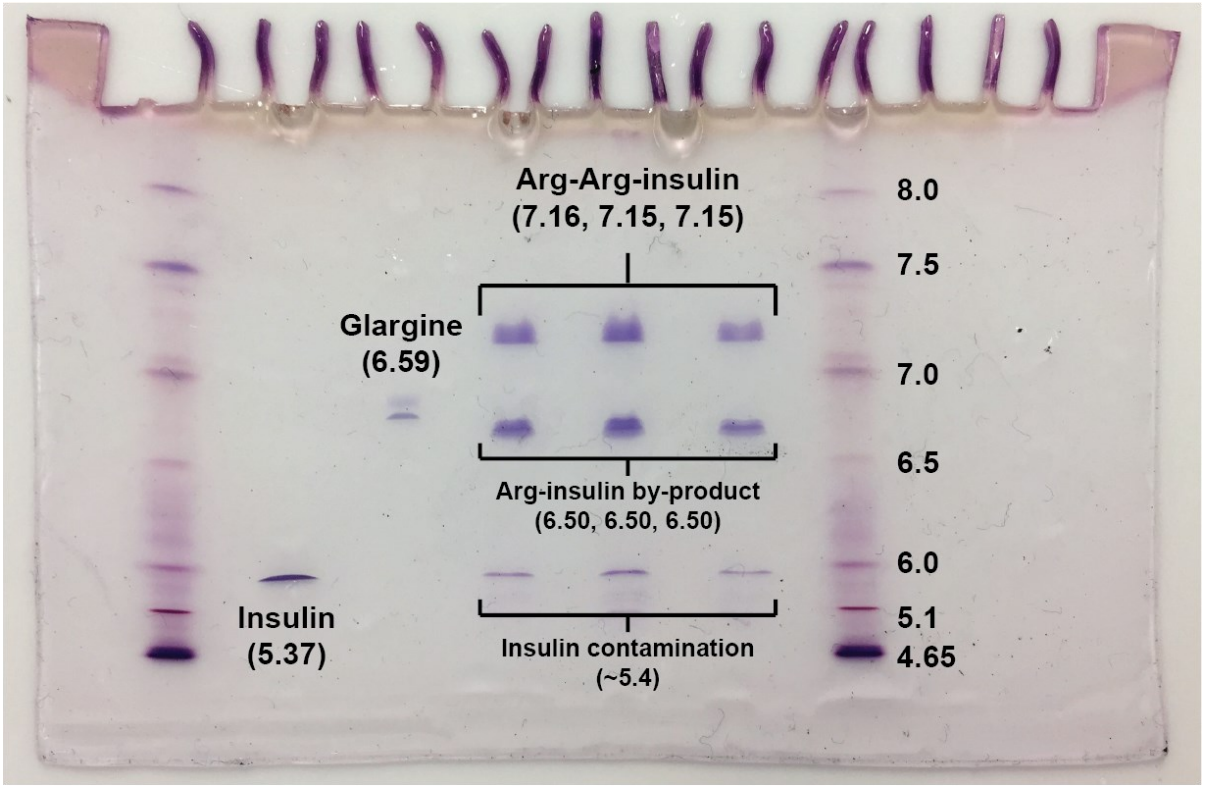

Figure 61 Arg-Arg-insulin isoelectric focusing. IEF is also consistent with the hypothesis of Arg hydrolysis

After the gel image was captured on a white background, the distance migrated by proteins in the gel was analyzed using Adobe Photoshop. pI of Arg-Arg-insulin was estimated by comparing its migration distance with the distances of protein standards. IEF shows that the pI of Arg-Arg-insulin is ~7.2. Another band at a pI equivalent with the Glargine is also seen in the sample. This is again consistent with the hypothesis of the species being Arg-insulin due to the hydrolysis of one of the arginines during the reaction (Figure 61).

P2-insulin

Though the peptidic Arg-Arg tag was able to raise the isoelectric point to the desired range, following problems limited the use of the tag for further studies: (a) stability during diazotization / esterification, and (b) purification as Arg-Arg-insulin coelutes with insulin. With peptidic tags, Lys-Lys-insulin could be another possibility which can have ~7.2 pI. However, lysine may complicate the synthesis as an imine bond can be formed between the ketone (on DMNPE) and the side chain, instead of hydrazine. Therefore, a new tag with two positive charges was designed to overcome these issues.

The idea was to create a tag with two pyrrolidine moieties from the precursor used for P-insulin, viz. 2-pyrrolidinoethylamine. However, a linker is required in order to conjugate two pyrrolidine moieties to a single photocleavable group. This can be achieved with a molecule containing two carboxylates for condensing two molecules of precursor, and an additional amine which can be used to link with DMNPE-acid. Such tags will raise the isoelectric point of insulin to ~7.2; 0.65 units

due to conjugation and 0.65 units x 2 times due to the addition of two charges. After extensive search, glutamic acid is identified as the ideal monoamino dicarboxylate linker.

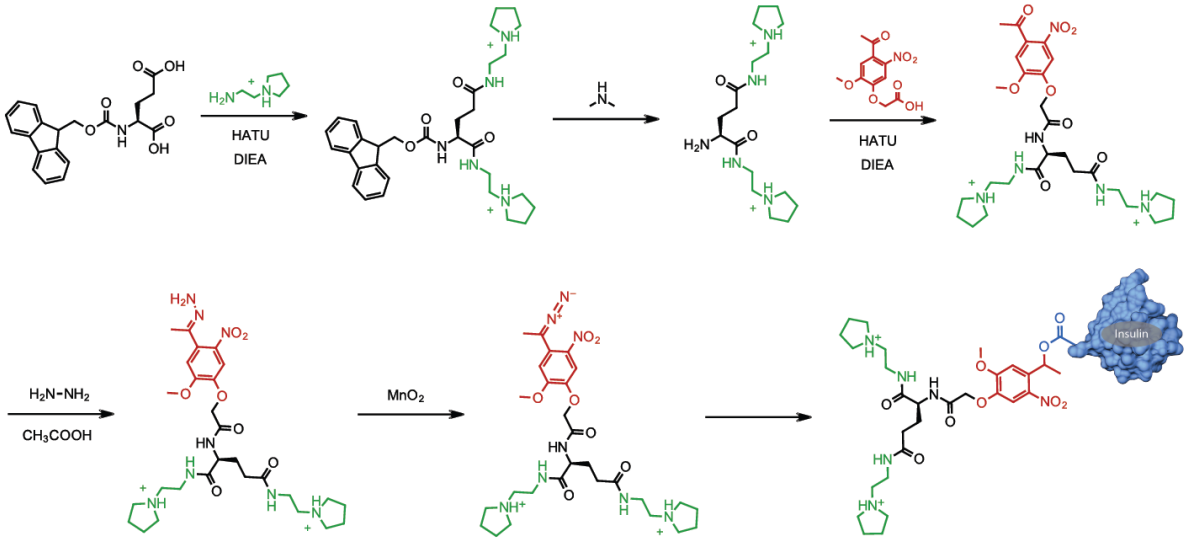

Figure 62 Synthesis of P2-insulin

The strategy is to begin the synthesis with Fmoc-protected glutamic acid. Condensation of 2-pyrrolidinoethylamine precursor will be performed on each of the carboxylic acid. Then, the Fmoc group will be removed and the free amine will be condensed with DMNPE acid. Further reactions i.e. hydrazone, diazo and insulin ester syntheses will be similar to all the other schemes discussed earlier (Figure 62).

Synthesis of Fmoc-P2

[1,3-bis-(2-pyrrolidin-1-yl-ethylcarbamoyl)-propyl]-carbamic acid 9H-fluoren-9-ylmethyl ester

200 mg Fmoc-glutamic acid (541.8 µmoles) and 612.6 mg of HATU (1.6 mmoles) were dissolved in 9 mL of NMP. Solution was allowed to stand for five

minutes. DIEA (1074 µmol, 187 µL) and 1-(2-aminoethyl)pyrrolidine (1.6 mmoles, 203.5 µL) were added to the solution and reacted for 3 hours. The product was purified using RP-HPLC, by injecting 4 mL of reaction mixture on a 250 x 21.2 mm, 10 µm, C18 column. It was collected from 36.5 – 45.0 min when run on a 0 – 100% acetonitrile gradient over 70 minutes at 5 mL/min. Analysis of Fmoc-P2 was performed on HPLC and LCMS (Figure 63). (Yield = 100% condensation with respect to Fmoc-glutamic acid).

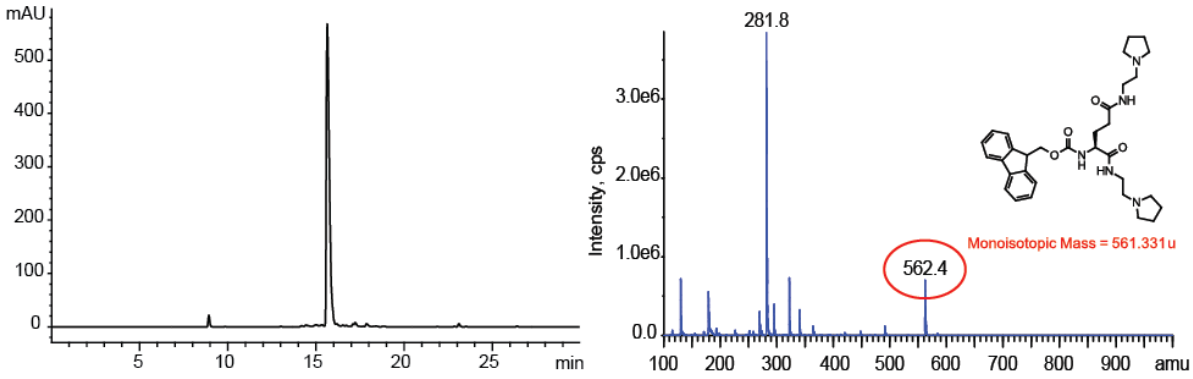

Figure 63 Fmoc-P2 analysis on HPLC (301 nm, left) and MS (right)

Synthesis of P2-DMNPE

2-[2-(4-acetyl-2-methoxy-5-nitro-phenoxy)-acetylamino]-pentanedioic acid bis-[(2-pyrrolidin-1-yl-ethyl)-amide]

Fmoc-P2 was dissolved in ethanol and quantified using UV-spectroscopy (ϵ_{301} = 6800 M^{-1} cm^{-1}). 440 µmoles of Fmoc-P2 was transferred into round bottom flask and dried. It was then dissolved in 20 mL of acetonitrile, followed by the addition of 20 mL of 40% dimethylamine solution for Fmoc removal. Dimethylamine has a very low boiling point; therefore, the reaction was performed for 30 minutes at room

temperature by *sealing* the flask. The solvent was then evaporated in vacuum (rotovap) with the water bath set at approximately 60 C. The dried crude was redissolved in 40 mL of 50% DIEA in methanol solution and dried at 60 C repeatedly for five times. The washed crude was again washed with cold ether multiple times and dried. The deprotected P2 was neither purified nor characterized. Assuming 100% Fmoc-deprotection, 440 µmoles of deprotected P2 was dissolved in 5 mL NMP. 660 µmoles (0.18 g) DMNPE-acid and 990 µmoles (0.38 g) HATU were also dissolved in this solution. 1.9 mmoles (345 µL) of DIEA was added and reaction was allowed to stand for 3 hours. P2-DMNPE was purified using RP-HPLC, by injecting 4 mL of reaction mixture on a 250 x 21.2 mm, 10 µm, C18 column in each run. It was collected from 32.5 – 36.0 min when run on a 0 – 100% acetonitrile gradient over 70 minutes at 5 mL/min. Analysis of P2-DMNPE was performed on HPLC and LCMS (Figure 64).

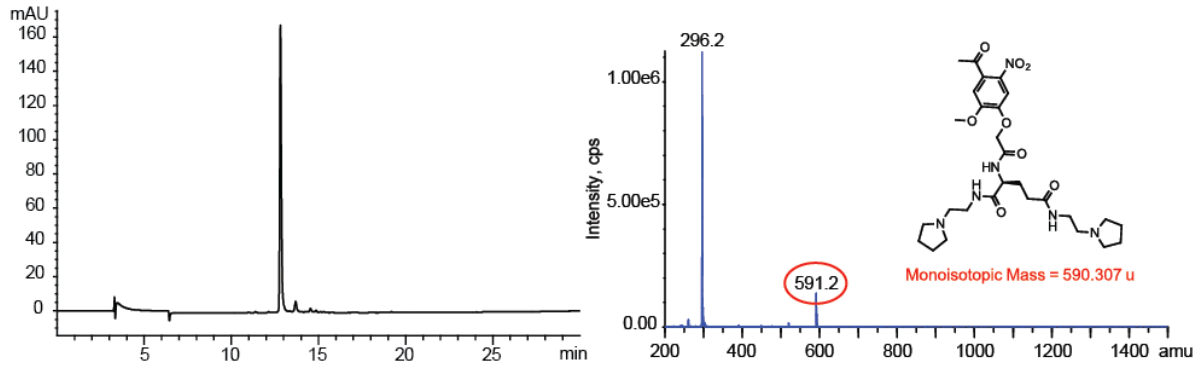

Figure 64 P2-DMNPE analysis on HPLC (345 nm, left) and MS (right)

Yield of this reaction was observed to be ~55%. Though 100% of the DMNPE-acid was condensed with amines, overall yield after purification was low due to loss of P2 amine during ether washes. Additionally, DMNPE-acid was observed to form condensation product with the dimethylamine. This means that the amine was not

removed from the reaction even in vacuum at 60 C. This is possibly due to the formation of dimethylamine – trifluoroacetate salts, which are retained in reaction as the salt form of the base should have a higher boiling point than the free base.

Synthesis of P2-hydrazone

2-{2-[4-(1-hydrazono-ethyl)-2-methoxy-5-nitro-phenoxy]-acetylamino}-pentanedioic acid bis-[(2-pyrrolidin-1-yl-ethyl)-amide]

P2-DMNPE was dissolved in minimal amount of ethanol:acetonitrile mixture (1:1) and quantified using UV spectroscopy (ϵ_{345} = 4470 M^{-1} cm^{-1}). 102.65 µmoles of P2-DMNPE were diluted to 6 mL with 1:1 ethanol:acetonitrile solution. 15 µL of glacial acetic acid and 261.2 µL of hydrazine monohydrate were added and allowed to react for 4 hours at 90 C. Reaction mixture was dried, and the crude material was washed multiple times with cold ether (Yield = 100% conversion of ketone to hydrazone).

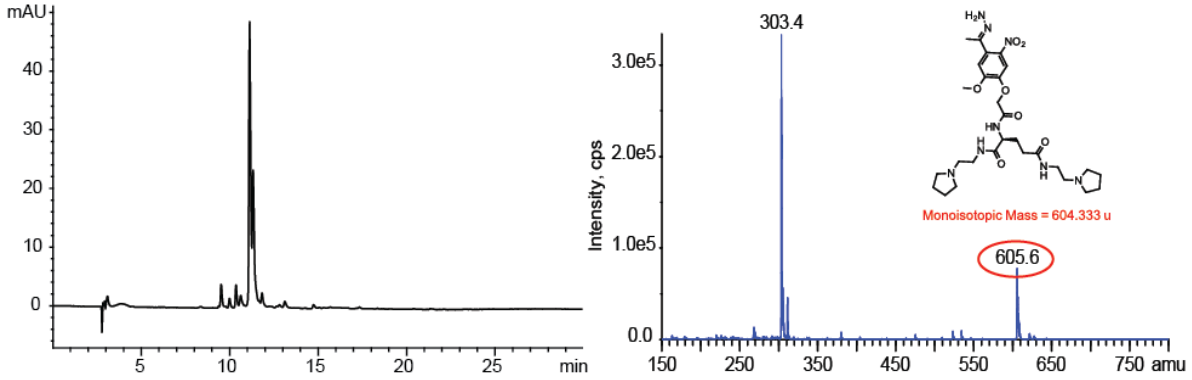

Figure 65 P2-hydrazone analysis on HPLC (345 nm, left) and MS (right)

Ether was discarded and partially purified P2-hydrazone was obtained as a yellowish-white material in the flask. The hydrazone was dried again in vacuum to remove any traces of ether. P2-hydrazone was dissolved in minimal quantity of

anhydrous DMSO and used immediately for the next reaction. The hydrazone was analyzed on HPLC and LCMS (Figure 65).

It should be noted that P2-hydrazone is very unstable and will form azines. So, the drying process should be completed as soon as possible. Also, the presence of traces of ether in the product is not recommended, as it results in an unwanted exothermic reaction and loss of yield in the successive reaction.

Synthesis of P2-diazo

2-{2-[4-(1-diazo-ethyl)-2-methoxy-5-nitro-phenoxy]-acetylamino}-pentanedioic acid bis-[(2-pyrrolidin-1-yl-ethyl)-amide]

P2-hydrazone was dissolved in least volume of dry DMSO and quantified using UV-spectroscopy (ϵ_{345} = 4470 M^{-1} cm^{-1}). Final concentration of the hydrazone was adjusted to 16.56 mM with anhydrous DMSO. 132 µmoles (16.56 mM) of P2-hydrazone was transferred into a glass reaction vial. 22.9 mmoles (2000 mg) manganese dioxide was added and shaken vigorously for 45 minutes. The reaction mixture was centrifuged at 15000 g for 5 minutes. The clear solution containing P2-diazo was collected into another Eppendorf tube. Manganese dioxide was washed with additional DMSO to recover any trapped diazo. Formation of P2-diazo was confirmed by its characteristic red color and an absorbance at 450 nm (Figure *66*). Solutions were pooled and used for the insulin reaction immediately. Yield of the reaction was not estimated due to instability of the diazo. It was assumed that 100% hydrazone is oxidized, and therefore reacted with insulin in a 1:1 mole ratio relative to the hydrazone.

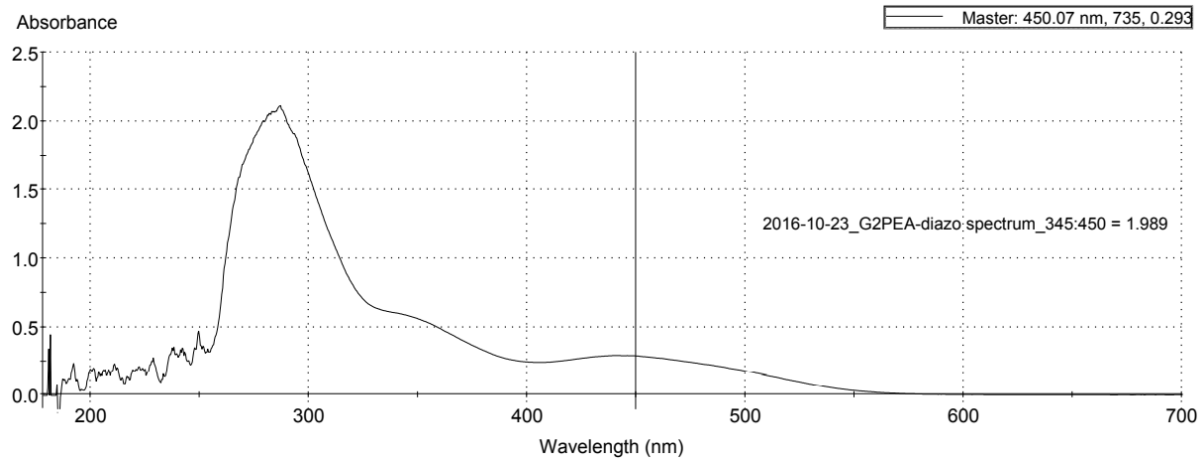

Figure 66 P2-diazo UV-visible spectrum

Synthesis of P2-insulin

132 µmoles of insulin (770 mg) was dissolved in 8 mL of dry DMSO. This insulin solution was prepared during the diazotization of P2-hydrazone, so that the diazo can be immediately mixed with the protein. P2-diazo solution (132 µmoles) was added to insulin solution and mixed homogenously. The reaction was carried out for 24 hours in dark. P2-insulin was purified by RP-HPLC on 250 x 4.6 mm, 5 µm, C18 column. The protein is collected from 27.2 - 33.4 minutes when run on a 24% - 38% acetonitrile gradient over 35 minutes, with a flow rate of 1 mL/min. Purified P2-insulin was analyzed on HPLC and MS (Figure 67). Yield was observed to be 10-15%. This is an estimate based on the integration of insulin versus P2-insulin proteins, obtained from a chromatogram of the P2-insulin reaction mixture. It should be noted that insulin and P2-insulin may co-elute on a standard 30-minute gradient. However, amounts of both the proteins can be determined by making use of the extinctions of both the proteins at 280 and 345 nm.

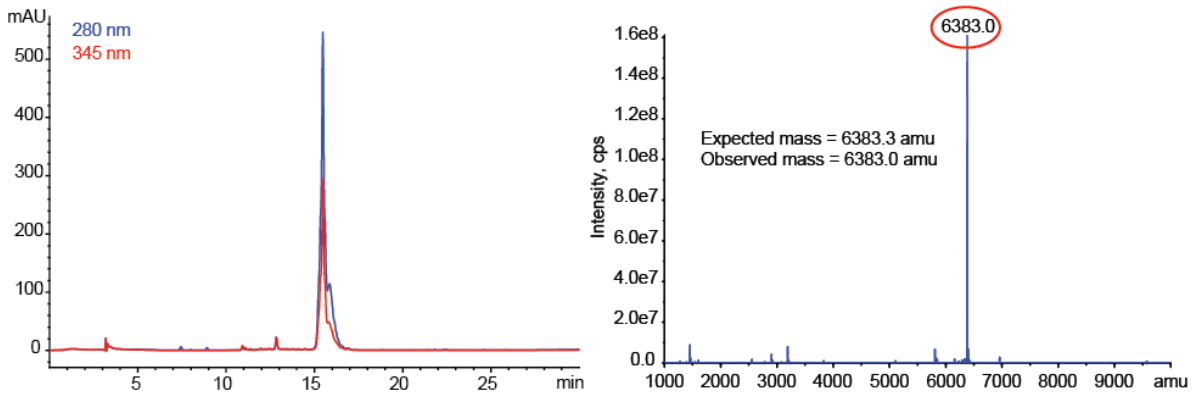

Figure 67 P2-insulin analysis on HPLC (left) and MS (right)

Determination of P2-insulin isoelectric point

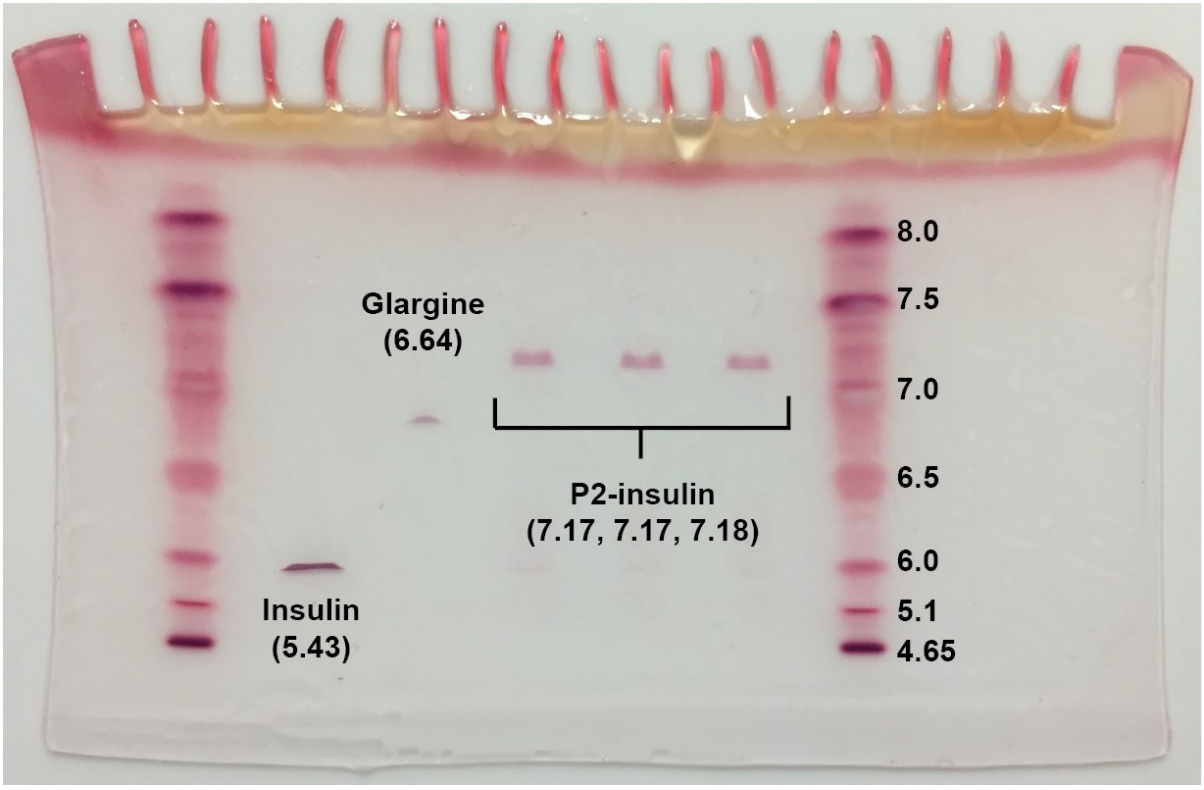

Figure 68 Isoelectric focusing gel electrophoresis of insulin, glargine and P2-insulin

0.5 nmoles/µL solutions of insulin, Glargine (diluted from Lantus formulation, (ϵ_{280} = 5128 M^{-1} cm^{-1}), and P2-insulin (ϵ_{345} = 4470 M^{-1} cm^{-1}) were prepared in DMSO,

diluted in IEF sample buffer. 1 nmol of each of the proteins, along with the standards were loaded on an IEF gel. Electrophoresis was performed as described earlier by varying the voltage at respective time intervals. Protein bands were fixed with glutaraldehyde and stained with a Crocein Scarlet-Coomassie Blue R-250 mixture. The gel was then destained with 40% methanol, 10% acetic acid solution.

After the gel image was captured on a white background, the distance migrated by proteins in the gel was analyzed using Adobe Photoshop. pI of P2-insulin was estimated by comparing its migration distance with the distances of protein standards. IEF shows that the pI of P2-insulin is also ~7.2, comparable to the pI of Arg-Arg-insulin. With this experiment, it is confirmed that the shifts in pI for insulin can be achieved using this model that a shift of 0.65 units in pI can be predicted with an addition of +1 charge to insulin (Figure 68).

Studies on P2-insulin solubility

One of the advantages with the charge tag approach is that the protein will have different solubilities at different pHs. Here, insulin was modified with the P2 tag to shift its isoelectric point from 5.4 to the physiological pH of skin, i.e. 7.2. Therefore, P2-insulin is expected to be insoluble at 7.2 but should be soluble at acidic conditions. This is beneficial for the development of a formulation. An acidic protein solution can be injected, which can easily pass through a 31G needle without any resistance. Previously, the FDA approved other biological molecules (Lantus, glucagon, etc.) which have to be injected as an acidic solution[45,46]. Therefore, the strategy to deliver

charge-tag insulin is by the use of an acidic formulation. To study this, solubility and behavior of P2-insulin at different pHs were studied.

P2-insulin versus insulin solubility

Insulin was modified with the P2 charge-tag with the goal of lowering protein solubility at physiological pH. Therefore, solubility of P2-insulin was determined in 10 mM PBS 7.2 and compared with the solubility of insulin. The method for determining the solubility is the same that was used for the non-polar insulins. 100 nmol of P2-insulin was suspended in 100 µL PBS and equilibrated for 2 hours by shaking. The samples were centrifuged at 15000 g for 4 minutes, and the supernatants were analyzed for P2-insulin and insulin in respective tubes. The charge-tag modification of insulin resulted in ~75x reduction in solubility at pH 7.2. Solubility in low µM range is comparable with the solubility of Lantus (Table 8, Figure 69). Determination of insulin solubility was not repeated as it was already performed for the non-polar tag variants. Therefore, P2-insulin solubility was directly compared with the solubility of insulin determined earlier. Thus, it can be concluded that this decrease in solubility is enough for the creation of protein depots in the skin.

Table 8 Solubility of insulin and P2-insulin in 10 mM PBS pH 7.2

Protein	Solubility (µM) ± S.D.	Times reduction
Insulin	1053 ± 158.1	--
P2-insulin	14.0 ± 1.3	~75

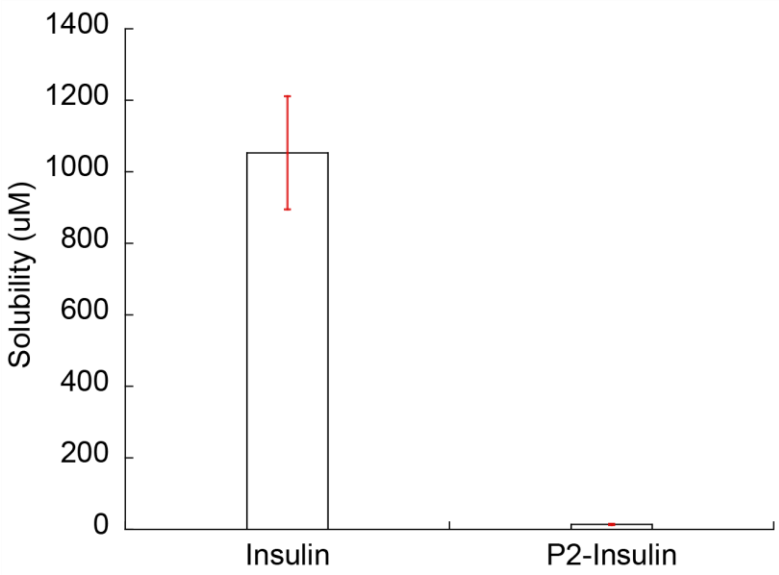

Figure 69 Comparison of insulin and P2-insulin solubilities in 10 mM PBS pH 7.2

pH dependent P2-insulin solubility

One of the requirements of the photoactivated depot is a high solubility in the acidic conditions. Higher concentration of P2-insulin in the formulation ensures that higher amount of the protein will be injected as a depot. Therefore, P2-insulin solubility was measured at pH 4 and 7.2 (Solubility at pH 7.2 was determined in previous experiment). The FDA approved the injection of Lantus at pH 4, and hence formulation for the PAD can be lowered to as low as 4 without any issues. Briefly, 200 nmol P2-Insulin was introduced into 100 µL 10 mM phosphate buffered saline at pH 4 and 7 in different tubes and allowed to reach equilibrium over a 2 h period. All the tubes had visible solid present at equilibrium, ensuring that saturation had been achieved. The visible solid was confirmed to be P2-insulin after the study, by solubilizing it in DMSO and analyzing by HPLC. The samples were centrifuged, and the supernatants analyzed by HPLC for modified insulin. As anticipated, P2-insulin

has a ~15.5x lower solubility at the neutral pH than at the acidic formulation pH (Table 9, Figure 70).

Table 9 Differential solubility of P2-insulin at pH 4.0 and pH 7.2

pH of buffer	P2-insulin solubility (μM)	Difference (x times)
4	216.0 ± 46.0	~15.5
7.2	14.0 ± 1.3	--

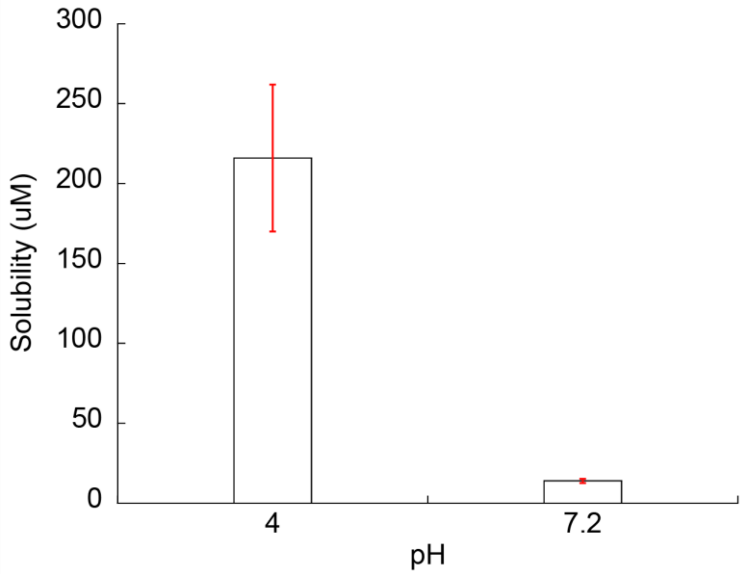

Figure 70 Differential solubility of P2-insulin at pH 4 and pH 7.2

The observed solubility trends are also depicted photographically in Figure 71. Here, 400 μL of a 75 μM P2-insulin solution in 10 mM pH 4 phosphate buffer was prepared. To this, 38 μL of a 0.1 N sodium hydroxide was added to bring the pH to 7.2, at which point immediate precipitation was observed. Upon vortexing, the suspension and the pH of the solution became homogenous. This tube was then irradiated for 10 min using a 365 nm LED light source (1.84 mW/cm^2) which

substantially clarified the suspension. To fully clarify this, the tube was centrifuged, removed the clarified buffer, added 400 µL of fresh buffer, and rephotolyzed the solution. The result was a clear solution of insulin. This experiment not only demonstrated that P2-insulin can instantaneously precipitate when the pH was raised to 7.2 (as in the case of an injection in skin), but also the precipitate can be photolyzed to release the native soluble insulin.

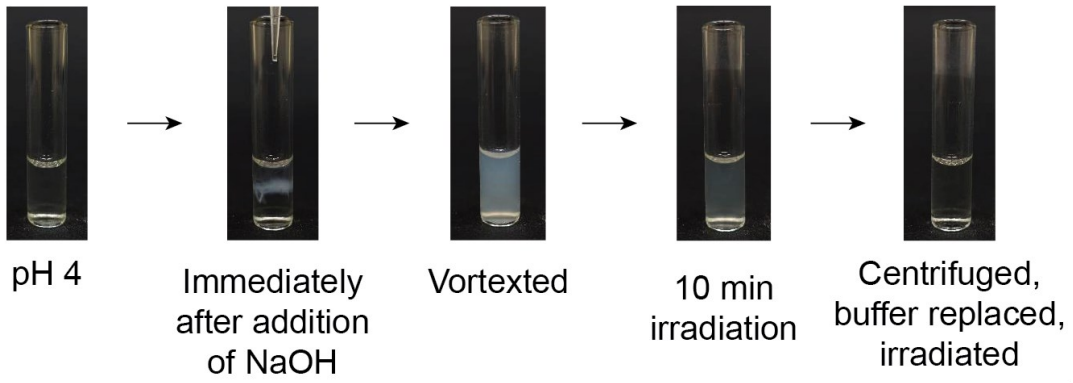

Figure 71 pH and light dependent behavior of P2-insulin

P2-insulin photolysis and insulin release

The previous experiment demonstrated that P2-insulin suspension clarifies on exposure to light. To closely examine the kinetics, two different experiments were performed – (a) photolysis in DMSO (homogenous), and (b) photolysis in PBS (heterogenous).

Photolysis in DMSO

40 µL of a 0.5 mM solution of P2-insulin (40 nmol) in DMSO was irradiated using a 365 nm LED light source with an absolute irradiance of 0.95 mW/cm^2 (distance from the bottom of the tube to the LED was 7 cm). At specific time intervals,

the reaction was sampled (2 µL DMSO samples were diluted to 10 µL with Bio-Rad IEF sample buffer) and analyzed using IEF gel electrophoresis. The figure shows the higher pI P2-insulin (upper band) being converted into the lower pI native insulin (lower band). The reactant and product molarities were quantitated, and the resulting insulin evolution shown in the plot. The kinetics are well fit by a single first order process, yielding a first order rate constant of 0.16 min ^{1}.

Insulin = P2-Insulin$_{t=0}$*[1-exp^{-kt}]

From this experiment, kinetics of the DMNPE based photorelease can be accurately determined as it was done without complications from variables like light intensity due to scattering of insoluble particles. In addition, this experiment also demonstrated that the photoreleased insulin has an isoelectric point that was shifted back to 5.4 (Figure 72).

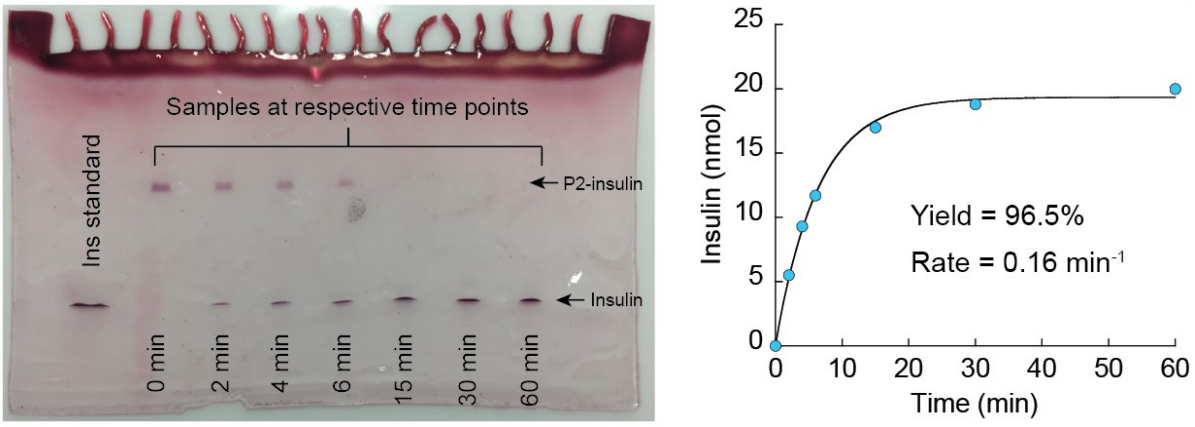

Figure 72 P2-insulin photolysis in DMSO

Photolysis in PBS

This experiment was done to study the kinetics under circumstances closer to the 'real world', where native soluble insulin should be released from insoluble

suspension in the skin at pH 7.2. This experiment was performed very similar to the photolysis of non-polar insulin variants. A pH adjusted suspension of P2-insulin (100 nmol) in 10 mM pH 7.2 PBS (100 µL) was irradiated with a 365 nm LED (absolute irradiance = 1.84 mW/cm^2), placed at 5 cm from the bottom of the tube. At specific time intervals, tube was centrifuged at 15000 g for 4 minutes to collect the total (100 µL) clear supernatant for insulin analysis. The un-photolyzed P2-insulin pellet was resuspended in fresh 100 µL buffer, and the photolysis was continued. A control tube was also prepared for the experiment containing 100 nmol per 100 µL buffer but was not exposed to light. 10 µL of the PBS supernatant of respective time points were diluted to 20 µL with IEF sample buffer and analyzed using isoelectric focussing. Insulin release was plotted as a function of time using the following equation.

$$\text{Insulin} = \text{P2-Insulin}_{t=0} * [1-\exp^{-kt}]$$

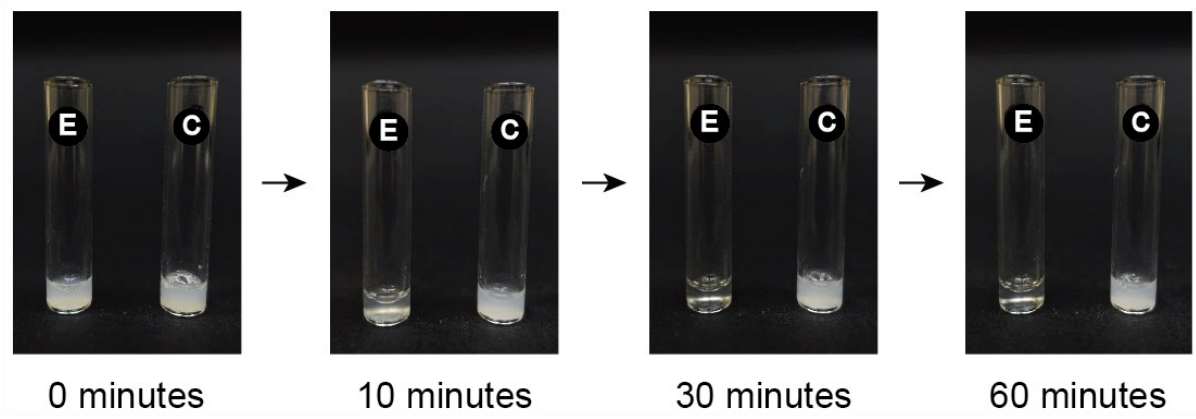

Figure 73 Light based solubilization of P2-insulin in PBS. E = experiment tube; C = control tube. Control was not irradiated throughout the experiment

The data was well fit to a first order rate law, which gave a first order kinetic constant of 0.075 min^{-1}, and a maximum concentration of 838 µM. This represents a

majority of the expected 1 mM released insulin. The gel also indicates no detectable P2-insulin in the supernatant. Control samples, in which P2-insulin was suspended and processed in an identical fashion, but remained unirradiated, showed no insulin released. This combined data shows a very facile and specific release of soluble insulin in response to light (Figure 73, Figure 74 and Figure 75).

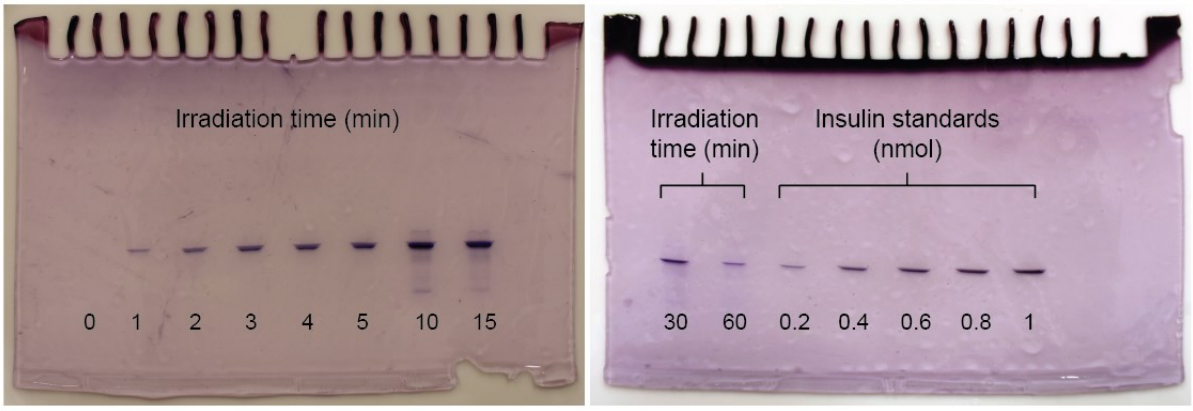

Figure 74 P2-insulin photolysis in PBS 7.2

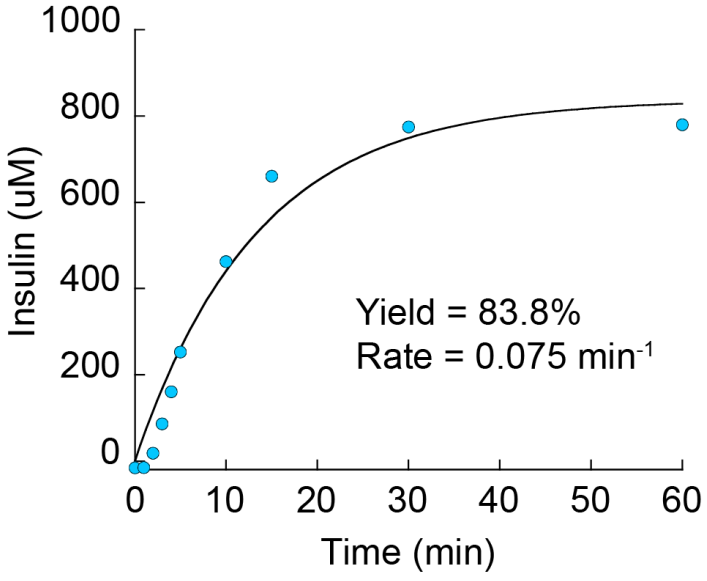

Figure 75 Insulin evolution from P2-insulin after irradiation in 10 mM PBS pH 7.2

Summary

In this work, new photoactivated materials were created by linking photolysis to an isoelectric point shift, which itself is linked to a solubility shift. Specifically, basic photocleavable tags were used for this purpose. These shift the normal pI of insulin from 5.4 to ~7.2. The result of this incorporation are materials that are completely soluble in mildly acidic solutions but precipitate upon injection into a pH 7 environment, i.e., the skin.

To achieve this, pI shifts were predicted based on the IEF studies on non-polar insulins and Glargine. Four different insulin variants were synthesized based on the predictions, demonstrating that their pI values were shifted in the expected manner. One of the four variants, P2-insulin, was analyzed in detail, demonstrating that it behaves as designed: It is soluble in a formulation pH of 4, but precipitates at pH 7.2, its approximate pI value. Upon irradiation, the photocleavable link to insulin is broken, and completely native and soluble insulin is released from the depot in a well behaved, first order fashion. These charge-tag insulin variants are also 90% therapeutic, form completely soluble and injectable formulations in mildly acidic conditions, form insoluble depots at neutral pH, efficiently release soluble protein from these depots when irradiated, and leave behind only small easily absorbed molecules after irradiation.

CHAPTER 5

DISCRETE PHOTOLYSIS

Introduction

In the previous studies with charge-tag and non-polar tag insulin variants, photolysis was performed in a continuous fashion. These experiments do not explain the nature of the behavior of the PAD materials completely. Ideally, the PAD materials should release native insulin only when exposed to light. It is expected that the PAD materials should not release insulin when they are not exposed to light. The control tube in the continuous photolysis experiments indicate whether insulin will be released in the absence of light or not. But these control tubes do not explain whether insulin will be released in dark, after irradiation. To determine accurately if the PAD material will release insulin during this dark period in between two irradiation periods, a discontinuous photolysis should be performed. This is a critical experiment to predict the behavior of PAD materials in animals – the depot should be able to deliver insulin only during the period of irradiation; but delivery during the dark periods (when not irradiated) is not desired and does not result in a tight blood glucose control.

In this experiment, the PAD material was irradiated with a 365 nm LED in discrete events, and the reaction will be analyzed for any insulin release beyond the irradiation period, i.e. during the dark periods. The polymer based first-generation PAD had ideal insulin release kinetics[30]. However, when the same first-generation PAD was later constructed on a Tentagel resin, the insulin photorelease kinetics

differed drastically, showing insulin release in the dark periods[31]. Therefore, the discrete photolysis experiments were performed with the next generation tag-insulin variants to predict their behavior in animals.

Method

A series of discrete photolysis experiments were performed in this study, with all the insulin variants. All the experiments were performed in a uniform way, by following the method described here. Particles of modified insulins were prepared at a concentration of 1 mM (150 nmol/150 µL) in 10mM PBS pH 7.2. The pH of the suspensions was adjusted to 7.2 with 0.1 N sodium hydroxide. Suspension was centrifuged at 15000 g for 5 minutes to separate the particles. The clear buffer was removed, and the particles were suspended in 150 µL of fresh buffer. 100 µL suspension containing 100 nmol was transferred into a 1 mL HPLC insert. Photolysis was performed such that the bottom of the tube was placed 5 cm away from the 365 nm LED.

The experiment for performed for a total duration of 2 hours. Prior to the first irradiation, a 0-minute sample was collected by centrifuging the sample and collecting 100 µL buffer. Particles were suspended in fresh buffer and irradiated for 1 minute. The reaction was centrifuged to collect the buffer (100 µL) at 5, 15, 30, 45 and 59 minutes. Particles were resuspended in fresh buffer (100 µL) after sampling at each time point. Remaining particles were photolyzed again for 1 minute, from 60^{th} to 61^{st} minutes. Sampling was continued in the same way during the second hour at 65, 75, 90, 105 and 120 minutes. 25 µL of the collected buffers were injected on HPLC (150 x

3.2 mm 5 µm C18) for insulin analysis. Amount of insulin in each sample was interpolated from an insulin standard curve.

Discrete photolysis of CD-insulin

The studies began with the discontinuous photolysis of CD-insulin. The experiment was performed as discussed and the data was analyzed on HPLC. To understand the total amount of insulin released from the particles, cumulative insulin amounts were calculated. The results are plotted which shows the cumulative amount of insulin released over time (Figure 76). The results are interpreted to know two different details about the nature of protein release: (a) slow release of insulin, and (b) equivalency of the cumulative insulin amounts in both the irradiation cycles.

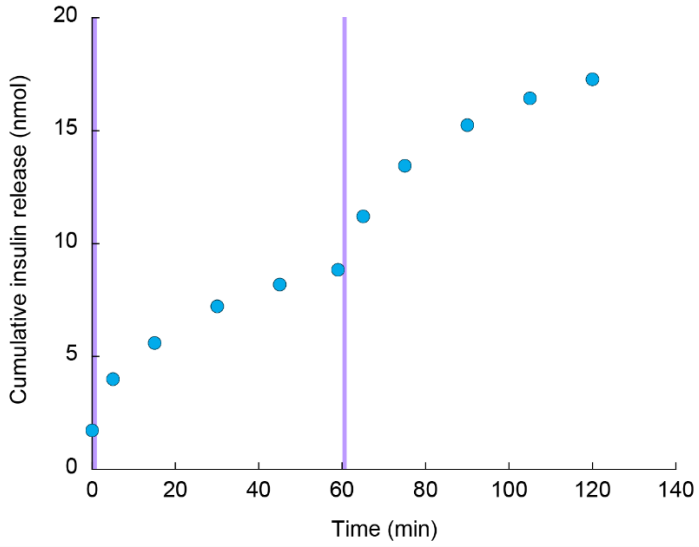

Figure 76 Insulin release from CD-insulin when irradiated in discrete 1 min events. Irradiation periods are highlighted as violet bars on the plot

Ideally, the photoactivated insulin should stop delivering insulin once the light exposure is turned off. But it was evident from the experiment that there was a slow

release of insulin, even during the un-irradiated period after irradiation. From this data, we can predict that the photoactivated insulin would release native insulin over longer time, having a pharmacokinetic profile that is slower than regular insulin.

Secondly, CD-insulin released 8.84 nmol of insulin in the first hour for an irradiation time of 1 minute, and 8.44 nmol of insulin in the second hour. This is an interesting observation that CD-insulin is behaving in an ideal way, releasing equal amounts of insulin on multiple, equal in time irradiation events. This behavior was not observed with previous materials, which also failed to release insulin from the depot upon a second irradiation in an animal model. Therefore, CD-insulin may confer longevity to the depot allowing release of protein with multiple irradiations over time.

A slow insulin release from the PAD is not ideal, and materials should be designed to avoid this problem if possible. Therefore, there is a need to study the behavior of all the next generation photoactivated insulins and solve the lag issue.

Discrete photolysis of all tag-insulin variants (effect of the type of tag)

Based on the conclusions made from the previous experiment, discrete photolysis studies of the rest of the tag-insulin variants were pursued. These include Val-Pro-Ile-insulin, Val-Val-Val-insulin, Ile-Ile-Ile-insulin and P2-insulin. All the four materials were processed as per the method and observations were recorded (Figure 77).

Firstly, all the three non-polar peptidic insulins released insulin in approximately equal amounts with multiple irradiations, though the absolute

amounts of released insulin for each species differ by small amounts. This again indicates that non-polar insulins can possibly deliver insulin in a predictable fashion when irradiated for multiple times in the animal models. However, P2-insulin did not deliver equal amounts of insulin upon multiple irradiations. The amount of insulin release upon second irradiation was only 64% of the amount released upon first irradiation. This phenomenon is not yet understood but is observed with other previous generation photoactivated insulin materials too.

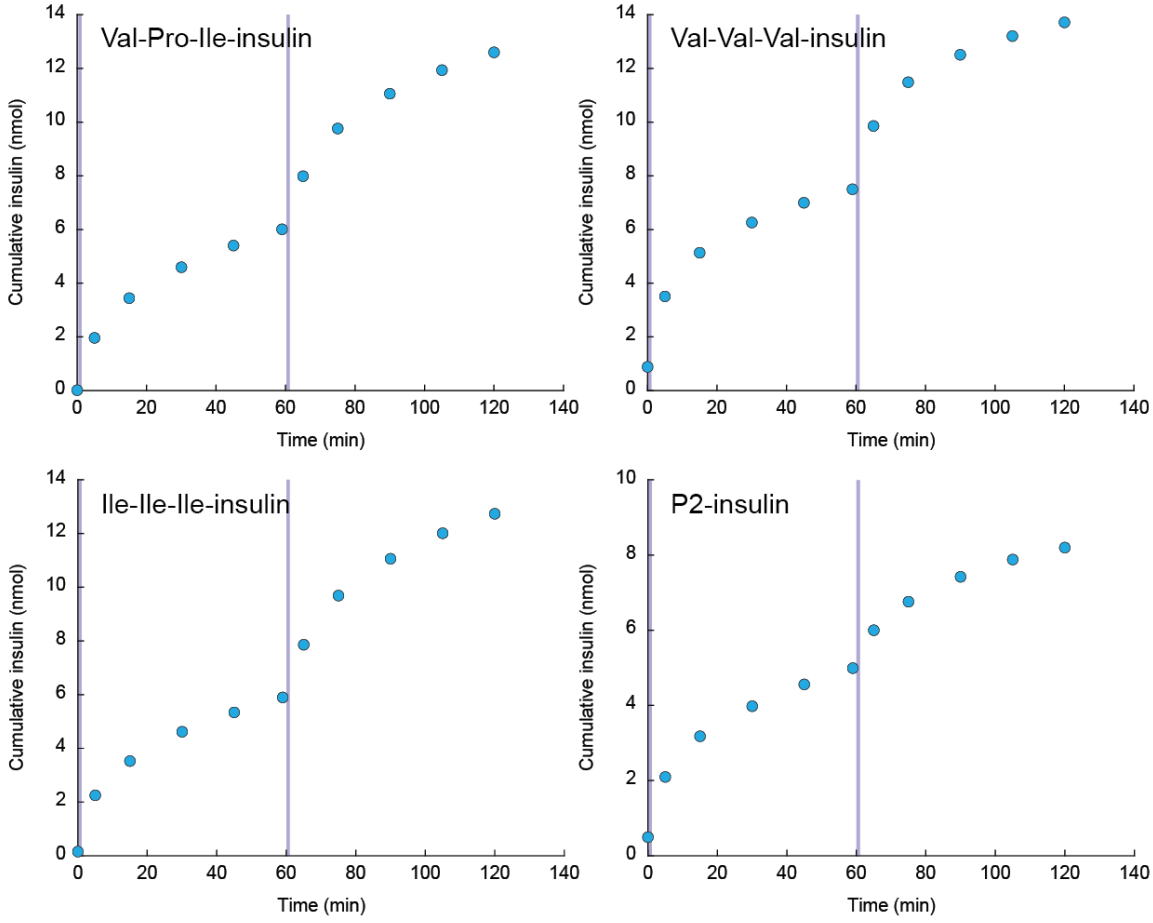

Figure 77 Insulin release from VPI-insulin, VVV-insulin, III-insulin and P2-insulin when irradiated in discrete 1 min events. Irradiation periods are highlighted as violet bars on the plots

Like CD-insulin, both the non-polar tag and the P2 charge-tag variants showed lag in insulin photorelease. The first-generation material, in which insulin was linked to an insoluble polyethylene glycol-based resin, also released insulin at a slow rate. Since non-polar, charged as well as solid insoluble supports have similar responses to the stimulus, it was concluded that the slow release may be independent of the nature of chemical modifications. Therefore, other possible reasons for the delay in release were investigated.

Effect of particle size on the rate of insulin release

One of the factors that can play a key role in the release of insulin is the size of the particles. Insulin variants are milled into fine particles at high μm ranges. These are insoluble particles which scatter the light, particularly the 365 nm light which can undergo scattering significantly as it has a lower wavelength. However, particles of a size have specific surface areas that are exposed to light during the photoreaction – this affects the rate of insulin release. When the same amount of insulin variants is milled into different sizes, smaller particles have an overall higher surface area. Therefore, the number of molecules exposed to the 365 nm light is higher and hence more insulin molecules may be released. This hypothesis was put to test by making CD-insulin of different particle sizes and performing discrete photolysis experiments using the method discussed above.

Preparation of particles of different size was a challenging task. Initially, attempts were made to mill CD-insulin with different sized magnetic beads which can assist in the formation of different sized insulin particles. However, the protein was

observed to be lost probably due to (a) non-covalent binding on the bead surface, or (b) protein denaturation. Hence, alternative methods of making the particles were explored. Another method was identified from the literature to make small particles of uniform sizes. This method was called the membrane extrusion method and was applied to produce particles of small molecules[47]. Though the particle size was small (~100-200 nm) and uniform, it was not applicable to proteins as the method requires the use of non-polar solvents in which insulin is insoluble.

Finally, CD-insulin particles of two different sizes were prepared using two different techniques (Figure 78). Following the regular method of milling during this experiment, the mean particle size (diameter) of CD-insulin was found to be 1208 nm. A theoretical calculation using the mean diameter gives a mean surface area ($4. .r^2$) of 4.58 μm^2. Then, CD-insulin particles of a different size were prepared by precipitating it in a 50 mM pH 6.0 phosphate buffer (without sodium chloride). In brief, 150 nmol CD-insulin was dissolved in 100 µL DMSO. This solution was added dropwise to the pH 6 buffer which was vigorously stirred. The pH of the buffer was adjusted to 6 because CD-insulin will have lowest solubility at its isoelectric point. The resulting particles had a mean diameter of 2837 nm and a mean surface area of 25.29 μm^2. Though the mean diameter was only about twice higher, the discrete photolysis experiment was performed since the surface area was significantly higher by about 5x. Observations are shown in Figure 79.

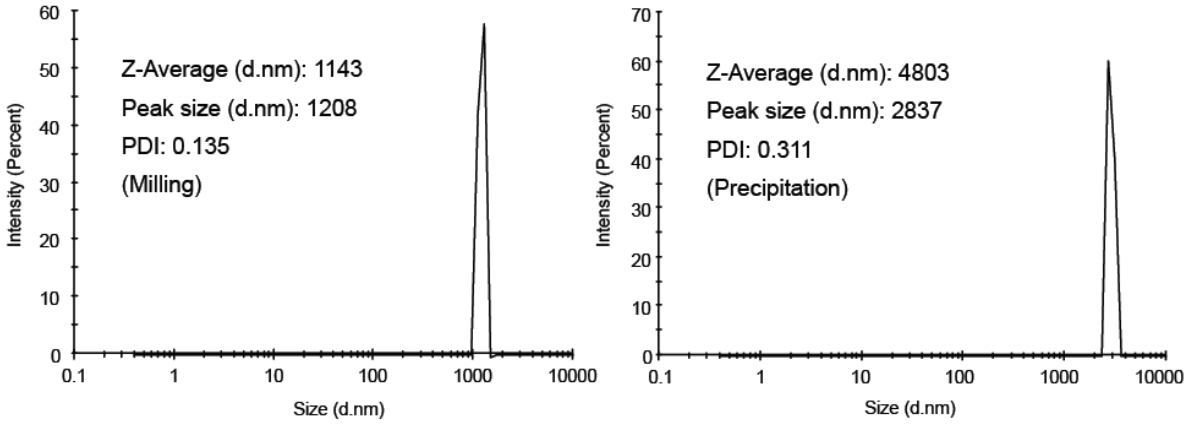

Figure 78 CD-insulin particles of different sizes analyzed using Zetasizer Nano

Again, CD-insulin particles of both sizes had a slow release. It is difficult to compare the rates of release due to difference in amounts release. To compare the rate, only the first hour data was considered; the amounts released were normalized to percentages and the data was overlaid on a single plot. This showed that the rate of release was same for the smaller particles (milling) when compared with the larger particles (precipitation). Therefore, it was concluded that the rate of insulin release could not be affected with particle size. Moreover, CD-insulin did not release equal amounts of insulin in both the irradiation cycles in this experiment. It may be possible that the exposure of protein to the buffer over longer periods may affect the rate of release due to exchange of salts with TFA as counter ions. Salts are known to lower the rate of DMNPE photolysis. In fact, it can also be expected that the amount of insulin released is lower for the second irradiation. If the rate of insulin release depends on the concentration of CD-insulin, the amount of native insulin should be lower as the concentration of CD-insulin after 1 hour should be lower. Since this

phenomenon is not completely understood, it should be noted that insulin release is not predictable and can vary between experiments.

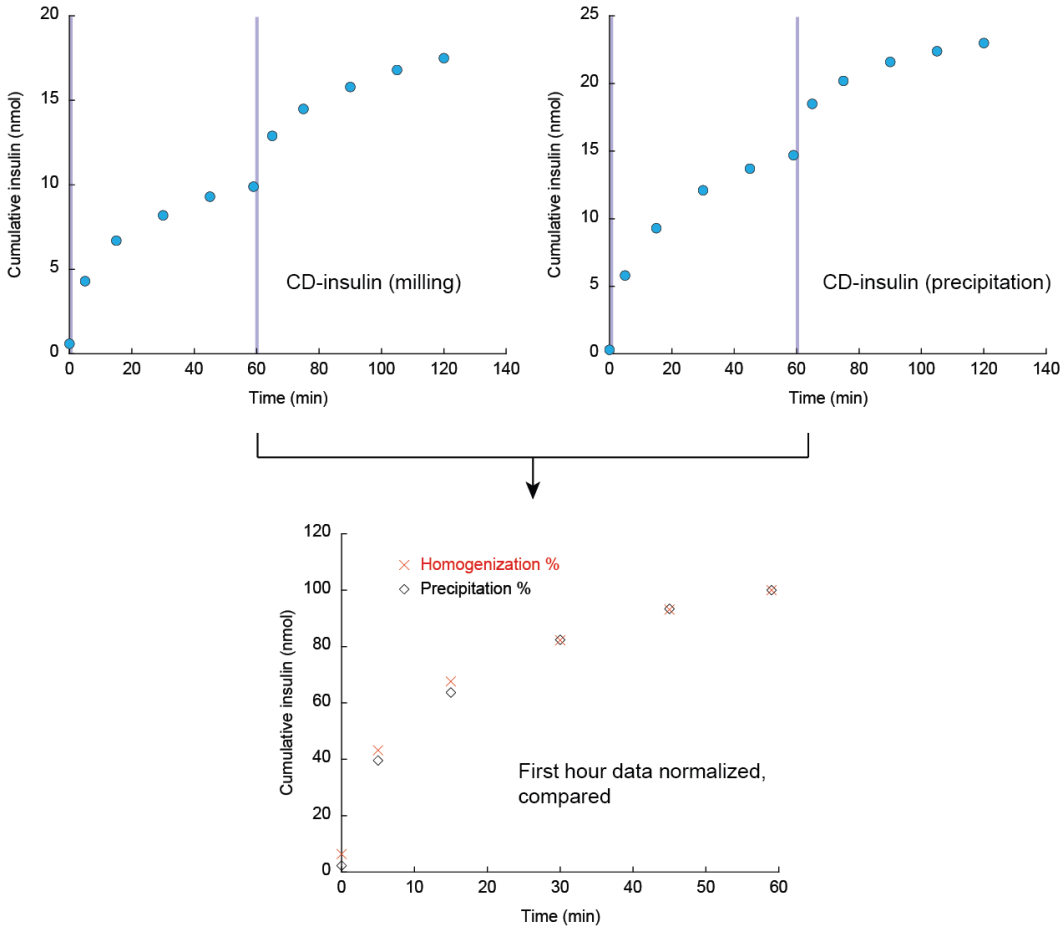

Figure 79 CD-insulin of different particle sizes release insulin in the same rate when photolyzed in discrete events

Effect of intermolecular insulin interactions on rate of insulin release

In the previous experiments, physical and chemical properties of the protein such as particle size and the nature of modification have been explored. However, not all chemical properties of the variants were investigated. The next generation insulin variants are made up of three different chemical moieties – (a) the tags, (b) insulin,

and (c) the photocleavable group. It is now clear that the tags do not affect the rate of insulin release. So, it is important to study the physicochemical nature of the protein itself and its effects on the rate of insulin release.

Insulin tends to interact with neighboring molecules to form stable multimers, especially in the presence of metal ions like zinc[48]. An insulin hexamer is particularly stable as a zinc complex, and it is this form that is used by the pancreas to store insulin before releasing into the blood[49]. Since insulin molecules are brought close to each other during the preparation of particles, it is possible that the proteins are bound tightly with the other molecules in a particle and hence are solvated at a lower rate. To test this hypothesis, new variant with CD-tag was synthesized using Lispro. Lispro is a fast-acting insulin developed by Eli Lilly by reversing the sequence of the last two residues of the B-chain towards the C-terminus. This minor structural difference weakens and breaks the complex at ~200x faster rate than native insulin, ensuring that insulin stays in its monomer form for majority of the time[50].

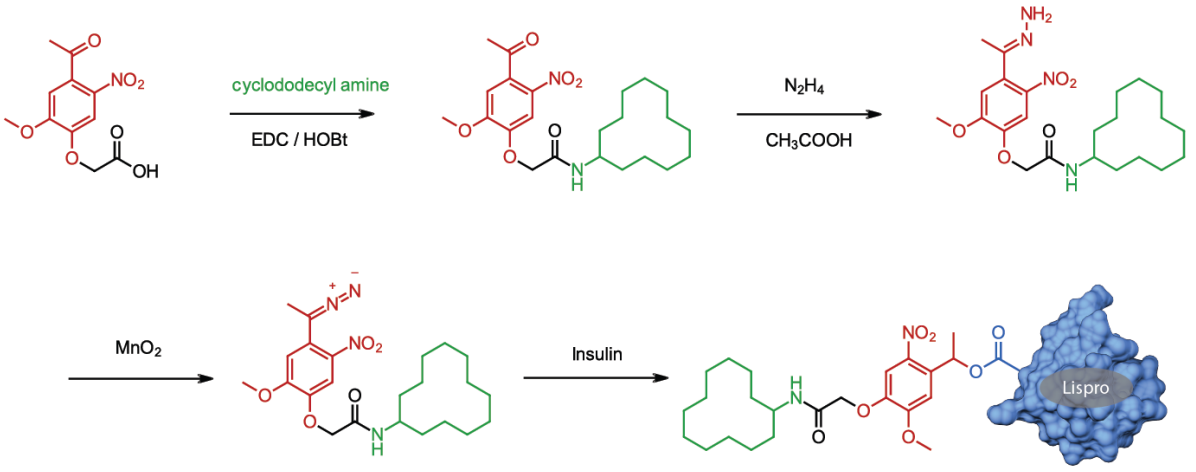

Figure 80 Synthesis of CD-Lispro

CD-Lispro was synthesis using the method described for CD-insulin (Figure 80). 1.13 µmol (50 µL diluted to 200 µL with DMSO) of CD-diazo was added to Lispro (1 µmol) in DMSO (300 µL). Reaction was incubated in dark at room temperature for 24 hours. CD-Lispro was purified using RP-HPLC using a 250 x 4.6 mm 5µm C18 column. The pure protein was collected from 18.3 to 20.0 minutes on a 0-30 minutes acetonitrile gradient at 1 mL/min. Solvents contained 0.1% trifluoroacetic acid. CD-Lispro was analyzed on HPLC and MS (Figure 81).

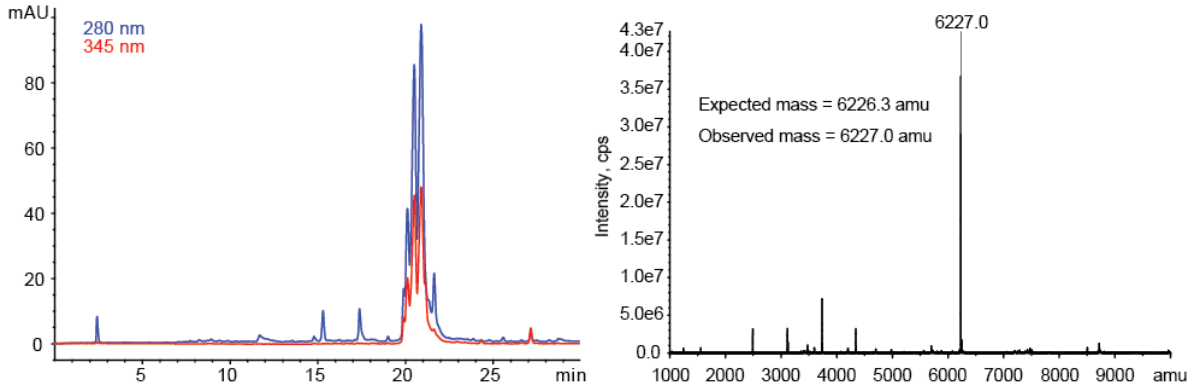

Figure 81 CD-Lispro analysis on HPLC (left) and MS (right)

After purification, discrete photolysis of CD-Lispro was performed by following the standard method discussed earlier. Similar to the pattern observed for CD-insulin, HPLC analysis showed that CD-Lispro also had a low rate of insulin release. It was concluded from this experiment that intermolecular interactions between insulin molecules also is not responsible for the lag in release of insulin. The data points at time 0 min are not closer to zero due to the contamination of insulin from purification of protein. Due to minor differences in the amount of insulin released, the photorelease data of only the first hour was normalized to percentages.

For this study, only CD-Lispro was photolyzed in a discrete manner. Discrete photolysis of CD-insulin was not repeated for this experiment for comparison. Data from the first sub-study in this chapter was used (Figure 82).

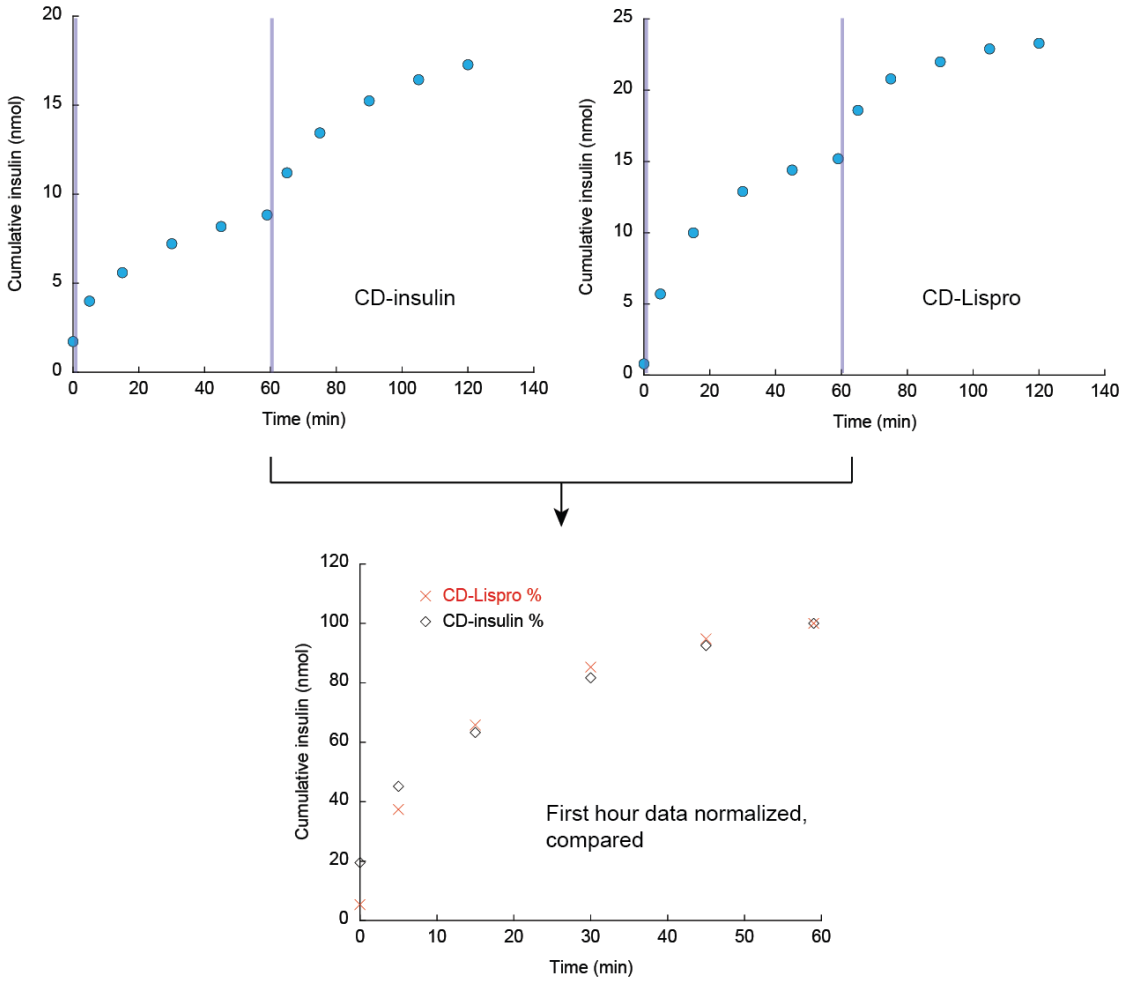

Figure 82 CD-insulin and CD-Lispro uncage insulin at a similar rate as seen when photolyzed in discrete periods

Effect of the rate insulin dissolution on rate of insulin release

Previous observations have shown that insulin is rapidly absorbed into the blood (C_{max} ~15 min) in diabetic rat models. However, the insulin released from the

photoactivated insulin is slowly absorbed[31,51]. This phenomenon can be consequence of the slow release of insulin from the depot.

Regular insulin injections contain the hormone that is already solvated in the formulation. Therefore, its absorption into the blood is limited only by the of rate of insulin diffusion into the blood circulation. But the slow release can be attributed to the dissolution of the protein itself. The photoactivated insulin variants are insoluble particles in a solid state. After photolysis, the native insulin that is produced is also in the solid state at that precise moment. This insulin in the insoluble form needs to be solvated before being absorbed into the blood for circulation. Here, the rate at which insulin is detected whether in the blood (*in vivo*), or in the buffer (*in vitro*) is limited by two steps – (a) insulin dissolution, and (b) insulin diffusion. Thus, the process can be thought to be slower since an additional step is involved here.

This hypothesis was tested by measuring the rate at which insulin goes into buffer. 383 nmol (2.22 mg) insulin was weighed in a 1 mL HPLC insert. The experiment was initiated by the addition of 500 µL 10 mM PBS pH 7.2 was added to the tube. It was shaken throughout the experiment to allow uniform dissolution. Sampling was performed over one hour, specifically at 5, 15, 30, 45 and 60 minutes by centrifuging at 15000 g for 5 minutes. At each time point, 500 µL of the buffer was removed and the particles were resuspended in fresh buffer. Analysis was performed on HPLC and insulin in each sample was determined using a standard curve.

The results indicate that insulin is not instantaneously soluble at pH 7.2 (Figure 83). Complete saturation was achieved at 30 minutes, however visually the buffer was

clear by ~20 minutes. Based on these observations, it can be concluded that the rate of insulin dissolution can play a key role in limiting the rate at which insulin is delivered from the photoactivated insulin.

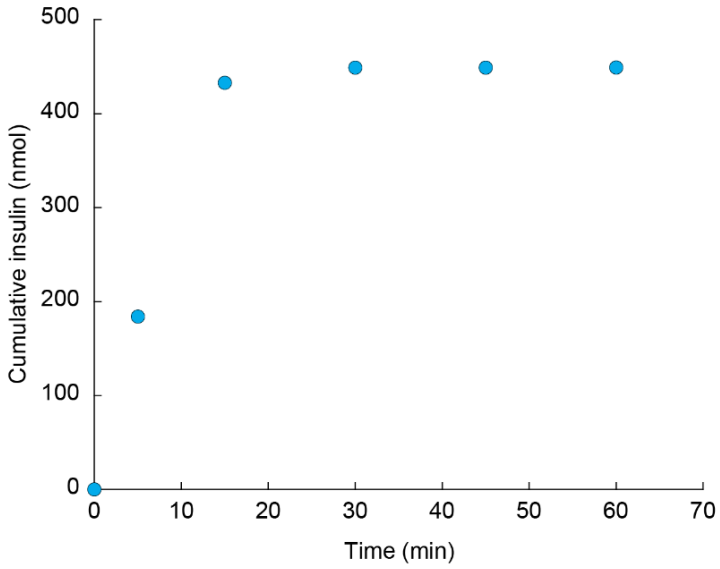

Figure 83 Insulin dissolution (rate) in 10 mM PBS pH 7.2

Role of photocleavable group in the mechanism of insulin release

Interesting observations were made from the discrete photolysis experiments of tag-insulin variants. Effects of the chemical nature of tag-insulin variants were studied moiety-by-moiety. It seems that both the tags and the protein do not influence the rate of insulin release. The only moiety that is common among all the different variants is the photocleavable group. It is therefore possible that the lag is caused by the photocleavable group.

Literature was extensively surveyed to know the mechanism of photocleavable group. The exact mechanism for the DMNPE ester photolysis is not determined yet. However, a few mechanisms were proposed based on their observations. One of these

mechanisms is now widely accepted and describes the photocleavage reaction in two steps (Figure 84). The first step involves the excitation of the photocleavable group and is a rapid process. However, the next step in which the carboxylic acid is uncaged is the slow rate determining step that may depend on the pH of the environment.

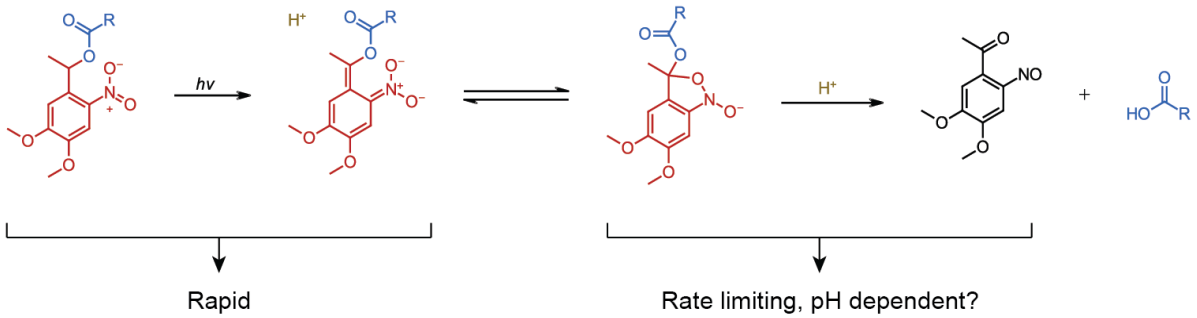

Figure 84 Possible mechanism of DMNPE photolysis. A rate limiting step can potentially lower the insulin release rate at pH 7

Interestingly, another group studying the rate of DMNPE photolysis describes how the rate is affected by pH of the environment[52]. It was observed that the reaction progresses at a very high rate in acidic conditions, and the rate goes down drastically as the pH is raised. Moreover, the same study also shows that the rate is also lowered in the presence of salts. Thus, it can be predicted from these observations that the rate of insulin photo-release can be lower under physiological conditions. This can be studied by photolyzing a caged model compound in 10 mM PBS and analyzed with the help of H-NMR. However, it was not pursued due to lack of time.

CHAPTER 6

IN VIVO STUDIES

Introduction

Testing the tag-insulin variants in animals will provide the ultimate answer to whether the tag approach can be further pursued and translated for clinical use. Of the eight different variants synthesized in the overall study, five materials (Val-Pro-Ile-insulin, Val-Val-Val-insulin, Ile-Ile-Ile-insulin, CD-insulin and P2-insulin) can be potentially used for testing the proficiency of the tag approach in animal models. Since all the four non-polar insulin variants are similar, only one best species was used as a representative of the category. Therefore, CD-insulin and P2-insulin, i.e. one from each category, were chosen to be tested in diabetic rats. The methods described here are approved by the University of Missouri - Kansas City Institutional Animal Care and Use Committee (IACUC Protocol number 1603-02).

T1D rodent model

A method was previously established to test the first-generation PAD in diabetic rats. The same method will be followed for the testing of the photoactivated tag-insulins so that the *in vivo* responses can be compared. Sprague Dawley rats (male) were purchased and type 1 diabetes was induced with an intraperitoneal injection of streptozotocin (65-70 mg/kg). The streptozotocin was diluted in 100 mM Na-Citrate buffer, pH 4.5 under sterile conditions. Streptozotocin destroys the islets of pancreas and therefore the rat cannot produce insulin, mimicking the condition of type 1 diabetes[53]. This T1D rodent model has a constant elevated blood glucose

concentration. The rat was confirmed to be diabetic when the blood glucose concentration is found to be >250 mg/dl on three consecutive days after the treatment with streptozotocin. The concentration can be brought down to normal levels only with the administration of exogenous insulin. In addition, Sprague Dawley rats are also known to be calm and can be easily handled. This is therefore an ideal model for the testing of photoactivated insulins.

Experimental method

The rats were anesthetized with isoflurane gas using a precision vaporizer (induced with 5% and maintained at 2-2.5%). When the rat reached the plane of surgical anesthesia, they were placed on a surgical warming pad throughout the experiment to maintain a baseline body temperature. The tail of the rat was nicked at the end (or the scab) with a sterile scalpel blade after sterilization with 70% ethanol; and this was performed to collect the blood from tail vein. The baseline glucose concentration was then determined.

200 nmol modified insulin was milled in 200 µL 100 mM PBS pH 7.2. The suspension was centrifuged, and the supernatant was removed. The pellet (of modified insulin) was resuspended in 50 µL 10 mM PBS 7.2. 35 µL of the suspension was diluted to 50 µL with 10 mM PBS and loaded in a syringe with 27 G needle.

A site of about 1 $inch^2$ patch of dorsal skin near the spine was identified as the site of PAD injection and shaved with a razor to remove the hair. The site was sterilized with 70% ethanol and the photoactivated insulin suspensions in PBS (150 nmol/50 µL, or 25 U/50 µL) were injected intradermally using a 27 G needle. The base

plate of the LED was stuck around the site of injection with glue. 20 minutes after the PAD injection, blood glucose and insulin levels were measured to determine if there was any leaching of insulin into the blood. The LED was then placed on the site of injection, the placement or alignment of which will be assisted with the magnets on the base plate. The depot was irradiated for a predetermined time by turning on the LED. For control rats, an aluminum foil was placed between the LED and base plate so that the light was blocked, and the depot not irradiated. After irradiation, blood was collected at predetermined time points for the next two hours to determine changes in glucose and insulin levels. After each collection, blood was centrifuged at 4000 rpm for 10 minutes to remove RBCs. Clear plasma was collected in an Eppendorf tube with a gel loading tip and frozen at -20 C until ELISA analysis. The rat was allowed to recover for a minimum of 3 days if multiple experiments were performed. This duration also provided enough time for any previously injected insulin materials to be eliminated from the body.

Determination of glucose and insulin concentrations:

At each time point, glucose concentration (mg/dl) is directly determined during the experiment using a Freestyle Lite Blood Glucose Monitoring System. However, the plasma was frozen until when the insulin concentration (nM) was determined using ALPCO Ultrasensitive Insulin ELISA kit, following the method described in the booklet. Plasma samples were diluted 15x with zero standard (provided in the kit) for analysis by ELISA.

Pilot study with CD-insulin

Our studies began (in Rat #44, IACUC protocol number 1603-02) with CD-insulin, the non-polar tag insulin variant with lowest solubility. As discussed, 150 nmol of CD-insulin particles were injected intradermally. Two minute-irradiation of the first-generation PAD resulted in a significant decrease in blood glucose. But the tag-insulin variants have ~6x more insulin density. Moreover, the duration of irradiation should be lowered since CD-insulin can leach into the blood as it does not have an absolute zero solubility. Therefore, the duration was reduced to 30 seconds. Glucose and insulin levels were plotted against time (Figure 85).

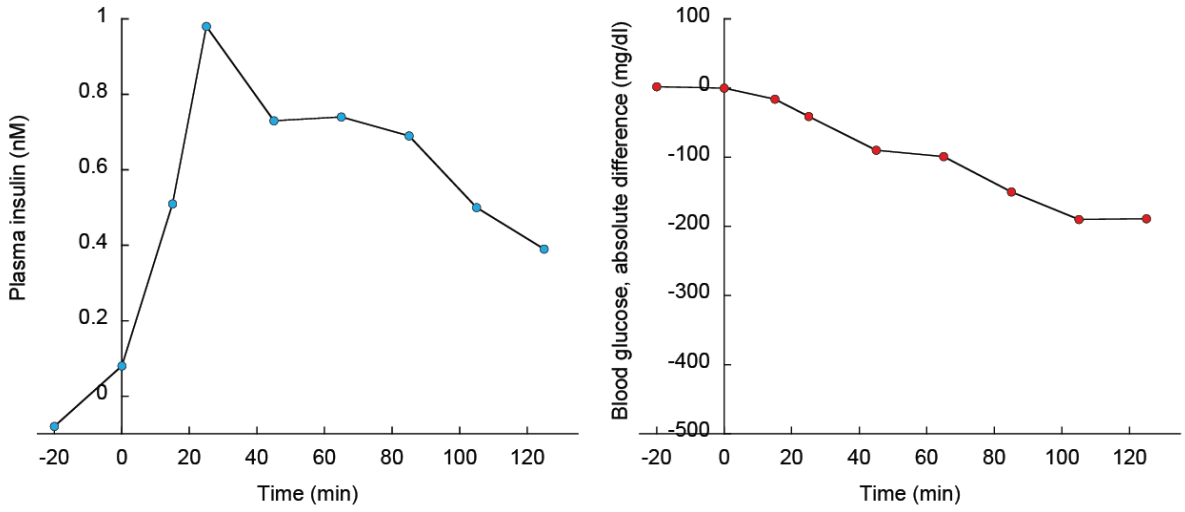

Figure 85 Blood glucose and plasma insulin profiles of CD-insulin. The depot was irradiated for 30 seconds

This experiment shows that insulin can be delivered into circulation in an amount that is significantly higher (C_{max} = 1 nM) than the first-generation PAD (C_{max} = 0.2 nM). The blood glucose levels fell from 313 mg/dL to 122 mg/dL at the end of two hours. This is ~190 units reduction in glucose levels, compared to the 180 units

reduction with the first-generation material. This result was achieved with a duration that is 1.5 minutes lesser than the duration of irradiation of the first-generation PAD. This improvement was possible only due to the tag approach, which not only improved the insulin density to 90% w/w, but also improved the density of photocleavable groups in the depot to enhance the rate of photochemistry and release therapeutic amounts of insulin.

Additionally, it should also be noted that there was minimal difference between the amount of insulin detected in plasma at -20 min and 0 min. This indicates that leaching of insulin from the depot cannot be detected even with the help of an ultrasensitive ELISA. This observation was also corroborated with the levels of glucose at those time points. Relative to the total reduction of glucose over 2.5 hours (191 units), the amount lowered was only 2 units, which is only 1% response. This study shows that the non-polar tags are successful at lowering insulin solubility and help make highly efficient photoactivated depots.

CD-insulin dose-response study – experimental design

Though it was evident from the previous experiment that the non-polar tags make good photoactivated depots, additional studies are required (along with controls) to know if the PAD can be translated into clinics. Multiple questions are required to be answered, but here the work will be focused on understanding the dose-response of CD-insulin in the T1D rat model. These studies are critical to know if the depot can deliver only the desired amount of insulin, due to varied times of irradiation, in response to blood glucose if automated. Blood glucose levels vary

person to person and time to time based on their carbohydrate consumption. Therefore, experiments were designed to know how much insulin will be delivered with different irradiation periods, and if an increase in amount delivered correlates with an increase in time.

Sample size determination

The power analysis was performed on the data from the single irradiation experiment with the first-generation PAD[31]. The highest amount of plasma insulin, detected at t=25 min in test group, was compared to the amount of plasma insulin at t=25 min in control group. These groups have a very large effect size of 3.64. For an =0.05 and power=0.9, the sample size was found to be 3. Though the experiments were performed prior to this statistical analysis, this indicates that the studies performed with three rats for each material should be enough.

Experimental design

The same amount of depot (150 nmol) was injected during each experiment. Five different experiments were performed on each rat, in which the depot was irradiated for 0, 15, 30, 45 and 60 seconds. The 0 second irradiation was the control experiment where an aluminum foil was placed between the light source and depot, and light was turned on for 60 seconds. Thus, this experiment not only acted as a control in which the depot was not irradiated (0 seconds), but also answered the question if insulin was released from the depot due the heat generated from a 60 sec irradiation of the LED. These experiments were performed in three rats in total to obtain the data in triplicates.

CD-insulin dose-response study: the first attempt

In Rat #45, 15 second irradiation of the depot had a highest insulin C_{max} of 0.25 nM at 45 minutes. But the corresponding blood glucose levels were only lowered by 120 units from 355 mg/dL to 232 mg/dL. In the next experiment on the same rat, when the depot was irradiated for 30 seconds, the C_{max} was found to be only 0.23 nM (65 minutes) and the blood glucose levels fell by only 164 units (Figure 86). Firstly, CD-insulin did not deliver insulin in a linear fashion, i.e. the insulin concentration was not doubled with the doubling of irradiation time. Second, the glucose levels did not drop in Rat #45 in comparison with Rat #44. Most importantly, skin reaction was observed at the site where CD-insulin was injected (discussed later). Similar results regarding the insulin insensitivity were also observed with Rat #46. The blood glucose was only lowered from 334 mg/dL to 277 mg/dL (difference = 57 units) over 2 hours.

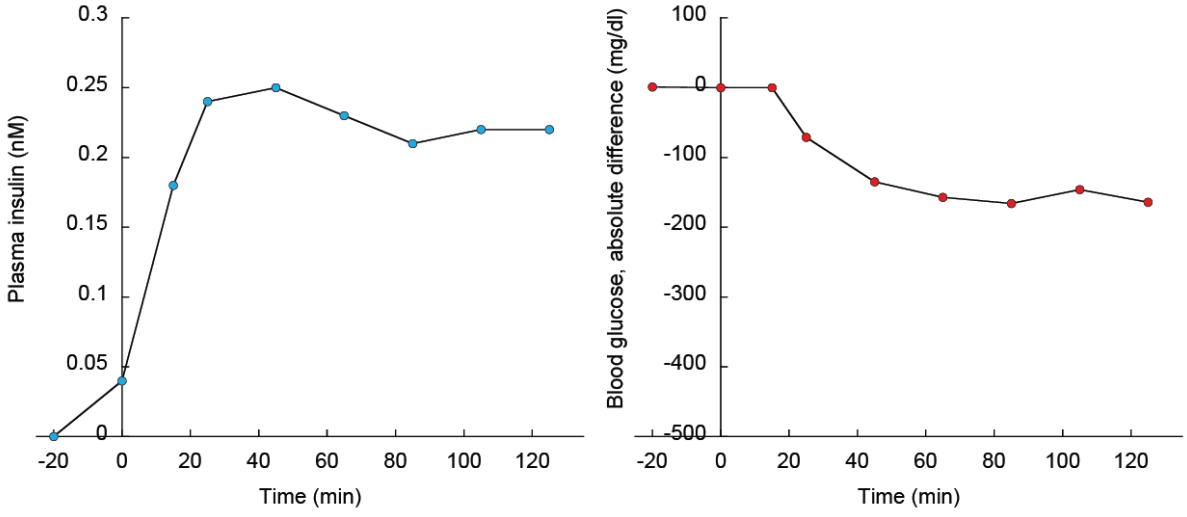

Figure 86 30 seconds irradiation of the depot in Rat 45 did not yield the same results. Both the insulin release and glucose response were lower compared to the observations in pilot study

These possibilities were discussed based on the results on Rat #45 insulin response:

a) Insulin photoreleased from CD-insulin was not biologically active, probably as the protein was processed in organic solvents.
b) The insulin purchased commercially itself was not active.
c) Rat #45 was insensitive to insulin.

The following possibilities were thought to be responsible for the skin reaction:

a) CD-insulin injection resulted in an immunogenic reaction at the site of injection.
b) Vehicle (PBS) was not sterile, and hence the reaction was observed due to infection.
c) Continuous exposure of UV light resulted in burning of the skin, which was a reaction at the site of injection.

In order to know the reasons for failure, new experiments were designed.

Test of insulin bioactivity or rat insensitivity to insulin

Bioactivity of photoreleased insulin

While pursuing first-generation PAD, insulin assay was established by injecting insulin solutions subdermally at a dose of 14.2 nmol/kg (2.36 IU/kg)[31]. This dose was also used by other research groups, and therefore insulin injection at this dose should lower the blood glucose of a diabetic rat by ~420 mg/dL. This information was utilized to study if the insulin released from CD-insulin was biological active. CD-insulin was photolyzed *in vitro* in PBS and the amount of insulin released into solution was determined using HPLC. Volume of PBS containing insulin

amount equivalent to a dose of 14.2 nmol/kg was injected in Rat #47 (Figure 87). The glucose concentration was only lowered from 405 mg/dL to 306 mg/dL (difference = 99 mg/dL). This is a very low response compared with the 420 mg/dL reduction in older studies. Thus, it was confirmed that either the photoreleased insulin was inactive, or the rat was insensitive to insulin. Therefore, another experiment was performed to further clarify this problem.

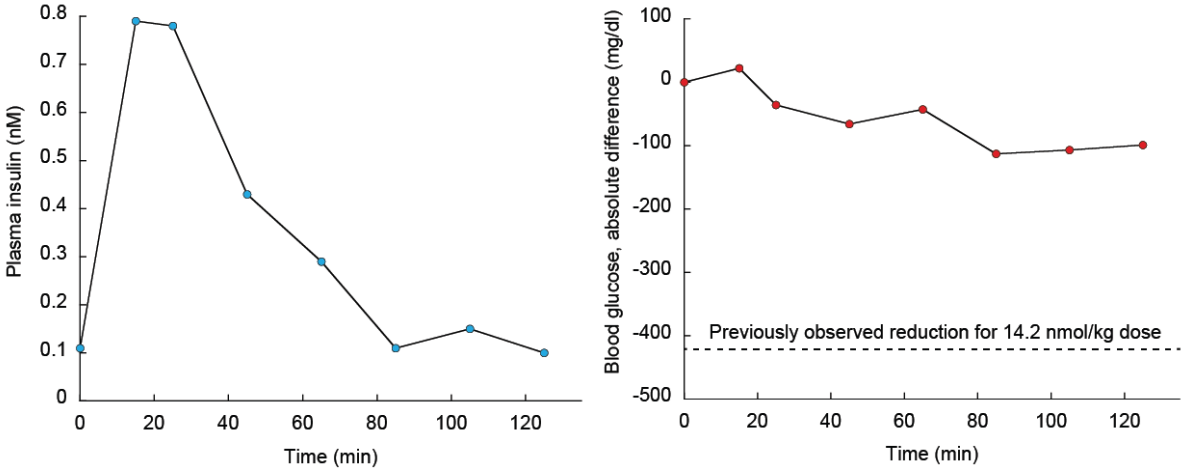

Figure 87 CD-insulin was photolyzed in PBS. Photoreleased insulin was injected in Rat #47 at a dose of 14.2 nmol/kg. Plasma insulin (left) and glucose (right) profiles are shown. Dotted line in the glucose plot shows the amount of reduction seen previously with the same dose of insulin

Bioactivity of commercial insulin

In this experiment, a solution of insulin purchased newly from the vendor was prepared in PBS. Insulin of dose 14.2 nmol/kg was injected subdermally in Rat #47 and the glucose was monitored. Plasma was not collected for insulin analysis. Again, Rat #47 did not respond to insulin and the glucose was only lowered from 379 mg/dL

to 318 mg/dL (difference = 61 mg/dL) over 65 minutes. Since the glucose drop saturated at that stage, the experiment was not continued for another hour. This low amount of reduction in blood glucose clearly tells that the rat is insensitive to insulin, as the insulin was purchased freshly from the vendor. There is again a possibility that the insulin obtained from the vendor is not biologically active. This was further verified by injecting the same Rat #47 with a pharmaceutical standard, Novolin R. Novolin R is a fast-acting insulin and is used clinically. Rat #47 was observed to be insensitive to Novolin R. This confirms that the problem was with the rats 45, 46 and 47, and that the CD-insulin was probably fine (Figure 88).

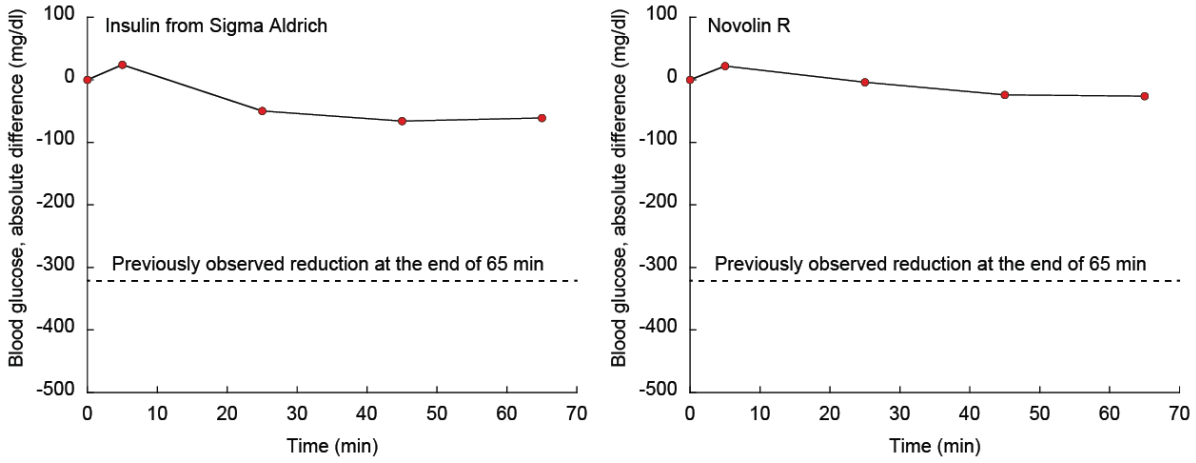

Figure 88 Blood glucose was not lowered when 14.2 nmol/kg insulin (Sigma Aldrich) and Novolin R were injected subdermally in diabetic rat

Tests to study reaction at the injection site

PBS (vehicle) injection: test of sterility and glucose drifting

In these studies, reasons for the reactivity at the injection site were explored. Rat #45 was anesthetized and the same volume of PBS, which was used for the

preparation of particles, was injected at -20 minutes. The experiment was performed for 2 hours according to the standard method, but the plasma was not collected for insulin analysis. Only the blood glucose was monitored at specific time points over 2-hour period (Figure 89).

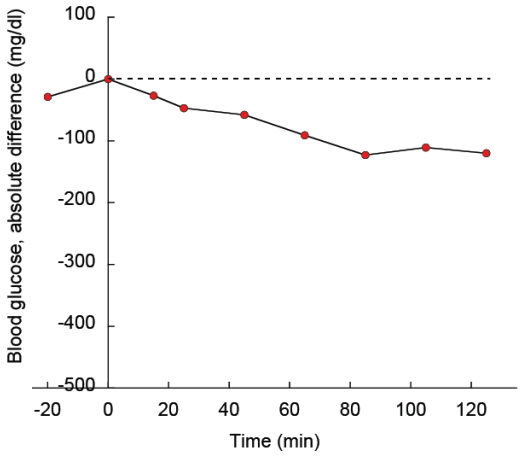

Figure 89 Blood glucose was observed to drift to lower concentrations even in the absence of insulin, probably due to "fasting" of rat while being under anesthesia

The blood glucose was not maintained at a constant level during the experiment. Even though insulin was not injected, the glucose levels were lowered from 424 mg/dL to 304 mg/dL (difference = 120 mg/dL) over 2 hours. Therefore, the reduction of glucose in any of the previous experiments may not be attributed to only insulin. These observations can be explained if the rat consumed any food just before the experiment. Any glucose that was absorbed into the blood was probably being used by the tissues during the experiment. Therefore, it was required to optimize the experiment to have a stable glucose profile throughout the period.

Also, the site of injection was observed for any reactions, which could occur due to microbial infections if the vehicle was not sterile. The site was monitored for ~48 hours and any skin reaction at the site was not observed. Therefore, it was concluded that the vehicle was not responsible for the skin reaction.

Identification of agent responsible for skin reaction

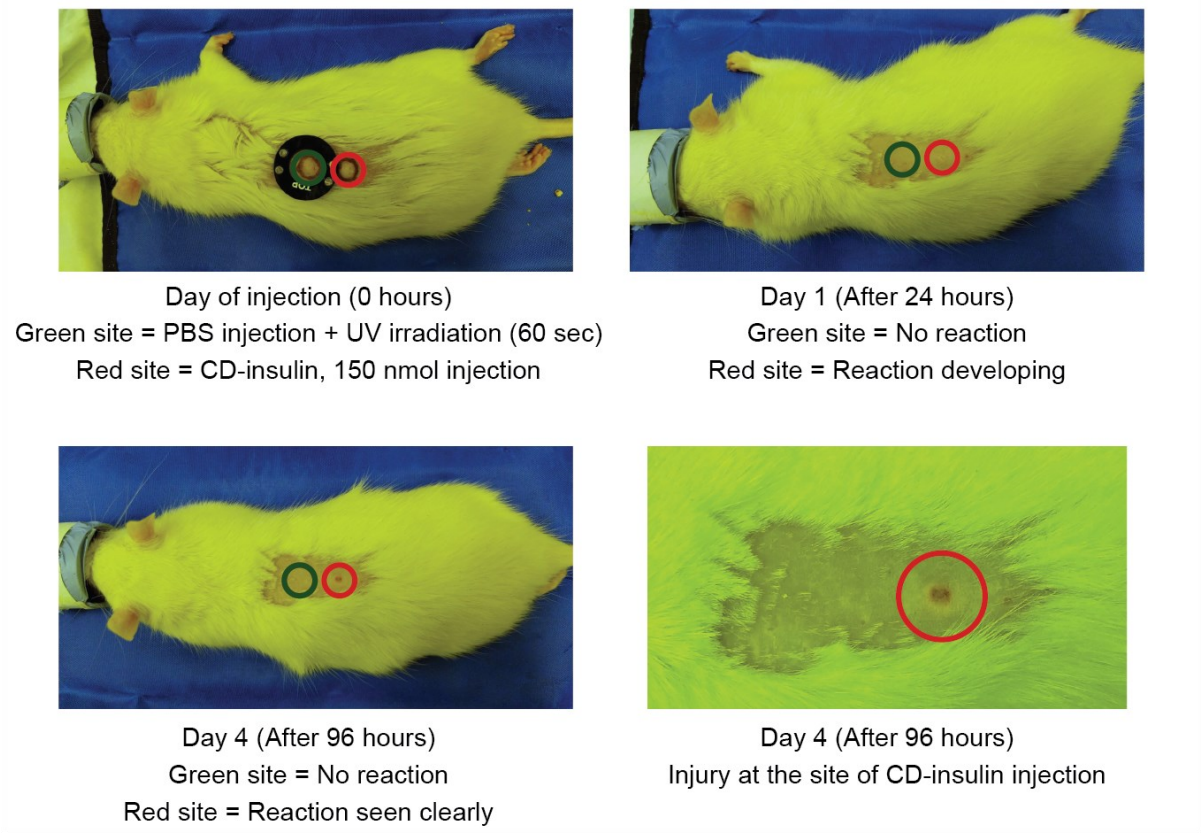

Figure 90 Skin reaction was observed at the site of CD-insulin injection

In this experiment (Figure 90), two injections – (a) 150 nmol CD-insulin in 50 µL PBS, and (b) 50 µL PBS were injected at two different sites in Rat #46. Site (a), i.e. the CD-insulin depot was not irradiated. But the site (b) where PBS was injected was irradiated with 365 nm LED for 60 seconds. The sites were monitored for two days for

any skin reactions. It was observed that the site (a) showed a skin reaction. However, site (b) where PBS was irradiated did not show any reaction.

Since site (b) was irradiated, neither light nor heat induced any injury. Injury was detected only at site (a), therefore the animal showed response to CD-insulin only. PBS also did not show any signs of injury, which was also observed in the previous experiment. It should be noted that not all rats showed reaction to the depot. The reason for this phenomenon was not yet understood.

Test of glucometer

In addition to the factors such as the health of the rat, or the bioactivity of insulin that affect the success of the experiment, one additional factor was required to be tested. This was the accuracy of the glucometer. All the responses so far were detected using the Freestyle Lite Blood Glucose Monitoring System. It was possible that the glucose detection itself was inaccurate. Therefore, the accuracy of the meter was determined by measuring glucose concentration from standard prepared in the laboratory. Glucose strips were dipped in standard solutions (100 mg/dL, 200 mg/dL, 300 mg/dL, 400 mg/dL and 500 mg/dL) and the observations were recorded. A new glucometer was also purchased (OneTouch Ultra 2 Glucose Diabetes Meter Kit) and the standards were measured. Both the results were compared (Figure 91).

It was observed that both the glucometers did not determine the glucose concentrations accurately. However, the new OneTouch glucometer was found to be more precise. The reason for the inaccuracy in measurements of standard solutions was later found from literature. Glucometers are designed to measure glucose

concentrations from viscous solutions containing dense cell populations such as the red blood cells[54,55]. Aqueous solutions of D-glucose are not ideal standards for calibrating clinically used point-of-care glucometers.

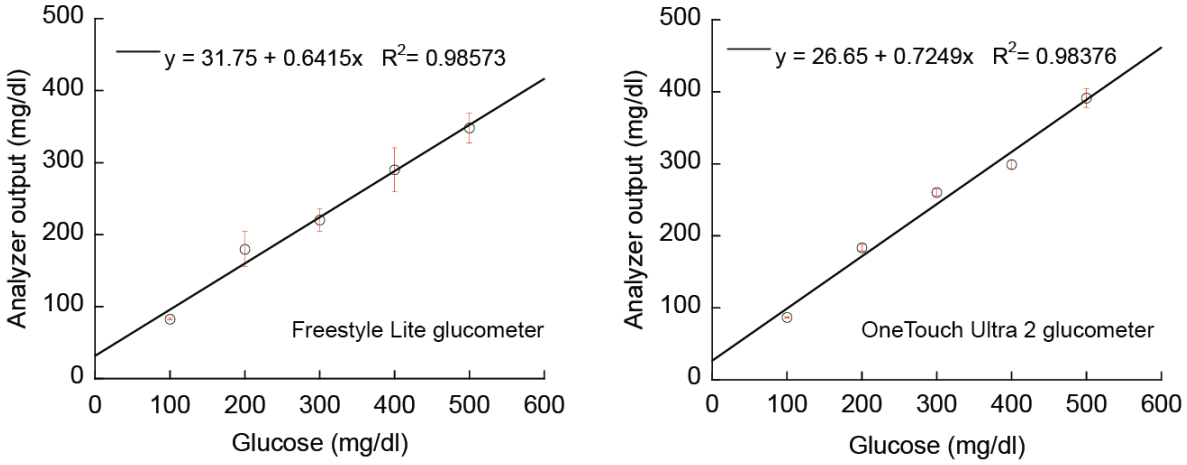

Figure 91 Test of glucometers with D-glucose standards. The OneTouch Ultra 2 glucometer was found to be more precise

Purchase of the new glucometer led to an interesting, yet very critical observation. Though the *in vitro* calibration experiments did not show any difference, a significant difference was observed in the measurements when both the glucometers were used to determine the glucose concentration from the rat blood. The older Freestyle Lite glucometer was particularly inaccurate at measuring blood glucose beyond 400 mg/dL. Therefore, the glucometer was showing outputs at around 380-420 mg/dL even when the true concentration of blood glucose was as high as >500 mg/dL. The new OneTouch Ultra 2 glucometer had an upper limit of detection of 600 mg/dL in blood.

The blood glucose concentration is measured typically when T1D was induced with streptozotocin. Previously, low blood glucose was detected even after streptozotocin injection, since the older glucometer did not function well. So, more streptozotocin was injected in the rats with the assumption that the baseline glucose levels will go higher. Though the rats condition worsened, the glucometer still showed lower response. But the OneTouch Ultra 2 glucometer seemed to show true values as they correlated well with the symptoms showed by rats. Therefore, the old Freestyle Lite glucometer was discarded the new experiments were performed only with the OneTouch Ultra 2 glucometer.

Optimizing conditions for new PAD experiments

Following modifications were made to the method after observing these problems and identifying a few causes of these problems.

1) Younger rats: Previously, rats were purchased based on weight and not their age. But it is known that the animal develops insensitivity to insulin as the rat ages[56]. Therefore, young (8-week old) rats were used for the successive experiments. This approach not only ensures that the rat will be sensitive to insulin, but also maintains uniformity throughout the experiment.
2) Lowering streptozotocin dose: Multiple doses of streptozotocin were given to previous rats to make them diabetic. This was because the older glucometer showed abnormal lower outputs. So, more streptozotocin was administered to increase the baseline glucose concentration. Due to higher doses, toxic symptoms of the drug/extreme diabetes were observed. Since the new

glucometer was able to detect higher blood glucose concentrations, we realized that a single dose of streptozotocin was enough to induce diabetes. In addition, the dose of streptozotocin was lowered to 62-65 mg/kg as younger rats were used for following experiments.

3) New glucometer: The new OneTouch Ultra 2 glucometer was used with OneTouch Ultra Blue test strips to measure blood glucose concentration. As discussed, this glucometer has a higher upper limit of detection. Therefore, determination whether the rat was diabetic or not after streptozotocin treatment was more accurate in the next experiments. Since the glucometer is also accurate, the measurements of the true drop in glucose levels were reliable.
4) Fasting before the experiment: The PBS injection sham experiment showed that the blood glucose levels were drifting while they were anesthetized during the two-hour experimental duration. This could happen if the rat consumed food few minutes before the experiment, and the excess glucose was being utilized or eliminated during the experiment – hence the glucose drift was observed. In order to avoid this problem, rats were fasted for at least 1.5 hours prior to the experiment in the successive experiments to have a stable glucose baseline during the experiment.
5) Treatment with long acting insulin after the experiment: The T1D rats were allowed to recover for 3 days after an experiment was performed. This means that the rat could develop insensitivity over time as it ages and any successive experiments on the same rat could possibly not yield good results. Therefore,

at the end of the experiment, rats were treated with a long acting insulin, Tresiba (degludec) to keep them healthy in between the experiments.

Final modifications in the PAD experimental methods

Sprague Dawley rats (8-week old, male) were purchased and type 1 diabetes was induced with an intraperitoneal injection of streptozotocin (62-65 mg/kg). The rat was confirmed to be diabetic when the blood glucose concentration is found to be >250 mg/dL on three consecutive days after the treatment with streptozotocin. For the PAD experiments, a baseline concentration of glucose at around 400-450 mg/dL was targeted. 2 hours prior to the experiment, rat was isolated for fasting by incubating it in a new cage. Food was not provided during this period, but the rat was provided with water. The rats were anesthetized, and the PAD experiment was performed as discussed in earlier. Glucose concentration was determined using OneTouch Ultra 2 glucometer, and insulin was determined from the 15x diluted plasma using ALPCO Ultrasensitive ELISA kit.

The successful CD-insulin dose-response study

The dose-response study was attempted by incorporating the modifications in the method. In brief, 150 nmol CD-insulin particles were injected subdermally in each experiment. Five different experiments (0, 15, 30, 45 and 60 seconds irradiation) were performed on each rat. The 0 second irradiation experiment (control) was performed by placing an aluminum foil between the light source and depot. These experiments were performed in three rats in total to obtain the data in triplicates. Rats #51, 52 and 53 were used in this study. Following results were obtained (Figure 92).

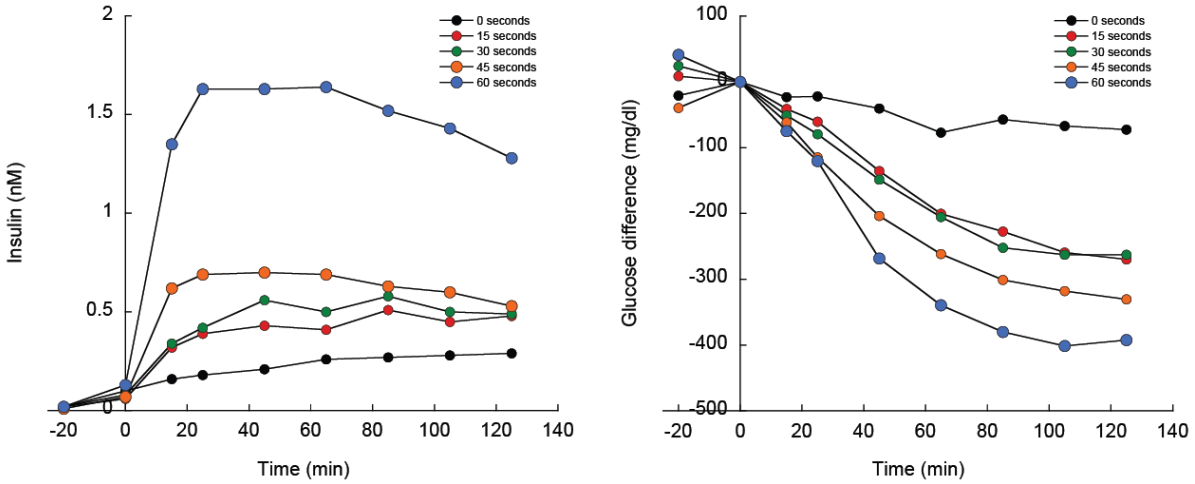

Figure 92 CD-insulin dose-response study: insulin and glucose profiles. Each point represents a mean of triplicate data. Error bars are not shown

Note on CD-insulin skin reaction: It was previously observed that CD-insulin causes reaction at the injection site. Such reactions were not observed since younger rats were used in the study. It is still not clearly understood if the reaction occurred due to (a) the age of the rat, or (b) insulin insensitivity, or (c) the toxic reactions of excess streptozotocin treatment.

A clear gradient response in both insulin and glucose profiles was observed with varying irradiation times. Higher the irradiation time, greater is the amount of insulin released from the depot and the drop in blood glucose concentrations. The linearity of the dose and effect relationship was determined by plotting the effect (decrease in glucose concentration, mg/dL) against the duration of depot irradiation (seconds). The data was found to be very linear with an R^2 of 0.85. This was the first dose-repose study of a photoactivated protein release in animals (Figure 93).

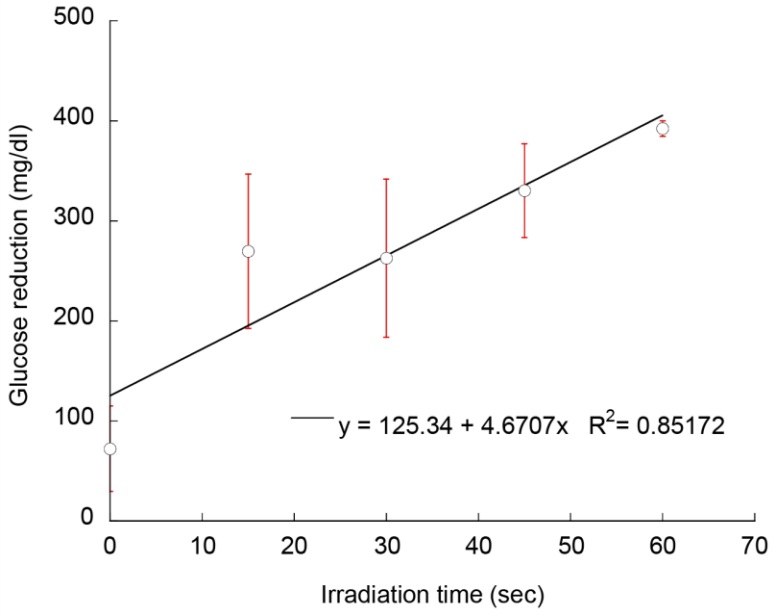

Figure 93 Linearity of the response in diabetic rats. Each data point represents mean and the standard deviations are shown as error bars

Comparison of CD-insulin with the first-generation PAD

The 60 second irradiation data of the CD-insulin was compared with the data reported using the first-generation PAD[31]. To compare the efficacy of CD-insulin, both the duration of irradiation and the amount of insulin released was considered. In these experiments, the first-generation PAD was irradiated for 120 seconds, whereas CD-insulin was exposed to light for only 60 seconds. The first-generation PAD had a C_{max} of ~0.16 nM, but CD-insulin profile had a 10x higher C_{max} of ~1.6 nM. Since the duration of irradiation was also 2x higher for first-generation PAD, we estimate that the efficacy of CD-insulin was ~20x higher than the first-generation PAD (Figure 94).

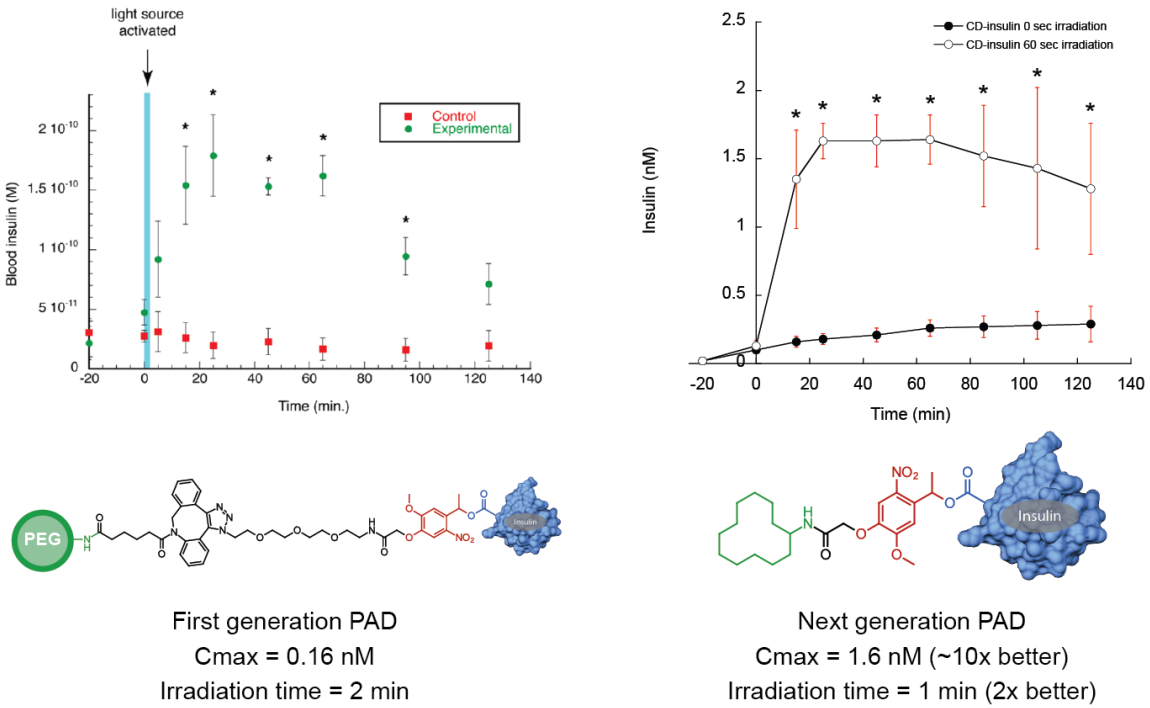

Figure 94 Comparison between the first and next generation PAD materials. ~20x increase in efficiency in animal models was possible due to tag approach

P2-insulin 60 second irradiation

Finally, an experiment was performed with P2-insulin, the charge tag insulin variant on Rats #53, 54 and 55. Though a soluble acidic formulation could be developed for P2-insulin to be injected in animal, a particulate suspension at pH 7.2 was prepared. This was done to maintain uniformity between the experiments and to compare the efficacy of charge tags and non-polar tags. Experiment was performed in a similar fashion. The method followed for injection is described shortly. 200 nmol P2-insulin was milled in 200 µL 100 mM PBS pH 7.2. The suspension was centrifuged, and the supernatant was removed. The P2-insulin pellet was resuspended in 50 µL 10 mM PBS 7.2. 35 µL of the suspension was diluted to 50 µL with 10 mM PBS and

injected subdermally in an anesthetized rat. Following observations were made (Figure 95).

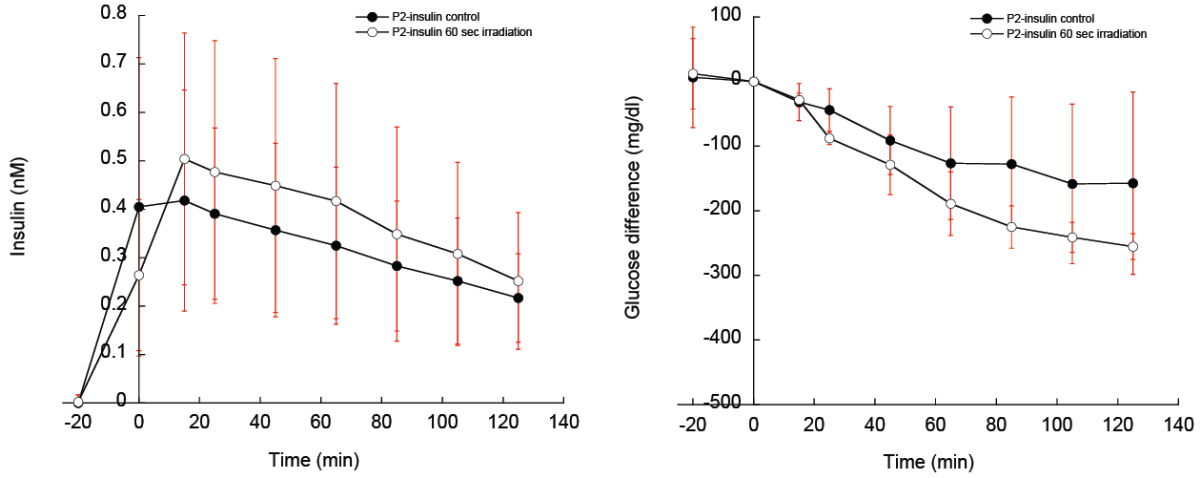

Figure 95 Insulin and glucose profiles determined in triplicates after irradiating P2-insulin depot in diabetic rats for 60 seconds. Standard deviations are shows as error bars

It was observed that a significant amount of insulin was detected in both control and test experiments. This was probably due to leaching and the higher solubility of P2-insulin (14 μM) versus CD-insulin (0.8 μM) at physiological pH. The amount of insulin released from the depot on irradiation was only slightly higher than that of the control. Therefore, further studies on P2-insulin were not pursued.

CHAPTER 7

SUMMARY, SCOPE AND CONCLUSIONS

Summary

The photoactivated insulin depot (PAD) was developed as a minimally invasive approach of insulin delivery for a tight glucose control in diabetics. In this approach, an inert insulin depot is injected under the skin, and the insulin delivery into circulation is controlled with the help of a light stimulus. A first-generation PAD was designed by linking photoactivated insulin to an insoluble polymer. Though the biocompatible polymer assisted in the retention of insulin at the site of injection, several issues were associated with its use. This study explores the potential of tags (small molecular modifications) for the construction of the PAD. Tags improve insulin density in the depot and can be easily eliminated from the site of injection after light activated delivery.

Tags retain insulin at the injection site by lowering the protein's solubility under physiological conditions. Two different types of tags, viz. non-polar/hydrophobic and charge tags were developed. The non-polar tags lower insulin solubility by hydrophobic effects. Four different insulin variants were developed with four varieties of non-polar tags, of which three tags were designed with hydrophobic peptides. The non-peptidic tag consists of a water insoluble cyclododecyl hydrocarbon. Non-polar tag insulin variants could be made into small particles with diameters in higher micron scales. These particles are injectable through a 31 G needle and can release insulin on exposure to light. Non-polar tags lowered

insulin solubility by about 1300 times. On the other hand, charge tags are basic in nature for insulin and raise the protein's isoelectric point from 5.4 to 7.2. Since proteins have lowest solubility at their isoelectric points, the charge tag insulin variant precipitates at the injection site. Charge tags have the advantage of being highly soluble at acidic pH and therefore, can be delivered as a soluble injection. P2-insulin, with a charge tag containing two positive charges, lowered the solubility of insulin by 75x and released insulin only on exposure to light in a first order fashion.

Tag insulin variants (one representative from each category of tags – CD-insulin and P2-insulin) were tested in a streptozotocin induced T1D rodent model. Firstly, the T1D rat model was optimized for performing PAD experiments. Then, the dose-response studies of CD-insulin were attempted, discussing the *in vivo* variable insulin release from PAD for the first time. CD-insulin is also ~20x better than the first-generation PAD. P2-insulin was observed to be leaching from the depot due to its solubility.

Tag approach: scope

The tag-approach developed in this study involves the chemical modification of proteins with light cleavable small molecules. The variety of functions that small molecules can provide is limitless and hence any protein can be modified with a variety of functional groups having different properties. Light sensitivity of the modification provides an additional advantage to the protein conjugate – the modification is not permanent and can be easily removed by exposure to light. In the case of PAD, newer tags can be further designed to improve the approach. In this

study, only two types of tags were explored to lower insulin solubility. Properties of the PAD can be potentially improved by either lowering the solubility to a lower range with peptidic tags, or the photo-release kinetics. Two such approaches will be discussed here.

Histidine tags

While pursuing the charge tag approach, insulin glargine and the formulation of Lantus was studied extensively. The long action of glargine was not solely dependent on the reduction of solubility due to isoelectric point shifts. Lantus formulation also consisted of zinc, in the presence of which insulin readily hexamerizes[57]. The formulation also consists of phenol as an anti-microbial. It has been studied by many researchers that phenol also stabilizes one of the forms of insulin hexamer[58]. Insulin is rapidly absorbed into the blood when it exists in its monomeric state. Quaternary structures of insulin (dimers, trimers and hexamers) are not easily absorbed. Therefore, Lantus works as a long acting insulin due to a combination of factors including (a) solubility reduction by isoelectric shifting and (b) enhancing complexation with the help of zinc and phenol.

In the charge tag approach, the P2-tag was designed to raise the isoelectric point of insulin to 7.2. One of the ideas to improve charge tag approach was the inclusion of zinc in formulation to assist in P2-insulin complexation and retention at the site of injection. Here, two important points were noted.

1) Since the chemical structure of native insulin was not preserved in P2-insulin, there is a possibility that hexamers may not form. Therefore, tags can prevent

the formation of insulin hexamers and quaternary structures of other proteins including aggregates.

2) Tertiary amines are known to complex well with zinc ions[59]. Therefore, it is also possible that the tag can compete with insulin for complexation. Design of such tags allows the development of a photoactivated insulin hexamer, which dissociates to monomers on exposure to light.

Therefore, a new peptidic tag with histidines (His-His-His-insulin variant) was designed. Histidine is an aromatic amino acid with a pK_a of ~6. The imidazole side chain of histidine will be protonated and charged at acidic pH, allowing a soluble formulation for a histidine insulin variant. But since the side chain exists in a deprotonated state, the PAD with aromatic side chains can possibly have a very low solubility in the skin (Figure 96).

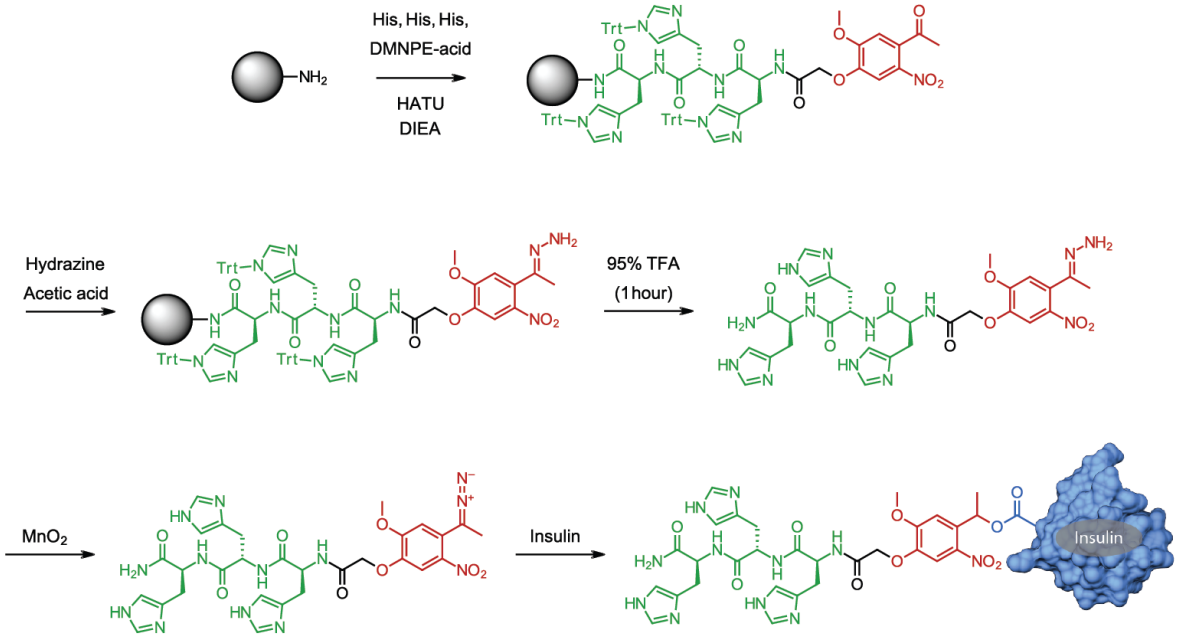

Figure 96 Synthesis of His-His-His-insulin

This was not pursued further because the yields of diazotization and insulin esterification reactions were very low. It was then hypothesized that the diazotization failed probably due to interactions of His-His-His-hydrazone of diazo complexed with manganese oxide and could not be isolated from the reaction. However, the impure protein was analyzed on mass spectrometer (Figure 97) and by isoelectric focusing (Figure 98) to know that conjugation of a single histidine raises the isoelectric point of insulin by 0.13 units. So, a tag with sequence Arg-His-His-His-His connected to insulin should raise the pI to 7.22.

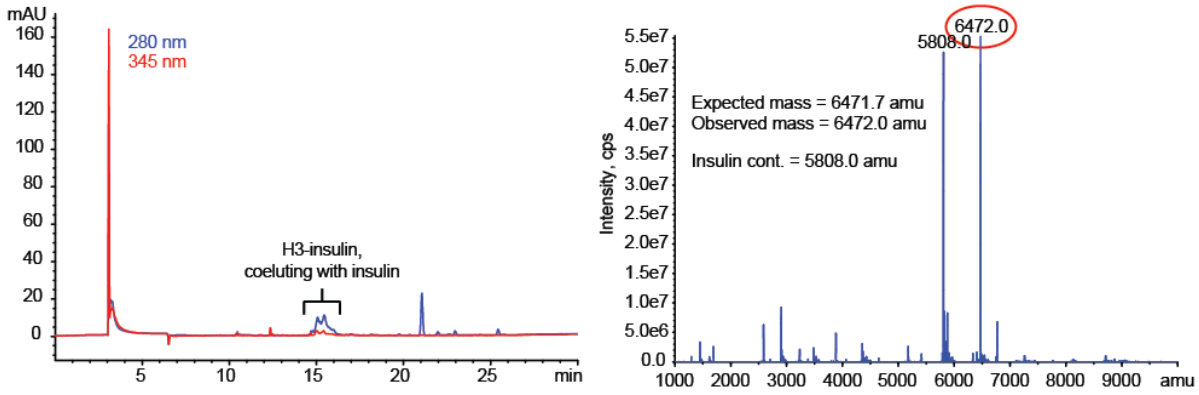

Figure 97 Analysis of His-His-His-insulin on HPLC (left) and MS (right)

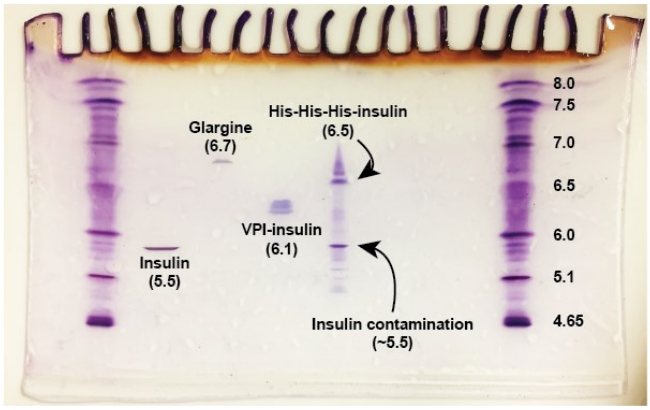

Figure 98 Isoelectric focusing of impure His-His-His-insulin

Amphiphilic tags

One of the advantages of peptidic tags that was discussed earlier is the allowance of protein conjugation with a variety of sequences. Non-polar peptidic tags were efficient in lowering the protein solubility, but the charge tags have the advantage of getting cleared at a faster rate due to their higher solubility after photolysis. Therefore, peptidic tags were designed to combine these two approaches to create a better PAD. Ile-Ile-Ile-insulin lowered the solubility by 350x and the P2-insulin by 75x. A combination of these two can potentially lower the solubility of insulin to as low ranges as that of CD-insulin.

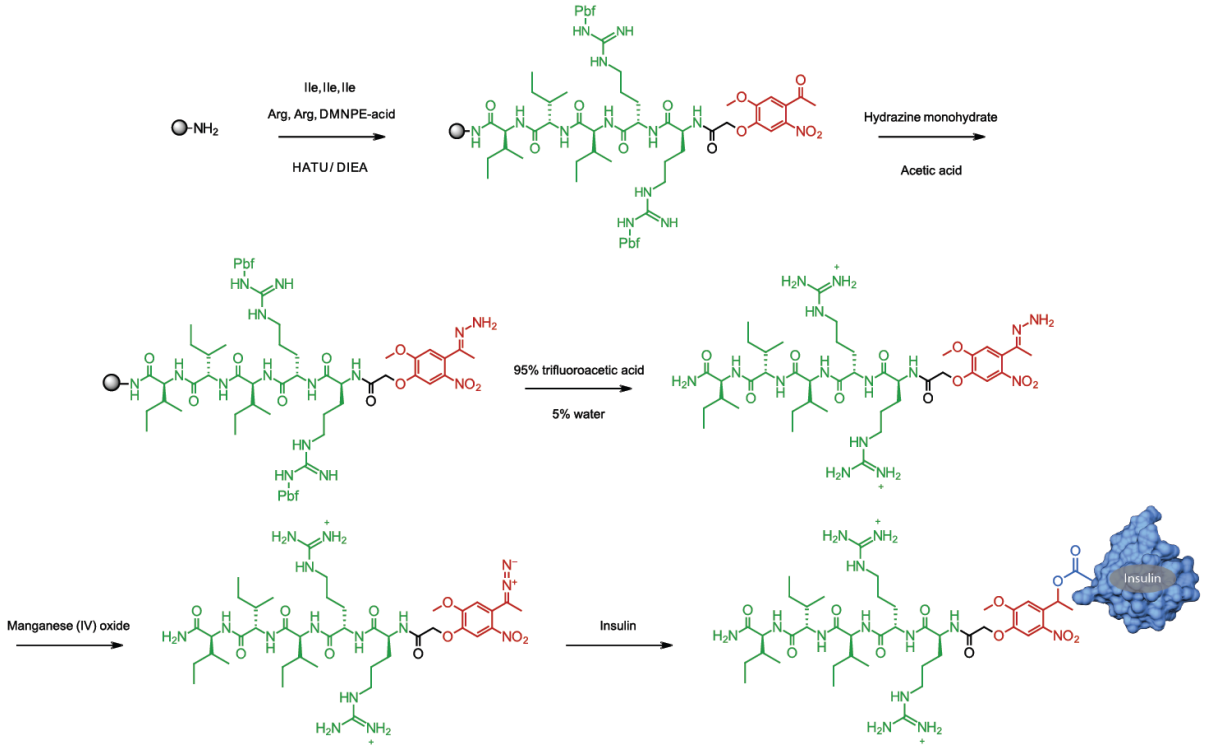

Figure 99 Synthesis of Ile-Ile-Ile-Arg-Arg-insulin

Peptidic tags were designed with isoleucine and arginines. Two charges are required to raise the pI to 7.2 and three isoleucines were utilized. Many sequences are

possible with these amino acids, but the best sequence was identified as Ile-Ile-Ile-Arg-Arg-insulin. It is recommended that the three isoleucines are towards the C-terminus of the peptidic tag; this ensures that the Ile-Ile-Ile will be exposed to aqueous conditions and lowers the solubility of protein. Synthesis of the protein was attempted and is shown in Figure 99. Again, studies on this tag were not pursued further as the diazotization and insulin esterification yields were very low.

Conclusions

Therefore, the tag approach is a simple yet highly applicable design that helped improve the PAD efficiency by ~20x *in vivo*. Improvements in the design of tags can further improve the efficacy of the PAD. The work done in this study also discusses the ability of the PAD to deliver insulin in a variable fashion. However, further studies are required to assess / improve the potential of PAD; including longevity and stability of the depot *in vivo*, new designs to engineer PAD to have its depot site in subcutaneous layer instead of subdermal layer, etc. If the PAD insulin delivery is automated with the help of a continuous glucose monitor, it has the potential to be translated into the clinic as an artificial pancreas and thus, can improve lives of many diabetics.

APPENDIX

Copyright Clearance Center RightsLink®

Home | Help | Email Support | Karthik Nadendla

ELSEVIER

Chapter: Chapter Six Chemical modification of proteins with photocleavable groups
Book: Methods in Enzymology
Author: Karthik Nadendla,Bhagyesh Sarode,Simon H. Friedman
Publisher: Elsevier
Date: 2019

Order Completed

Thank you for your order.

This Agreement between Karthik Nadendla ("You") and Elsevier ("Elsevier") consists of your license details and the terms and conditions provided by Elsevier and Copyright Clearance Center.

Your confirmation email will contain your order number for future reference.

Printable Details

License Number	4812820805132
License date	Apr 19, 2020

Licensed Content

Licensed Content Publisher	Elsevier
Licensed Content Publication	Elsevier Books
Licensed Content Title	Methods in Enzymology
Licensed Content Author	Karthik Nadendla,Bhagyesh Sarode,Simon H. Friedman
Licensed Content Date	Jan 1, 2019
Licensed Content Pages	16
Journal Type	S&T

Order Details

Type of Use	reuse in a thesis/dissertation
Portion	figures/tables/illustrations
Number of figures/tables/illustrations	2
Format	electronic
Are you the author of this Elsevier chapter?	Yes
Will you be translating?	No

About Your Work

Title	Next generation photoactivated insulins for the development of a light activated artificial pancreas
Institution name	University of Missouri-Kansas City
Expected presentation date	May 2020

Additional Data

Portions	Figure 3 and Figure 4

Hydrophobic Tags for Highly Efficient Light-Activated Protein Release

Author: Karthik Nadendla, Bhagyesh R. Sarode, Simon H. Friedman
Publication: Molecular Pharmaceutics
Publisher: American Chemical Society
Date: Jul 1, 2019

REFERENCES

(1) Hall, J. E. Guyton and Hall Textbook of Medical Physiology. 2011. *Saunders Elsevier Philadelphia, PA* **1946**, 12899–19103.

(2) Gillespie, K. M. Type 1 Diabetes: Pathogenesis and Prevention. *Cmaj* **2006**, *175* (2), 165–170.

(3) Stumvoll, M.; Goldstein, B. J.; van Haeften, T. W. Type 2 Diabetes: Pathogenesis and Treatment. *Lancet* **2008**, *371* (9631), 2153–2156.

(4) Allen, F. M. *Studies Concerning Glycosuria and Diabetes*; Wm Leonard, 1913.

(5) Joshi, N.; Caputo, G. M.; Weitekamp, M. R.; Karchmer, A. W. Infections in Patients with Diabetes Mellitus. *N. Engl. J. Med.* **1999**, *341* (25), 1906–1912.

(6) Vlassara, H.; Palace, M. R. Diabetes and Advanced Glycation Endproducts. *J. Intern. Med.* **2002**, *251* (2), 87–101.

(7) Selvin, E.; Steffes, M. W.; Zhu, H.; Matsushita, K.; Wagenknecht, L.; Pankow, J.; Coresh, J.; Brancati, F. L. Glycated Hemoglobin, Diabetes, and Cardiovascular Risk in Nondiabetic Adults. *N. Engl. J. Med.* **2010**, *362* (9), 800–811.

(8) Association, A. D.; others. Diagnosing Diabetes and Learning about Prediabetes. 2016. 2019.

(9) Bild, D. E.; Selby, J. V; Sinnock, P.; Browner, W. S.; Braveman, P.; Showstack, J. A. Lower-Extremity Amputation in People with Diabetes: Epidemiology and Prevention. *Diabetes Care* **1989**, *12* (1), 24–31.

(10) Lindsberg, P. J.; Roine, R. O. Hyperglycemia in Acute Stroke. *Stroke* **2004**, *35* (2), 363–364.

(11) Sampanis, C. H. Management of Hyperglycemia in Patients with Diabetes Mellitus and Chronic Renal Failure. *Hippokratia* **2008**, *12* (1), 22.

(12) Hirsch, I. B.; Farkas-Hirsch, R.; Skyler, J. S. Intensive Insulin Therapy for Treatment of Type I Diabetes. *Diabetes Care* **1990**, *13* (12), 1265–1283.

(13) Ter Braak, E. W.; Woodworth, J. R.; Bianchi, R.; Cerimele, B.; Erkelens, D. W.; Thijssen, J. H. H.; Kurtz, D. Injection Site Effects on the Pharmacokinetics and Glucodynamics of Insulin Lispro and Regular Insulin. *Diabetes Care* **1996**, *19* (12), 1437–1440.

(14) Bilotta, F.; Guerra, C.; Badenes, R.; Lolli, S.; Rosa, G. Short Acting Insulin Analogues in Intensive Care Unit Patients. *World J. Diabetes* **2014**, *5* (3), 230.

(15) Norrman, M.; Hubálek, F.; Schluckebier, G. Structural Characterization of Insulin NPH Formulations. *Eur. J. Pharm. Sci.* **2007**, *30* (5), 414–423.

(16) Wang, F.; Carabino, J. M.; Vergara, C. M. Insulin Glargine: A Systematic Review of a Long-Acting Insulin Analogue. *Clin. Ther.* **2003**, *25* (6), 1541–1577.

(17) Havelund, S.; Plum, A.; Ribel, U.; Jonassen, I.; Vølund, A.; Markussen, J.; Kurtzhals, P. The Mechanism of Protraction of Insulin Detemir, a Long-Acting, Acylated Analog of Human Insulin. *Pharm. Res.* **2004**, *21* (8), 1498–1504.

(18) Jonassen, I.; Havelund, S.; Hoeg-Jensen, T.; Steensgaard, D. B.; Wahlund, P.-O.; Ribel, U. Design of the Novel Protraction Mechanism of Insulin Degludec, an Ultra-Long-Acting Basal Insulin. *Pharm. Res.* **2012**, *29* (8), 2104–2114.

(19) Rolland, F.; Winderickx, J.; Thevelein, J. M. Glucose-Sensing Mechanisms in Eukaryotic Cells. *Trends Biochem. Sci.* **2001**, *26* (5), 310–317.

(20) Pingel, M.; Vølund, A. Stability of Insulin Preparations. *Diabetes* **1972**, *21* (7), 805–813.

(21) McGill, J. B.; Ahn, D.; Edelman, S. V; Kilpatrick, C. R.; Cavaiola, T. S. Making Insulin Accessible: Does Inhaled Insulin Fill an Unmet Need? *Adv. Ther.* **2016**, *33* (8), 1267–1278.

(22) Oleck, J.; Kassam, S.; Goldman, J. D. Commentary: Why Was Inhaled Insulin a Failure in the Market? *Diabetes Spectr.* **2016**, *29* (3), 180–184.

(23) Latres, E.; Finan, D. A.; Greenstein, J. L.; Kowalski, A.; Kieffer, T. J. Navigating Two Roads to Glucose Normalization in Diabetes: Automated Insulin Delivery Devices and Cell Therapy. *Cell Metab.* **2019**, *29* (3), 545–563.

(24) Ahern, J. A. H.; Boland, E. A.; Doane, R.; Ahern, J. J.; Rose, P.; Vincent, M.; Tamborlane, W. V. Insulin Pump Therapy in Pediatrics: A Therapeutic Alternative to Safely Lower HbA1c Levels across All Age Groups. *Pediatr. Diabetes* **2002**, *3* (1), 10–15.

(25) Saboo, B. D.; Talaviya, P. A. Continuous Subcutaneous Insulin Infusion: Practical Issues. *Indian J. Endocrinol. Metab.* **2012**, *16* (Suppl 2), S259.

(26) Barnard, K. D.; Skinner, T. C. Cross-Sectional Study into Quality of Life Issues Surrounding Insulin Pump Use in Type 1 Diabetes. *Pract. Diabetes Int.* **2008**, *25* (5), 194–200.

(27) Paul, N.; Kohno, T.; Klonoff, D. C. A Review of the Security of Insulin Pump Infusion Systems. *J. Diabetes Sci. Technol.* **2011**, *5* (6), 1557–1562.

(28) Kuroda, K.; Takeshita, Y.; Kaneko, S.; Takamura, T. Bending of a Vertical

Cannula without Alarm during Insulin Pump Therapy as a Cause of Unexpected Hyperglycemia: A Japanese Issue? *J. Diabetes Investig.* **2015**, *6* (6), 739–740.

(29) Friedman, S. H. Replacing Pumps with Light Controlled Insulin Delivery. *Curr. Diab. Rep.* **2019**, *19* (11), 122.

(30) Jain, P. K.; Karunakaran, D.; Friedman, S. H. Construction of a Photoactivated Insulin Depot. *Angew. Chemie Int. Ed.* **2013**, *52* (5), 1404–1409.

(31) Sarode, B. R.; Kover, K.; Tong, P. Y.; Zhang, C.; Friedman, S. H. Light Control of Insulin Release and Blood Glucose Using an Injectable Photoactivated Depot. *Mol. Pharm.* **2016**, *13* (11), 3835–3841.

(32) Woo, Y. C.; Park, S. S.; Subieta, A. R.; Brennan, T. J. Changes in Tissue PH and Temperature after Incision Indicate Acidosis May Contribute to Postoperative Pain. *Anesthesiol. J. Am. Soc. Anesthesiol.* **2004**, *101* (2), 468–475.

(33) Holmes, C. P. Model Studies for New O-Nitrobenzyl Photolabile Linkers: Substituent Effects on the Rates of Photochemical Cleavage. *J. Org. Chem.* **1997**, *62* (8), 2370–2380.

(34) Nadendla, K.; Sarode, B. R.; Friedman, S. H. Hydrophobic Tags for Highly Efficient Light-Activated Protein Release. *Mol. Pharm.* **2019**, *16* (7), 2922–2928. https://doi.org/10.1021/acs.molpharmaceut.9b00140.

(35) Nadendla, K.; Sarode, B.; Friedman, S. H. *Chemical Modification of Proteins with Photocleavable Groups*, 1st ed.; Elsevier Inc., 2019. https://doi.org/10.1016/bs.mie.2019.04.008.

(36) Jain, P. K.; Shah, S.; Friedman, S. H. Patterning of Gene Expression Using New Photolabile Groups Applied to Light Activated RNAi. *J. Am. Chem. Soc.* **2011**, *133* (3), 440–446.

(37) Abelt, C. J.; Pleier, J. M. Stereoselective Azine Formation in the Decomposition of Phenyldiazomethanes. *J. Am. Chem. Soc.* **1989**, *111* (5), 1795–1799.

(38) Kolb, V. M.; Kuffel, A. C.; Spiwek, H. O.; Janota, T. E. On the Mechanism of Formation of Azines from Hydrazones. *J. Org. Chem.* **1989**, *54* (11), 2771–2775.

(39) Wintersteiner, O.; Abramson, H. A. The Isoelectric Point of Insulin Electrical Properties of Adsorbed and Crystalline Insulin. *J. Biol. Chem.* **1933**, *99* (3), 741–753.

(40) Hennessey Jr, J. P.; Scarborough, G. A. An Optimized Procedure for Sodium Dodecyl Sulfate-Polyacrylamide Gel Electrophoresis Analysis of Hydrophobic Peptides from an Integral Membrane Protein. *Anal. Biochem.* **1989**, *176* (2), 284–289.

(41) Irvine, D. J.; Swartz, M. A.; Szeto, G. L. Engineering Synthetic Vaccines Using Cues from Natural Immunity. *Nat. Mater.* **2013**, *12* (11), 978–990. https://doi.org/10.1038/nmat3775.

(42) Scopes, R. K. *Protein Purification: Principles and Practice*; Springer Science & Business Media, 2013.

(43) Nadendla, K.; Friedman, S. H. Light Control of Protein Solubility Through Isoelectric Point Modulation. *J. Am. Chem. Soc.* **2017**, *139* (49), 17861–17869. https://doi.org/10.1021/jacs.7b08465.

(44) Honegger, A.; Hughes, G. J.; Wilson, K. J. Chemical Modification of Peptides by Hydrazine. *Biochem. J.* **1981**, *199* (1), 53–59.

(45) Luzio, S. D.; Beck, P.; Owens, D. R. Comparison of the Subcutaneous Absorption of Insulin Glargine (Lantus®) and NPH Insulin in Patients with Type 2 Diabetes. *Horm. Metab. Res.* **2003**, *35* (07), 434–438.

(46) Joshi, A. B.; Rus, E.; Kirsch, L. E. The Degradation Pathways of Glucagon in Acidic Solutions. *Int. J. Pharm.* **2000**, *203* (1–2), 115–125.

(47) Guo, P.; Hsu, T. M.; Zhao, Y.; Martin, C. R.; Zare, R. N. Preparing Amorphous Hydrophobic Drug Nanoparticles by Nanoporous Membrane Extrusion. *Nanomedicine* **2013**, *8* (3), 333–341.

(48) Huus, K.; Havelund, S.; Olsen, H. B.; van de Weert, M.; Frokjaer, S. Chemical and Thermal Stability of Insulin: Effects of Zinc and Ligand Binding to the Insulin Zinc-Hexamer. *Pharm. Res.* **2006**, *23* (11), 2611–2620.

(49) Emdin, S. O.; Dodson, G. G.; Cutfield, J. M.; Cutfield, S. M. Role of Zinc in Insulin Biosynthesis. *Diabetologia* **1980**, *19* (3), 174–182.

(50) Brange, J.; Vølund, A. Insulin Analogs with Improved Pharmacokinetic Profiles. *Adv. Drug Deliv. Rev.* **1999**, *35* (2–3), 307–335.

(51) Sarode, B. R.; Kover, K.; Friedman, S. H. Visible-Light-Activated High-Density Materials for Controlled in Vivo Insulin Release. *Mol. Pharm.* **2019**, *16* (11), 4677–4687.

(52) McCray, J. A.; Trentham, D. R. Properties and Uses of Photoreactive Caged Compounds. *Annu. Rev. Biophys. Biophys. Chem.* **1989**, *18* (1), 239–270.

(53) Furman, B. L. Streptozotocin-Induced Diabetic Models in Mice and Rats. *Curr. Protoc. Pharmacol.* **2015**, *70* (1), 5–47.

(54) Shin, J.-Y.; Nam, H.-H.; Lee, K.-J. Estimation of Glucose Concentration Using Adaptive Calibration Curve in Different Hematocrit Levels. *Electron. Lett.* **2013**, *49* (9), 584–585.

(55) Arabadjief, D.; Nichols, J. H. Assessing Glucose Meter Accuracy. *Curr. Med. Res. Opin.* **2006**, *22* (11), 2167–2174.

(56) Qiang, W.; Weiqiang, K.; Qing, Z.; Pengju, Z.; Yi, L. Aging Impairs Insulin-Stimulated Glucose Uptake in Rat Skeletal Muscle via Suppressing AMPK$ $. *Exp. Mol. Med.* **2007**, *39* (4), 535–543.

(57) Goykhman, S.; Drincic, A.; Desmangles, J. C.; Rendell, M. Insulin Glargine: A Review 8 Years after Its Introduction. *Expert Opin. Pharmacother.* **2009**, *10* (4), 705–718.

(58) Derewenda, U.; Derewenda, Z.; Dodson, E. J.; Dodson, G. G.; Reynolds, C. D.; Smith, G. D.; Sparks, C.; Swenson, D. Phenol Stabilizes More Helix in a New Symmetrical Zinc Insulin Hexamer. *Nature* **1989**, *338* (6216), 594–596. https://doi.org/10.1038/338594a0.

(59) Dalla Cort, A.; Mandolini, L.; Pasquini, C.; Rissanen, K.; Russo, L.; Schiaffino, L. Zinc--Salophen Complexes as Selective Receptors for Tertiary Amines. *New J. Chem.* **2007**, *31* (9), 1633–1638.

VITA

Karthik Nadendla was born on September 23, 1988 in Rajahmundry, India. He received his Master of Pharmacy degree (Biotechnology, 2012) from Manipal University, India. He was trained in the areas of drug manufacturing, drug design and plant biotechnology at Dr. Reddy's Laboratories, Doble Lab (IIT Madras, India) and Huchzermeyer Lab (Leibniz Universität Hannover, Germany) respectively. For about a year, he also worked at Sandor Lifesciences Pvt. Ltd. as a biochemist and was involved in the development of tests for the detection of inborn errors of metabolism.

In 2014, Karthik moved to the United States of America to pursue his doctoral research at the Friedman Lab (University of Missouri-Kansas City). Here, he worked on the development of the photoactivated insulin depot and helped design highly efficient next generation materials with the 'tag-approach' discussed in this text. His work is published in peer reviewed journals and recognized by scientific communities such as F1000. Karthik continues to work on biomedical problems and attempts to develop better therapies using his expertise in the area of protein chemistry.